



TECHNISCHE UNIVERSITÄT MÜNCHEN

Lehrstuhl für Biotechnologie der Nutztiere

*ROSA26* dual fluorescent reporter pigs and generation of a  
porcine model for pancreatic cancer

Shun Li

Vollständiger Abdruck der von der Fakultät Wissenschaftszentrum Weihenstephan für Ernährung, Landnutzung und Umwelt der Technischen Universität München zur Erlangung des akademischen Grades eines

Doktors der Naturwissenschaften

genehmigten Dissertation.

Vorsitzender: Univ.-Prof. Dr. W. Schwab

Prüfer der Dissertation:

1. Univ.-Prof. A. Schnieke, Ph. D.

2. apl. Prof. Dr. D. K. M. Saur

Die Dissertation wurde am 30.06.2014 bei der Technischen Universität München eingereicht und durch die Fakultät Wissenschaftszentrum Weihenstephan für Ernährung, Landnutzung und Umwelt am 24.09.2014 angenommen.

## Abstract

The *ROSA26* locus in mouse, human and rat has been widely used in genetic modification as it can be targeted with high efficiency and a gene of interest inserted into the *ROSA26* locus can be expressed stably and ubiquitously. Here the porcine *ROSA26* gene was also identified and four exons were confirmed on chromosome 13.

Cre/loxP site-specific recombination is a powerful and versatile tool that allows for precisely controlled conditional gene expression and many other genetic modifications in mice. This work extends this system to pigs, with a particular focus on conditional and tissue-specific expression of oncogenic mutations to model human cancers. Cre reporter strains that reveal the location, pattern and extent of Cre recombination *in vivo* are an important component of this technology. This work reports viable pigs with a dual fluorochrome cassette under the control of a strong synthetic promoter that switches expression after Cre-recombination, from membrane-targeted tandem dimer Tomato to membrane-targeted green fluorescent protein. The reporter cassette was placed at the porcine *ROSA26* locus by conventional gene targeting using primary mesenchymal stem cells, and animals generated by nuclear transfer. Gene targeting efficiency was high, and analysis of foetal organs and primary cells indicated that the reporter is highly expressed and functional. This indicates that the porcine *ROSA26* locus conserves the functions of its orthologues in mouse, human and rat. Cre reporter pigs will provide a multipurpose indicator of Cre recombinase activity, an important new tool for the rapidly expanding field of porcine genetic modification.

The other part of this work is to generate a porcine model for pancreatic cancer. A conditional transcription stop cassette (LSL) was inserted into the intron 1 of porcine KRAS, and the KRAS<sup>G12D</sup> was inserted into exon 2. Thus, KRAS<sup>G12D</sup> can be expressed after Cre recombination. Furthermore, Cre recombinase was placed into a site after the stop codon of porcine PDX-1 locus. These targeted cells were evaluated *in vitro* and can be used for nuclear transfer.

## Zusammenfassung

Der ROSA26 Locus wird sowohl in der Maus als auch im Menschen und der Ratte häufig für Genetic Engineering verwendet, da hier mit hoher Effizienz exogene Gene eingefügt werden können, deren Expression anschließend stabil und ubiquitär erfolgt. In der vorliegenden Arbeit wurde das porcine ROSA26-Gen identifiziert und vier Exons auf Chromosom 13 verifiziert.

Das Cre/loxP-Rekombinationssystem ist ein wichtiges und flexibel einsetzbares Werkzeug, welches genau gesteuerte Genexpression sowie viele weitere genetische Modifikationen ermöglicht. In dieser Arbeit wurde das System auf Schweine ausgeweitet, mit besonderem Fokus auf die konditionelle und gewebsspezifische Expression von onkogenen Mutationen für Modelle menschlicher Krebserkrankungen. Cre-Reporterstämme, die genaue Lokalisierung, Muster und Ausmaß der Cre-Rekombination abbilden, spielen hierbei eine wichtige Rolle. Im Rahmen dieser Arbeit wurden lebensfähige Reporterschweine erzeugt, die eine doppelt fluorochrome Kasette tragen. Diese wird von einem stark exprimierten synthetischen Promoter gesteuert, welcher nach Cre-Rekombination von der Expression von membranlokalisierten *Tomato* zu membranlokalisierten GFP wechselt. Die ganze Kasette wurde mit Hilfe von konventionellem *Gene Targeting* in den porcinen ROSA26 Locus in primären mesenchymalen Stammzellen integriert, aus welchen in einem weiteren Schritt via Kernttransfer Schweine generiert wurden. Die Effizienz des *Gene Targetings* war hoch und die Analyse foetaler Organe und primärer Zellen zeigte, dass der Reporter stark exprimiert wird und funktional ist. Hieraus lässt sich schließen, dass der porcine ROSA26 Locus die Funktionen seiner Orthologe in Maus, Mensch und Ratte konserviert hat. Cre-Reporterschweine können vielfach für die Detektion von Cre-Rekombinase-Aktivität eingesetzt werden und stellen einen wichtigen Baustein in der Entwicklung des schnellwachsenden Feldes der porcinen genetischen Modifikationen dar.

Um ein porcines Modell für Pankreaskreb zu erstellen, wurde ein konditionelle Transkriptions-Stop-Kasette (LSL) in Intron 1 des porcinen KRAS integriert, während KRAS<sup>G12D</sup> in Exon 2 integriert wurde. Somit kann KRAS<sup>G12D</sup> nach Cre-Rekombination exprimiert werden. Weiterhin wurde Cre-Rekombinase nach dem Stop-Codon im porcinen

PDX-1 Locus platziert. Die so modifizierten Zellen wurden *in vitro* analysiert und können nun für den Kerntransfer eingesetzt werden.

# Contents

<b>1</b>	<b>Introduction .....</b>	<b>1</b>
1.1	Pancreatic cancer .....	1
1.1.1	Pancreatic ductal adenocarcinoma (PDAC) .....	1
1.1.2	Molecular genetics of PDAC .....	2
1.2	Animal models of pancreatic cancer .....	5
1.2.1	Mouse models of pancreatic cancer .....	5
1.2.2	Pigs as model in biomedicine .....	6
1.3	Genetically modified (GM) animals .....	7
1.3.1	Direct transgenesis .....	7
1.3.2	Cell-mediated DNA transfer .....	10
1.3.3	Genome editing .....	12
1.3.4	Gene-targeted animals .....	14
1.3.5	Gene-targeted pigs .....	16
1.3.6	Cre/loxP system .....	17
1.4	Reporter animal strains .....	18
1.4.1	Reporter genes .....	18
1.4.2	Random reporter strains .....	20
1.4.3	Mouse Cre reporter strains .....	21
1.4.4	<i>ROSA26</i> locus .....	22
1.4.5	<i>ROSA26</i> reporter strains .....	23
1.5	Functions of reporter animal lines .....	24
1.5.1	Live cell imaging .....	24
1.5.2	Cell lineage tracing .....	26
1.5.3	Cell cycle indicator .....	27
1.5.4	For immunological research and cancers .....	29
1.6	Aim of this project .....	30
<b>2</b>	<b>Material and methods .....</b>	<b>32</b>
2.1	Material .....	32
2.1.1	Chemicals .....	32
2.1.2	Enzymes .....	33
2.1.3	Kits .....	34
2.1.4	Media, solutions, cells and supplements for molecularbiology and microbiology ..	34
2.1.4.1	Bacterial growth media .....	34
2.1.4.2	Solutions and supplements for molecular biology and microbiology .....	34
2.1.4.3	Antibiotics for microbiology .....	35
2.1.4.4	Bacterial strains .....	36
2.1.5	Media, solutions, supplements and cell lines for mammalian cell culture .....	36

---

2.1.6	Primers .....	37
2.1.7	Consumable Supplies.....	38
2.1.8	Cloning vectors and plasmids.....	39
2.1.9	Laboratory equipment.....	39
2.1.10	Softwares.....	41
2.2	Methods.....	41
2.2.1	Molecular biology methods.....	41
2.2.2	Microbiology methods.....	50
2.2.3	Tissue culture methods .....	51
2.2.3.1	General cell culture.....	51
2.2.3.2	Freezing and thawing of cells .....	52
2.2.3.3	Isolation of porcine cells .....	53
2.2.3.4	Transfection of mammalian cells .....	55
2.2.3.5	Selection of transfected cells and picking clones .....	57
2.2.3.6	PCR and RT-PCR from cell culture .....	57
2.2.3.7	$\beta$ -Galactosidase staining of eukaryotic cells.....	58
2.2.3.8	Cell preparation for somatic cell nuclear transfer (SCNT) .....	58
2.2.3.9	Cre transduction .....	58
2.2.3.10	Cryosection.....	58
2.2.3.11	Whole animal Tomato fluorescence .....	59
<b>3</b>	<b>Results .....</b>	<b>60</b>
3.1	Identification of porcine ROSA26 gene .....	60
3.2	Construction of ROSA26 gene targeting constructs.....	61
3.2.1	Construction of the GCROSA targeting vector .....	61
3.2.2	Construction of the TGROSA targeting vector .....	62
3.2.3	Linearization of targeting vectors.....	63
3.3	Porcine ROSA26 gene targeting .....	63
3.3.1	Transfection and selection of MSC clones .....	64
3.3.2	PCR screening for gene targeting events.....	64
3.3.3	RT-PCR analyses of ROSA26 targeted clones .....	65
3.3.4	Southern blot analyses of ROSA26 targeted clones .....	66
3.3.5	lacZ staining and activation of mCherry for GCROSA targeted MSC cell clones.. .....	67
3.3.6	Activation of mEGFP expression for TGROSA targeted MSC clones.....	69
3.4	Generation of ROSA26 targeted fetuses and pigs .....	70
3.4.1	Analysis of GCROSA targeted piglets by PCR and southern blot.....	71
3.4.2	Analysis of GCROSA targeted piglets by RT-PCR.....	72
3.4.3	lacZ staining and activation of mCherry for fibroblasts derived from GCROSA piglet .....	73
3.4.4	Analysis of TGROSA fetuses and piglet by PCR and southern blot.....	74
3.4.5	Analysis of TGROSA targeted piglets by RT-PCR .....	75
3.4.6	mTomato fluorescence detection for TGROSA fetuses and live piglet #258 ..	76

---

3.4.7	Activation of mGFP for fibroblasts derived from TGROSA foetus .....	78
3.5	Porcine PDX-1 gene targeting.....	79
3.5.1	Transfection and selection of pKDNF clones .....	79
3.5.2	PCR screening for gene targeting events.....	80
3.5.3	Southern blot analysis of PDX-1 targeted clones .....	81
3.6	Porcine KRAS gene targeting .....	82
3.6.1	KRAS gene targeting vector .....	82
3.6.2	Transfection and selection of pKDNF clones .....	83
3.6.3	PCR screening for gene targeting events.....	83
3.6.4	RT-PCR analyses of KRAS targeted clones .....	85
3.6.5	Southern blot analyses of KRAS targeted clones.....	87
<b>4</b>	<b>Discussion .....</b>	<b>89</b>
4.1	Gene targeting of porcine ROSA26.....	89
4.1.1	Identification of the porcine ROSA26 gene and its importance .....	89
4.1.2	Construction of the targeting vectors .....	90
4.1.3	Targeting efficiency of the ROSA26 locus .....	91
4.1.4	Activity of the ROSA26 promoter.....	92
4.1.5	Ubiquitously expression of genes placed in the ROSA26 locus.....	93
4.1.6	Placing gene of interests into porcine ROSA26 locus through RMCE .....	94
4.2	Somatic cell nuclear transfer .....	95
4.2.1	Factors influencing efficiency of generating genetically modified pigs by SCNT... .....	95
4.2.2	Cell cycle synchronization between donor cells and recipient oocytes .....	97
4.3	TALENs and CRISPR/Cas9 for genome engineering .....	98
4.4	PDX-1 gene targeted locus .....	100
4.5	Outlook .....	101
<b>5</b>	<b>References:.....</b>	<b>105</b>
<b>6</b>	<b>Abbreviations .....</b>	<b>130</b>
<b>7</b>	<b>Appendix.....</b>	<b>133</b>
<b>8</b>	<b>Acknowledgement.....</b>	<b>140</b>

# 1 Introduction

## 1.1 Pancreatic cancer

Pancreas is one of the most important digestive organs in the human body that regulates two major physiological processes: protein and carbohydrate digestion and homeostasis of glucose [1]. There are different types of pancreatic neoplasms, as defined by their histological resemblance to various normal pancreatic cellular constituents [2]. These multiple tumor types possess distinct histological and genetic features, and among them, pancreatic ductal adenocarcinoma (PDAC) is the most common type of pancreatic neoplasm, accounting for more than 85 % of pancreatic tumor cases. Not only PDAC is the fourth leading cause of cancer death in the United States [3] but also is one of the lethal human cancer across the world [4]. Despite many efforts in the past decades, PDAC is still a major unsolved health problem and has poor prognosis, with a median survival of less than 6 months and a 5-year survival rate of only 3% [5]. Although around 15-20% of patients undergoes potentially curative resection, the 5-year survival was only 20% [5]. The therapeutic methods, such as surgery, chemotherapy, radiotherapy, or combinations of these, have minimal impact on the course of the aggressive neoplasm [4]. So, it is very urgent to find out effective approaches to prevent, diagnose, and treat pancreatic cancer. Therefore, it is of important to conduct a more in-depth analysis of its molecular biology and develop refined animal models.

### 1.1.1 Pancreatic ductal adenocarcinoma (PDAC)

Pancreatic Intraepithelial Neoplasia (PanIN), Mucinous Cystic Neoplasm (MCN), and Intraductal Papillary Mucinous Neoplasm (IPMN) are three precursors to PDAC identified after clinical and histopathologic studies [6,7]. Among these precursor lesions, PanIN is the most common and well studied one [2], and it originates in small terminal (<5 mm) pancreatic ducts [6]. Based on the degree of divergent morphologic alterations, PanINs are further classified as three stages PanIN-1, PanIN-2 and PanIN-3 (Figure 1.1). PanIN-1 can be further subdivided into PanIN-1A and PanIN-1B. In PanIN-1A stage, the normal ductal epithelium cells are transformed into tall columnar cells with basally located nuclei and abundant



supranuclear mucin, whereas the epithelial lesions in PanIN-1B stage have a papillary micropapillary or basally pseudostratified architecture, and the other respects are identical to PanIN-1A. PanIN-2 lesions have some nuclear abnormalities, including enlarged nuclei, nuclear crowding, some loss of polarity, pseudo-stratification and hyperchromatism. PanIN-3 lesions are characterised by a loss of nuclear polarity, severe nuclear atypia, occasionally abnormal mitoses, nuclear irregularities, prominent nucleoli and intraluminal necrosis [8]. Ultimately, the highest grade PanINs transform into PDAC, which is characterised by invasive growth and having a dense stroma of fibroblasts and inflammatory cells, called desmoplasia [2]. Compared with PanINs, MCNs and IPMNs are less common precursor lesions and macroscopically visible cystic neoplasms [9]. MCNs are mucinous epithelial cystic lesions in association with a distinctive ovarian-type stroma [10]. IPMNs are similar with PanINs at the cellular level and arise in the mucin-producing pancreatic duct where they enlarge the duct system by abundant mucin production and intraductal growth of the neoplasm [11]. Finally, these precursor lesions described above may evolve towards PDAC [12].

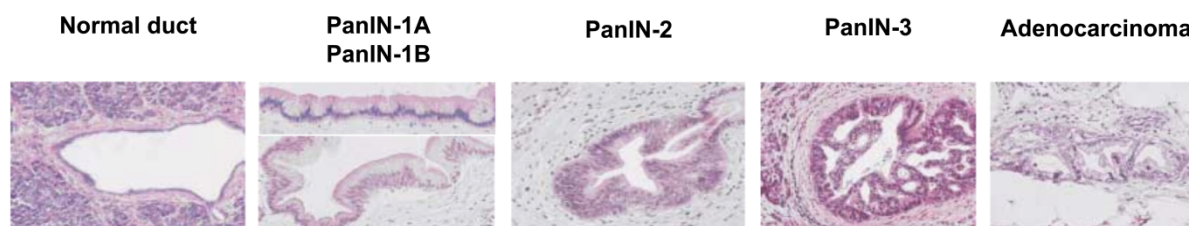


**Figure 1.1: Characterization of different stages of PanINs and PDAC.**

### 1.1.2 Molecular genetics of PDAC

Research into the molecular genetic mechanisms of pancreatic cancer revealed that the process towards PDAC involves oncogenes activation, loss of tumor suppressor genes, telomere shortening. For instance, KRAS (Kirsten rat sarcoma viral oncogene homolog) mutations, loss of CDKN2A (Cyclin-dependent kinase inhibitor 2A), TP53 (Tumour protein 53) and SMAD4 (SMAD family member 4), telomere shortening are confirmed to contribute to pancreatic carcinogenesis [5,13,14].

Activating oncogene KRAS mutations are the earliest genetic alterations observed in the progression series of PDAC. At least 99% of PanIN-1 lesions have shown KRAS mutations,

indicating its activation is a vital initial step in carcinogenesis of PDAC [15]. KRAS is a member of the RAS family and encodes a guanosine triphosphate (GTP)-binding protein that mediate a wide variety of cellular signaling pathway, such as proliferation, differentiation, cellular survival, motility, and cytoskeletal remodeling [16,17]. Ras protein cycles between an inactive GDP-bound form and active GTP-bound form [18]. In the inactive state, Ras is initially bound to GDP. Then this form is converted into the GTP bound form when GDP is removed from RAS, allowing GTP to bind, triggered by extracellular signaling through growth factor receptors. On the other hand, the active GTP-bound form is converted to the GDP-bound form when GTP is hydrolyzed by the intrinsic GTPase activity, which can be accelerated by GTPase activating proteins (GAPs) [2]. The KRAS activating mutations result in loss of the intrinsic GTPase activity of Ras protein and GTP cannot be hydrolysed into the GDP-bound form [19,20]. Therefore, the Ras protein remains always in the activated state and permanently activates downstream signaling events even in the absence of extracellular signals that may contribute to carcinogenesis [21]. KRAS is activated by point mutations and most often activating mutation in PDAC occurs in KRAS codon 12 resulting in amino acid substitution of glycine with aspartate [2,22,23]. In addition, there are also some other KRAS mutation in codon 15, 16, 18, 31, 59 and 61 found in the patients with adrenocortical tumours [24,25]. Activated KRAS leads to persistent stimulation of several downstream signaling pathways, for example: the phosphoinositide-3-kinase PI3K-AKT signaling pathway and RAF/mitogen-activated protein (MAP) kinase pathway that drive many hallmarks of the cancer [9,13,26].

The loss of function of the tumor suppressor gene CDKN2A, caused by mutation, deletion or promoter hypermethylation, occurs in 80-95% of sporadic pancreatic adenocarcinomas [27,28]. The CDKN2A encodes two tumor suppressors (p14/ARF and p16/INK4A) through different first exons and alternative reading frames in shared downstream exons. The vast majority of CDKN2A loss arises from the PanIN-2 stage. The protein p14/ARF stabilize tumour suppressor TP53 by inhibiting MDM2 (Mouse double minute 2 homolog). p16/INK4A act to inhibit CDK4/CDK6 mediated phosphorylation of retinoblastoma (RB), thus regulating the G1 checkpoint and blocking cells entry into the S (DNA synthesis) phase of the cell cycle.

p16/INK4A inactivation plays an important role in pancreatic carcinogenesis; and germline and sporadic mutations have been identified that target p16/INK4A, but spare p14/ARF.

The tumour suppressor gene TP53 acts to regulate many interrelated cellular processes including cell cycle progression, DNA repair and apoptosis [29,30]. Inactivation of TP53 through mutation is observed in more than 50% of pancreatic adenocarcinomas [28], and TP53 mutations mostly arise in later-stage PanIN-3 lesions [31]. Wild type TP53 acts like a tumor suppressor because it facilitates normal cell cycle progression by regulating the G1-S checkpoint and maintaining a G2-M arrest [32]. Thus, cells can be maintained in normal growth, genomic stability or induced to apoptosis in response to variety of cellular stresses [33]. Inactivation of TP53 facilitates rampant genomic instability and influences PTEN (Phosphatase and tensin homolog), which inhibits the AKT signaling pathway in pancreatic cancers [13]. In addition, TP53 inactivation in tumours may be associated with their aggressive biological behavior due to the finding that TP53 controls both growth and epithelial cell differentiation [34].

Another common alteration in pancreatic adenocarcinoma is the loss of SMAD4 observed in high-grade PanIN-3 lesions [35]. The loss of SMAD4 is achieved either by homozygous deletion or intragenic mutation with the loss of the second allele with a frequency of about 55% of pancreatic ductal adenocarcinomas [36]. SMAD4 encodes a transcriptional regulator that is an integral component of the TGF- $\beta$  signaling cascade, which plays an integral role in tumor initiation and progression [37,38]. There are three TGF- $\beta$  ligands (TGF- $\beta$ 1, TGF- $\beta$ 2 and TGF- $\beta$ 3), which can bind to serine/threonine kinase cell surface receptors type II and lead to phosphorylation of type I receptor. The type I receptor phosphorylates the downstream mediators SMAD2 and SMAD3 proteins. The phosphorylated SMAD2 and SMAD3 complexes together with SMAD4 enter the nucleus to regulate gene transcription involved in a variety of cellular processes including cell differentiation, cell cycle control and growth [39,40]. Inactivation of SMAD4 thus disrupts the TGF- $\beta$  signaling and the loss of SMAD4 is a key event in abrogating the TGF- $\beta$  mediated tumor cell growth and metastasis [41].

## 1.2 Animal models of pancreatic cancer

The therapeutic methods (such as surgery, chemotherapy, radiotherapy, or combinations of these) in PDAC remain poor in effect [4]. The development of animal models for pancreatic cancer is still the essential method to evaluate different strategies for treatment, early detection, chemoprevention and finally helping the patients to overcome pancreatic cancer. The reveal of the molecular genetic basis of PDAC, such as activation of KRAS and inactivation of the p16INK4A, TP53 and SMAD4 tumor suppressors, open an avenue to generate animal models to mimic human pancreatic cancer [42].

### 1.2.1 Mouse models of pancreatic cancer

Since the sophisticated ability to experimentally manipulate of mouse genome, mouse is widely used as the animal model for a series of human diseases [42–44]. The generation of mouse models for pancreatic cancer started as early as in 1987 [45,46], but the one model that has closest resemblance to human pancreatic cancer was established by Hingorani et al. in 2003 [47]. This mouse model has a KRAS<sup>G12D</sup> mutant allele blocked by inserting loxP floxed transcriptional stop cassette (LSL) into intron 1. Then LSL-KRAS<sup>G12D</sup> mice were further crossed with the mice expressing Cre recombinase under the control of pancreas specific promoter PDX-1 (Pancreatic and duodenal homeobox 1) or Ptf1a/P48 (pancreas-specific transcription factor 1a) to activate the KRAS<sup>G12D</sup> mutant allele. Such alteration in the compound mice showed all three stages of PanINs identical to the conditions in human. However, the low frequency of spontaneous development into invasive PDAC suggests that activation of oncogenic KRAS is not sufficient to induce the invasive stage of pancreatic adenocarcinoma. Therefore, multi-transgenic mouse models were generated to capture the progress to invasive and metastatic PDAC. A number of such multi-transgene mouse models have been generated, which combined PDX-1-Cre/LSL-KRAS<sup>G12D</sup> or Ptf1a/P48-Cre/LSL-KRAS<sup>G12D</sup> with deletions or mutations of p53 [48], Ink4 [49], Smad4 [50], Mist [51] or TGFβ [52] (Table 1.1). For instance, the PDX-1-Cre, LSL-KRAS<sup>G12D</sup>, LSL-Trp53<sup>R172H/-</sup> transgenic mouse model was generated by activation of both the KRAS<sup>G12D</sup> and Trp53<sup>R172H</sup> alleles only in mouse pancreas through interbreeding with PDX-1-Cre

transgenic animals. This mouse model showed the full spectrum of preinvasive lesions at ten weeks of age and developed differentiated PDAC afterwards. They showed dramatically shortened median survival of approximately 5 months, significantly less than PDX-1-Cre/LSL-Trp53<sup>R172H/-</sup>, PDX-1-Cre/LSL-KRAS<sup>G12D</sup> and wild type mice. Moreover, these triple mutant animals showed abdominal distension, cachexia, hemorrhagic ascites, and metastasis in the liver, diaphragm and adrenals, and all of them died before 12 months.

**Table 1.1: Mouse models of pancreatic adenocarcinoma**

Genotype	Time to tumor development (month)	Pancreatic cancer phenotype	Survival (month)
PDX-1-Cre; LSL-KRAS <sup>G12D</sup>	6	PDAC; penetrant PanIN; age dependent increase severity; occasionally PDAC with long latency	16
PDX-1-Cre; LSL-KRAS <sup>G12D</sup> ; LSL-Trp53 <sup>R172H</sup>	2-3	PDAC; Accelerated PanIN; well differentiated PDAC	5-6
PDX-1-Cre; KRAS <sup>G12D</sup> ; Ink4a/Arf <sup>fllox/fllox</sup>	2	PDAC; accelerated development of PanIN; poorly differentiated PDAC	2-3
PDX-1-Cre; KRAS <sup>G12D</sup> ; Smad4 <sup>fllox/fllox</sup>	2-3	IPMN; PDAC	2-6
P48 <sup>Cre/+</sup> ; LSL-KRAS <sup>G12D</sup>	8	PDAC; penetrant PanIN; age dependent increase severity; occasionally PDAC with long latency	16
Ptf1a <sup>Cre/+</sup> ; LSL-KRAS <sup>G12D</sup> ; Tgfb <sup>fllox/fllox</sup>	1	PDAC; accelerated PanIN; PDAC development	2
Mist1 <sup>KRASG12D/+</sup>	2	Accelerated development of acinar-derived PanIN; mixed subtypes pancreatic cancer	10.8

PDAC: Ductal adenocarcinoma of the pancreas; PanIN: Pancreatic intraepithelial neoplasia; IPMN: Intraductal papillary mucinous neoplasia

## 1.2.2 Pigs as model in biomedicine

In spite of huge progress of generating a wide range of mouse models for various human diseases, mice still have limited value for preclinical studies due to their considerable differences from human in size and lifespan [53]. However, the pig is an animal very similar to human in terms of size, anatomy, genetics and physiology [54]. More specifically, from genetical point of view, the size and the composition of the porcine genome are comparable to that of human; in terms of physiology, both pigs and human are omnivorous and their organs generally share common functional features. Therefore, nowadays pigs are widely used as

models in biomedicine research e.g. xenotransplantation [55], cancer [56,57], diabetes [58], cardiovascular disease [59], atherosclerosis [60], cutaneous pharmacology [61], wound repair [62], ophthalmological studies [63] and toxicology research.

### **1.3 Genetically modified (GM) animals**

A genetically modified animal is an animal whose genetic material (DNA) has been altered by using genetic engineering techniques, and which does not occur naturally by mating. So far, genetically altered animals have been produced in a wide range of species (Table 1.2).

Transgenic vertebrates have been produced in species with both scientific and commercial value including fish, amphibians, birds, and mammals. While transgenic invertebrate species mainly include some model organisms such as the arthropod fruit fly *Drosophila melanogaster*, and the nematode *Caenorhabditis elegans*, and organisms with commercial value including dwarf surfclams, eastern oysters and the Japanese abalone [64]. For mammals, transgenic animals are being generated mainly for two distinct fields of applications: agriculture and human medicine. During the past few decades, genetically modified mammals have been produced mainly based on methods which can be divided into 3 categories: direct transgenesis, cell-mediated transgenesis and genome editing.

#### **1.3.1 Direct transgenesis**

Direct transgenesis methods include DNA microinjection, sperm mediated gene transfer, transposon-mediated DNA transfer, viral transduction.

DNA microinjection: DNA microinjection is a popular and most direct method for creating transgenic animals. By this method, a very fine glass pipette is used to manually inject exogenous DNA into the eggs. In 1974, Jaenisch and Mintz microinjected the simian virus 40 (SV40) viral DNA into explanted mouse blastocysts and generated the first transgenic mice [65]. Later, Gordon et al. microinjected a recombinant plasmid composed of segments of herpes simplex virus and simian virus 40 viral DNA into pronuclear of fertilized mouse oocytes and also obtained the transgenic mice [66]. This approach was subsequently extended into

livestock to generate transgenic rabbits, sheep and pigs [67]. Although this method is straightforward, it has several limitations. First of all, it always leads to transgenic DNA randomly integrated into host genomic DNA. Thus, host genomic DNA close to the site of integration often undergoes various forms of sequence deletion, duplication or rearrangement as a result of transgene incorporation. If such alteration is sufficiently drastic, it may disrupt the function of host genes at the integration site and constitute insertional mutagenesis, causing an aberrant phenotype. It is also inefficient, with approximately 1-4% of injected eggs resulting in transgenic offspring among different species [68–70].

**Table 1.2: A part of reported transgenic animals in some species.**

Species	References
<b>Mammals</b>	
Mice ( <i>Mus musculus</i> )	Gordon et al. (1980), Joyner and Sedivy (2000), Vintersten et al. (2004) Muzumder et al.(2007), Armstrong et al. (2010)
Rats ( <i>Rattus rattus</i> )	Hamra et al. (2002), Kato et al. (2004), Hirabayashi et al. (2005), Agca et al. (2008)
Rabbits ( <i>Oryctolagus cuniculus</i> )	Fan and Watanabe (2003), Flisikowska et al. (2011), Song et al. (2013)
Sheep ( <i>Ovis aries</i> )	McCreath et al. (2000), Denning and Priddle (2003), Wheeler (2003)
Pigs ( <i>Sus domestica</i> )	Lai et al. (2002), Houdebine (2009), Kragh et al. (2009), Yang et al. (2011), Luo et al. (2011), Leuchs et al. (2012), Flisikowska et al. (2012), He et al. (2013), Ye et al. (2013)
Cattle ( <i>Bos taurus</i> )	Donovan et al. (2005), Richt et al. (2007), Houdebine (2009)
Goats ( <i>Capra hircus</i> )	Wheeler (2003), Houdebine (2009)
Dogs ( <i>Canis familiaris</i> )	Hong et al. (2009) Sasaki
Marmosets ( <i>Callithrix jacchus</i> )	Sasaki et al. (2009)
Rhesus monkeys ( <i>Macaca mulatta</i> )	Yang et al. (2008), Yuyu et al. (2010)
<b>Birds</b>	
Chickens ( <i>Gallus gallus</i> )	Mozdziak and Petite (2004)
Japanese quail ( <i>Coturnix japonica</i> )	Huss et al. (2008)
<b>Amphibians</b>	
Frogs ( <i>Xenopus laevis</i> and <i>Xenopus tropicalis</i> )	Macha et al. (1997), Sinzelle et al. (2006), Ishibashi et al. (2008)
<b>Fish</b>	
Zebra fish ( <i>Danio rerio</i> )	Zelenin et al. (1991), Davidson et al. (2003), Huang et al. (2008)
Goldfish ( <i>Carassius auratus</i> )	Houdebine and Chourrou (1991), Wang et al. (1995)
Nile tilapia ( <i>Oreochromis niloticus</i> )	Martinez et al. (2000), Maclean et al. (2002), Hrytsenko et al. (2009)
Carp ( <i>Cyprinus carpio</i> )	Yoshizaki et al. (1991)
Channel catfish ( <i>Ictalurus punctatus</i> )	Dunham et al. (2002)
Atlantic salmon ( <i>Salmo salar</i> )	Sin et al. (2000), Houdebine (1997)
<b>Invertebrates</b>	
Arthropod fruit fly ( <i>Drosophila melanogaster</i> )	Rubin and Spradling (1982), Fujioaka et al. (2000)
Nematode ( <i>Caenorhabditis elegans</i> )	Fire (1986), Mello et al. (1991)
Mollusk Japanese abalone ( <i>Haliotis diversicolor suportexta</i> )	Tsai et al. (1997)
Mollusk Eastern oyster ( <i>Crassosostrea virginica</i> )	Cadoret et al. (1997)
Mollusk dwarf surfclam ( <i>Mulinia lateralis</i> )	Lu et al. (1996)

Sperm mediated gene transfer (SMGT): SMGT as a method to obtain transgenic mammals was firstly established using sperm cells as vectors for introducing foreign DNA into mouse eggs [71]. This method was also applied in rats, rabbits and pigs with efficiencies around 50-80% [72–75]. However, this method has undergone considerable problems of reproducibility. It also reported that transgenes introduced by using this way frequently suffer rearrangement [76].

Transposon-mediated DNA transfer: Transposons are natural mobile genetic elements of genomes. Based on the different transposition mechanism, transposons can be categorized into two groups: class I transposons (retrotransposons), which use copy-and-paste mechanism via RNA intermediate; class II transposons (DNA transposons), which transpose through a cut-and-paste mechanism. Generally, DNA transposons are used for genetic engineering because they can direct the integration of a transgene [77]. Transposon systems have been extensively used for developing methods of human gene therapy and identifying oncogenes in mice, while they are less frequently used in large genetically modified animals [78].

Viral transduction: Two types of retroviral vectors have been developed for producing transgenic animals: vectors derived from the genome of prototypic retrovirus (such as MLV) and vectors derived from the genome of a more complex retrovirus (such as lentiviruses) [68]. By using retroviral vectors based on prototypic retroviruses, transfer of foreign genes into animal genome has already been accomplished [79]. Although embryos can be infected with retroviruses up to midgestation stage, oocytes to 16 cell stage are frequently used for infection with recombinant retroviruses containing foreign genes of interest [80]. After infection, the entered retroviral RNA reverse transcribed into DNA in cells and the integration of the DNA provirus into the host genome is mediated by specific nucleotide sequences at the ends of the retroviral genome and the retroviral integrase [81–83]. However, this method has some limitations, for example: the transgenes transferred by a retroviral vector can be silenced in the transgenic animal [84]; completion of infection process requires that the host cells are undergoing the S phase of cell cycle, causing effective retrovirus infection only in mitotically active cells [80]; the retroviral long-terminal-repeats can interfere with mammalian promoters



to misdirect or suppress host gene expression [68]; it is difficult to package a gene of more than 10 kb size because of the small size in volume of such prototypic viruses [68]. Yet, the development of lentiviral vectors brings a breakthrough in using viral vectors to generate transgenic animals [85,86]. There are some improvements of lentiviral vectors, such as, lentiviral vectors have been developed with incorporated enhancer elements to increase the expression of transgenes; viral enhancer and promoter sequence within the retroviral long-terminal-repeats (LTRs) have been deleted and replaced by tissue specific promoter or ubiquitous promoter sequences to reduce the effect of misregulating host genes by the viral LTRs [87–89]; some lentiviral vectors even carry tetracycline regulatable transgenes to regulate the expression of the transgene is desired [90]. Therefore, lentiviral transgenesis is one of the most efficient methods for generating transgenic animals due to their capacity for infecting a large spectrum of host cells and cells at different cycle stages. By using this method, a range of transgenic animals, such as mouse, rat, pig, cattle and chicken, have been successful generated [87,91–95].

### **1.3.2 Cell-mediated DNA transfer**

Transgenic animals can also be generated via the method of cell-mediated DNA transfer. By using this method, it requires that the transgenic cells can be used either for chimera formation or somatic cell nuclear transfer (SCNT). Cell-mediated DNA transfer is widely used for precise genetic modification through gene targeting which is based on the mechanism of homologous recombination (HR). HR represents the precise way to engineer the genome because defined changes can be introduced into specific genomic loci while leaving the rest of the genome unperturbed (Figure 1.2) [96,97]. Gene targeting by HR is a powerful tool to precisely manipulate the genome for a wide range of purposes [98–101]. For gene targeting, the targeting DNA can integrate into the genome of the cells through two possible ways: random integration and HR [102]. In mammalian somatic cells, gene targeting by homologous recombination is a very rare event because for every 1 gene targeting event, there will be  $10^5$  to  $10^7$  random integrants [103]. However, the relative rate of gene targeting in mouse ESCs is 10-100 fold higher than that found in mammalian somatic cells [102]. Thus, genetically

manipulated mouse ES cells were often injected into blastocysts, and then the injected embryos can be implanted into a foster mother to generate chimeric mice. As there are no confirmed ES cells in pig, the somatic cell nuclear transfer (SCNT) was widely used for the generation of transgenic pigs. SCNT is a technique in which the nuclei of somatic cells are transferred into enucleated oocytes, thereby reprogramming future development (Figure 1.3). SCNT can be used to generate genetically engineered animals by using modified donor cells [104].

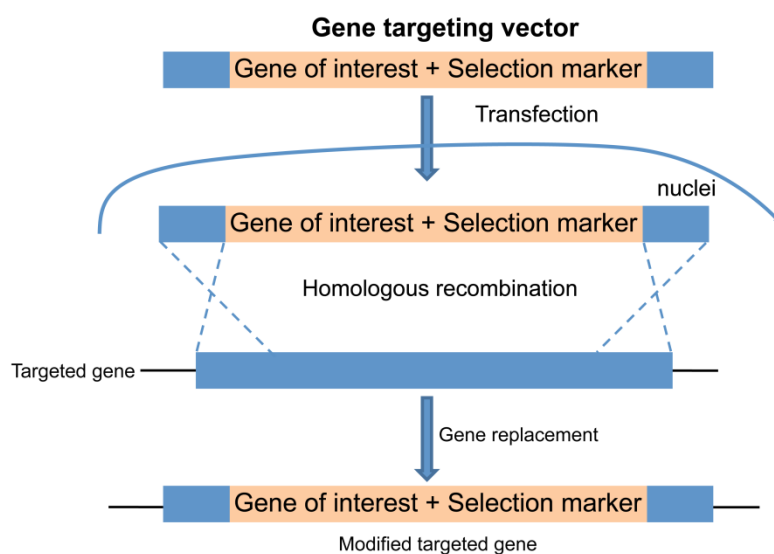


**Figure 1.2: Schematic of gene targeting via HR.** The gene targeting vector contains left and right homologous arms which are designed according to the targeted gene. When extracellular DNA is transfected into cells, gene replacement occurs by homologous recombination.

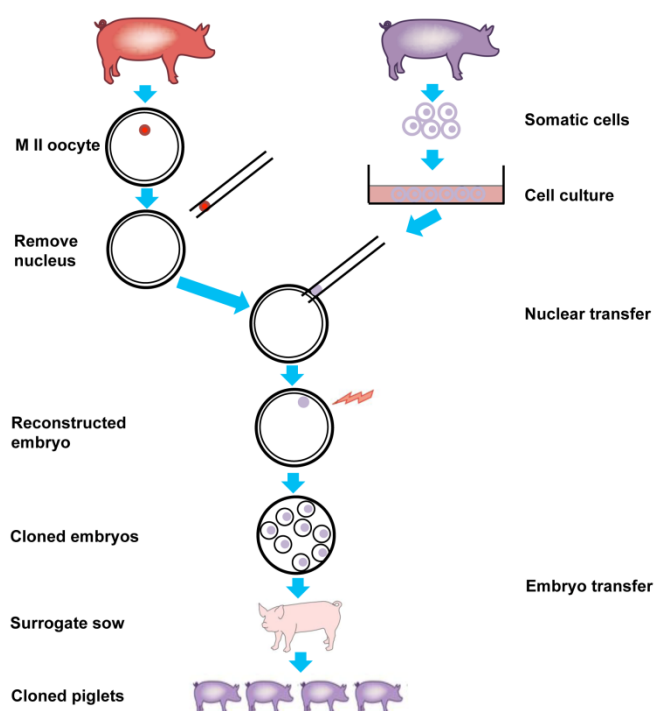


**Figure 1.3: Schematic diagram of SCNT.** A matured oocyte derived from oocyte donor pig is enucleated and then the nuclear from somatic cells of nuclear donor pig is transferred into enucleated oocyte. After electrofusion, reconstructed embryos are activated and cultured in vitro. Then, the embryos can be implanted into a surrogate sow to generate cloned animals.

The technique of somatic cloning in mammals was established by using blastomeres from early stage embryos as donor cells in the 1990s [105]. “Dolly” the sheep, as the landmark report in 1997, was the first mammal cloned using SCNT [106]. Subsequently, human factor IX transgenic sheep was also produced by nuclear transfer [107]. Afterwards, SCNT was rapidly extended to generate transgenic goats, cattle and pigs [108–112]. Therefore, with nuclei obtained from either mammalian stem cells or differentiated adult cells, SCNT is an especially important development in species beyond the mouse model. In particular, this technology allows to obviate the difficulties in identifying and isolating pluripotential domestic animal stem cells [80]. In addition, if all of the donor cells are transgenic, the offspring via SCNT are 100% transgenic.

### 1.3.3 Genome editing

Genome editing is a method that DNA is removed, inserted, or replaced from a genome by using artificially engineered site-specific nucleases. Those site-specific nucleases allow precise and efficient genetic modification by inducing targeted DNA double-strand break (DSBs) that stimulate the non-homologous end joining (NHEJ) and HR. Three recent engineered nucleases, including customised zinc finger nucleases (ZFN), transcription activator-like (TAL) effector nucleases (TALENs), and clustered regularly interspaced short palindromic repeats/CRISPR associated endonuclease cas9 (CRISPR/Cas9) have been widely used in several organisms [113–119].

Taking TALENs as an example, TAL effectors (TALEs) were discovered from the plant pathogenic bacteria genus *Xanthomonas* and composed of N- and C-termini for localization and activation, and DNA-binding domains (Figure 1.4) [120–122]. The DNA binding domain consists of a series of 33-35 amino acid repeats that each recognizes a single base pair [123]. Each amino acid repeat is highly conserved except for two variable amino acids at positions 12 and 13 which convey the specific DNA-binding properties (Figure 1.4) [124]. Usually, the

end of the tandem repeat region is truncated and referred to as a “half repeat” [123]. A specific TALEN is created by fusing the functional endonuclease *FokI* with TALEs. As *FokI* works in a dimeric way, therefore, a pair of TALENs is required to make a cut at a specific site of the genome [121,125–127]. A pair of designed TALENs binds to targeted DNA sequences flanking a spacer sequence (usually 14-18 bp), where the *FokI* heterodimerization forms (Figure 1.5). The dimeric *FokI* then cuts in the spacer DNA region, causing a double strand DNA break (DSB). DSB can be repaired by NHEJ or HR pathway (Figure 1.6). By NHEJ pathway, it often generates small insertions and/or deletions (indels), a useful means of inactivating a chosen gene. DSBs can stimulate HR pathway in the presence of homologous donor DNA, enabling insertion of an exogenous DNA sequence into a specified chromosomal locus [119,128,129].

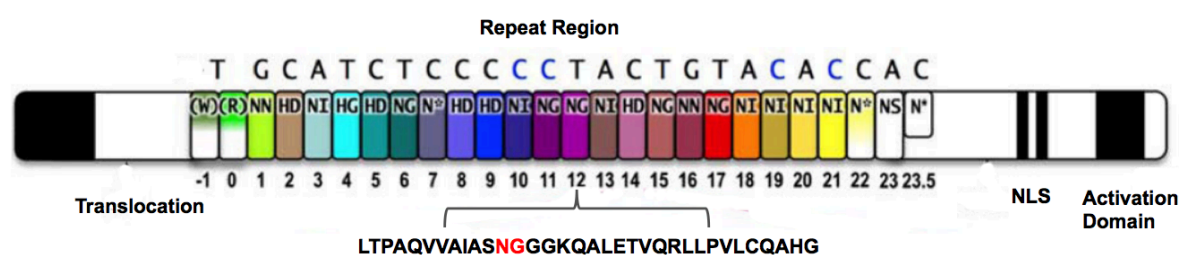


**Figure 1.4: Structure of TAL effectors.** Top, TAL effectors contain a N-terminal translocation domain, a tandem repeats region for recognizing targeted nucleotide sequence, a nuclear localization signal (NLS) and C-terminal region for transcriptional activation. Below, Individual TALE repeats contain 34 amino acids that recognize a single base pair via two repeat variable diresidues (RVDs) at position 12-13.

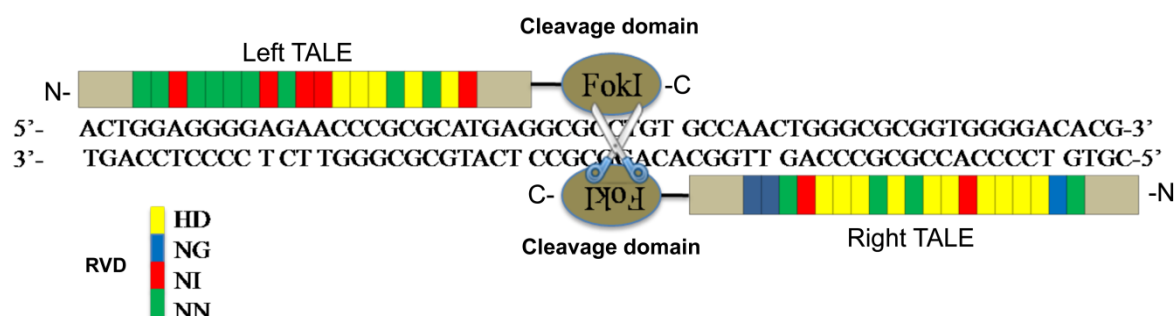


**Figure 1.5: Schematic of a pair of TALE nuclease (TALEN) dimer bound to DNA sequence.** A pair of TALENs binds on a targeted DNA sequence, allowing *FokI* dimerisation. Cleavage by the *FokI* nuclease domains occurs in the spacer sequence that locates between the two TALE DNA binding sites.

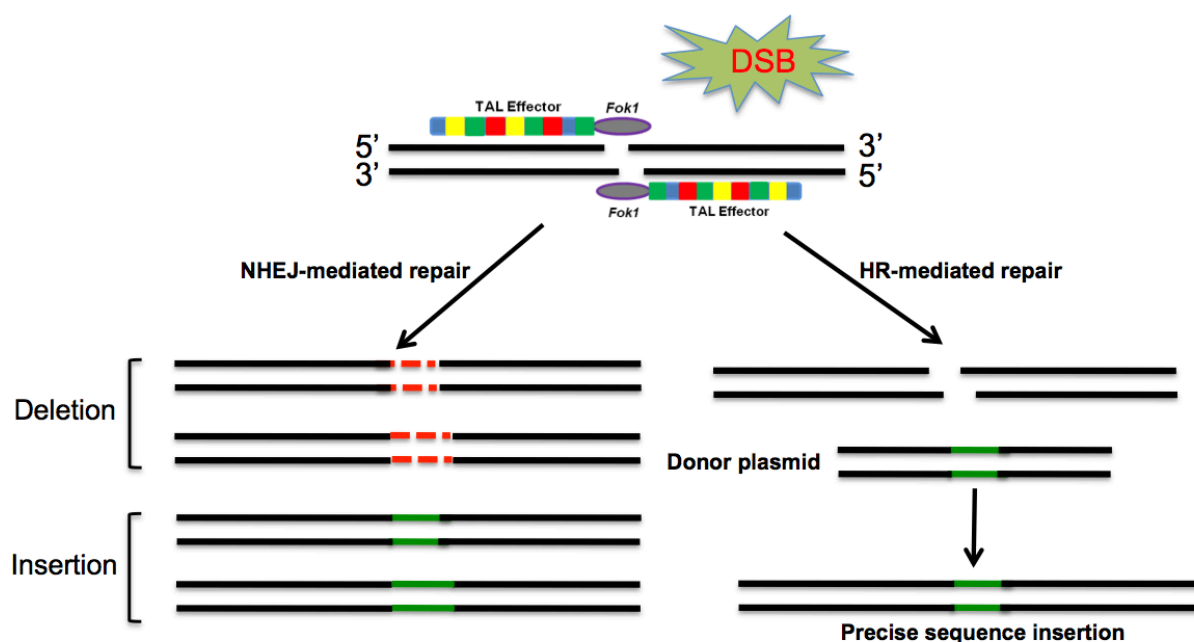


**Figure 1.6: DNA repair pathways after a nuclease-induced DNA double-strand breaks (DSBs).** In the absence of donor template, the DSBs is repaired by error-prone non-homologous end joining (NHEJ), yielding small insertion or deletion (indel) mutations at the targeted DNA sequence. In the presence of donor template with extended homology arms, DSB can be repaired by homologous recombination (HR), which lead to insertion of precise DNA sequences.

### 1.3.4 Gene-targeted animals

Gene targeting, defined as the introduction of site-specific modification into the genome by homologous recombination, paved the way towards the analysis of mammalian functional genomics [130]. Smithies et al [131] was first reported gene targeting in mammalian cells for the human  $\beta$ -globin gene. In 1981, two groups reported murine embryonic stem cells (ESCs) isolated from the inner cell mass of blastocysts [132,133]. Since the rapid development of murine embryonic stem cells (ESCs) technology, the combination of gene targeting with ESCs allows to generate targeted mice conveniently (Figure 1.7) [134]. The first successful gene targeting in murine ESCs was achieved for the selectable hypoxanthine phosphoribosyl transferase (HPRT) gene locus [135,136]. Subsequently, targeting of non-selectable genes, such as *c-abl* and *int-2*, also reported after development of strategies for homologous recombination [137,138]. Isolation of ES cells from humans, monkeys and rats has been successfully achieved [139–141], but isolation of ES cells from livestock species has made

limited progress. Although, embryo-derived pluripotent cell lines have been reported in cattle and pig, successful germ-line chimeric offspring have not yet been reported [142]. The failure of ES cell isolation has hampered development and applications of gene targeting technologies in livestock animals. Combining gene targeting with SCNT has opened the avenue for targeted genetic manipulations of domestic animals (Figure 1.7). McCreath et al. [143] reported the first gene targeted large animal which was produced by placing a therapeutic transgene at the ovine alpha1(I) procollagen (COL1A1) locus. Subsequently, other gene targeted large animals, such as rabbit, pig and cattle, were reported as well [55,113,144,145].

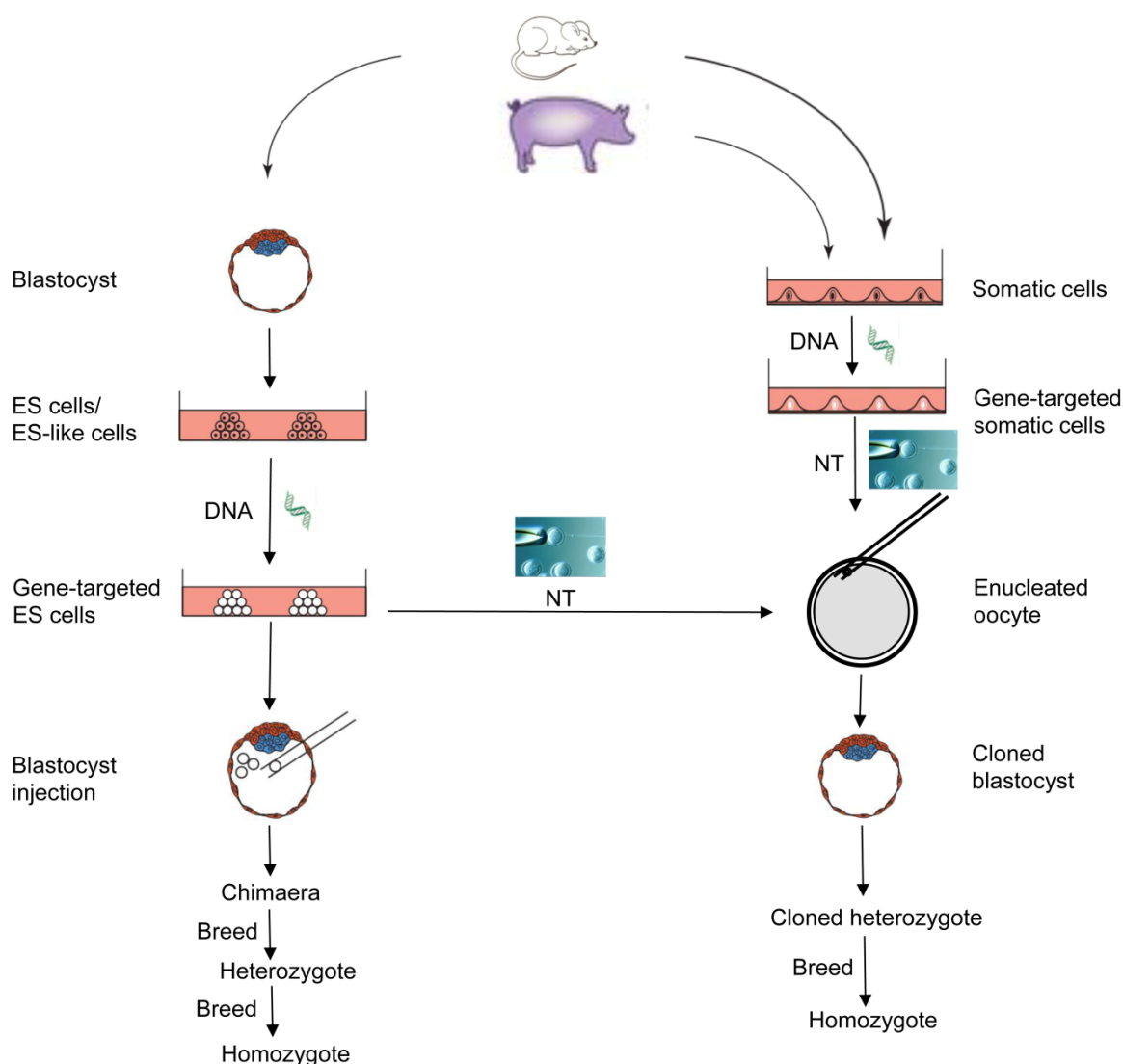


**Figure 1.7: Schematic of gene targeting in mice and livestock.** For mice, gene targeted embryonic stem (ES) cells can be either injected into blastocyst or used for nuclear transfer (NT) to generate gene-targeted mice. While ES cells isolated for domestic animals has limited progress, thus gene

targeted and nuclear transfer (NT) are combined to produce gene-targeted livestock.

### 1.3.5 Gene-targeted pigs

The first gene targeted pig, carrying heterozygous knock-out of  $\alpha$ -1,3-galactosyltransferase (GGTA1) gene, was generated for xenotransplantation to avoid hyperacute rejection (HAR) in pig-to-human transplantation [55,144]. Shortly after, a homozygous GGTA1 knock-out pig was produced [146], which provide a potential resource for xenotransplantation experiments. The first gene targeted porcine disease model was established for studying cystic fibrosis (CF). CF is an autosomal recessive disease caused by mutations in the gene expressing the CF transmembrane conductance regulator (CFTR). The most common mutation is a deletion of a phenylalanine residue at amino acid position 508 ( $\Delta$ F508) of the protein [147]. CFTR expressed predominantly in epithelia is an anion channel [148]. Previously created CF mouse models failed to develop the lung and pancreatic disease that cause most of the morbidity and mortality in humans with CF [149,150]. Therefore, gene targeted pigs were generated with the CFTR gene either disrupted or containing the most common CF associated mutation ( $\Delta$ F508) [148]. The homozygous CFTR gene knock out pigs were further bred, which showed replicating abnormalities seen in newborn patients with CF [151]. The first gene-targeted pigs for cancer were produced by inactivating breast cancer associated gene 1 (BRCA1) causing predisposition to breast cancer using adeno-associated virus-mediated method [152]. Our chair is also engaged in generating a series of human cancer and cancer predisposition models in pigs. So far, we have reported the first gene-targeted 'oncopigs' which are carrying truncated mutations in the adenomatous polyposis coli (APC) gene at sites orthologous to germ line mutations responsible for an inherited form of colorectal cancer, familial adenomatous polyposis (FAP) [57]. We have also produced gene-targeted pigs carrying a conditionally activated mutant form of the key tumour suppressor p53,  $TP53^{R167H}$ , orthologous to mouse  $Trp53^{R172H}$  and human  $TP53^{R175H}$ , to model Li-Fraumeni syndrome and other cancers [153].

### 1.3.6 Cre/loxP system

The Cre recombinase of the P1 bacteriophage is a 38.5 kDa protein and belongs to the integrase family of site-specific recombinases [154,155]. It can efficiently catalyze the recombination between two of its consensus 34 base pair DNA recognition sites (loxP sites) which consists of a core spacer sequence of 8 bp and two 13 bp palindromic flanking sequences (Figure 1.8) [156]. The orientation of the loxP site was defined by the asymmetric core sequence. Each 13 bp inverted repeat serves as a binding site for the recombinase, whereas the 8 bp spacer region participates in strand exchange during the recombination reaction. The Cre/loxP recombination system requires no additional sequence elements or co-factors for efficient recombination [157]. The postrecombination loxP sites are formed from the two complementary halves of the prerecombination sites. Cre recombinase can induce deletion, inversion or chromosomal translocation events depending on the orientation and location of the loxP sites (Figure 1.9) [157]. DNA flanked by two loxP sites with the same direction is deleted upon recombination, whereas DNA flanked by two loxP sites with the opposite direction is inverted upon recombination. Cre recombinase mediates a chromosomal translocation if the loxP sites are located on different chromosomes [158]. Since the Cre/loxP system has been successfully applied in mammalian cells and *in vivo*, it became a powerful tool for the generation of conditional gene activation and knock out [159,160]. Nowadays, our chair is extending the Cre/loxP system to pigs.

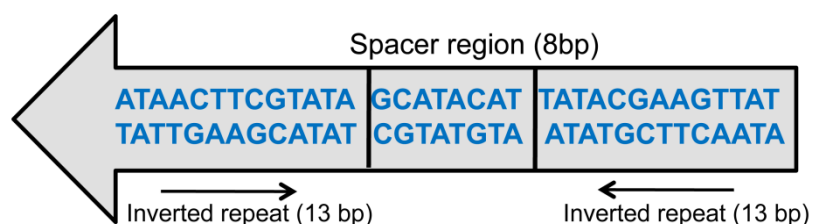


**Figure 1.8: Wild-type loxP sequence.** The loxP site contains an asymmetric 8 bp spacer region flanked by 13 bp inverted repeats where the Cre recombinase can recognize and bind to.



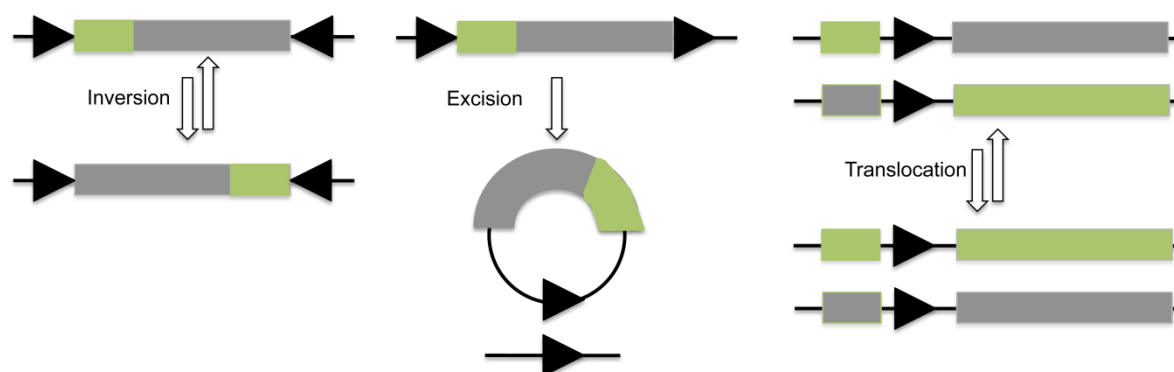


**Figure 1.9: The Cre/loxP recombination system.** Cre mediated inversion, excision and translocation recombination events between two loxP sites, which depends on the direction and location of two loxP sites.

## 1.4 Reporter animal strains

### 1.4.1 Reporter genes

Reporter genes refer to certain genes with a readily measurable phenotype that can be easily distinguished from a background of endogenous proteins [161]. Generally, reporter genes are chosen based on the sensitivity, dynamic range, convenience, and reliability of their assay [161–163]. Here reporter protein shall be classified into two categories: non-fluorescent proteins and fluorescent proteins.

#### Non-fluorescent proteins

**Chloramphenicol acetyltransferase (CAT):** CAT is a bacterial enzyme and the first reporter gene used to monitor transcriptional activity in cells [162]. Chloramphenicol, an inhibitor of prokaryotic protein synthesis, can be detoxified by CAT through catalyzing the transfer of acetyl groups from acetyl CoA to the 3'-hydroxyl-position of chloramphenicol. This enzyme is stable [164,165] and no endogenous expression is detected in mammalian cells. Although an automated ELISA has been developed, facilitating its application, the sensitivity of this assay is still not as high as for other reporters [162,166].

**$\beta$ -galactosidase:** The lacZ gene, which encodes  $\beta$ -galactosidase, is a well-characterized bacterial enzyme and one of the most commonly used reporter genes in molecular biology

[167].  $\beta$ -galactosidase can catalyze the hydrolysis of X-Gal and produce a blue product, which can be easily visualized. Therefore, it has the advantage over CAT because the assays tend to be simple.

### Fluorescent proteins

Green fluorescent protein (GFP): The GFP from the jellyfish, *Aequorea victoria*, discovered in 1962 by Shimomura [168], is a protein composed of 238 amino acid residues (26.9 kDa) that exhibits bright green fluorescence when exposed to light in the blue to ultraviolet range [169,170]. Its discovery triggered a hot research interest in the structure, biochemistry, and biophysics of GFP-like fluorescent proteins, which resulted in an avalanche of scientific reports about fluorescent proteins and their applications to solve a series of basic issues in molecular and cell biology [171]. GFP and its variants, such as enhanced yellow (EYFP) and enhanced cyan (ECFP), have been developed and are nowadays used in a wide range of areas [4,5]. GFP has become well established as a marker of gene expression in cell and molecular biology [173]. In 1997, Okabe et al. [174] generated the first 'green mouse', which expressed enhanced green fluorescent protein (EGFP) driven by a CAG promoter (chicken beta-actin promoter combined with the cytomegalovirus enhancer element). The successful generation of such 'green mice' suggested that EGFP expression is non-toxic in mouse. Variants of green fluorescent protein (EYFP and ECFP) were also rapidly used in mice for living imaging [175,176]. Later GFP and its variants were also applied in other species such as pig [177,178].

Red fluorescent protein (RFP): The emission spectra of GFP variants (YFP and CFP) are very close and it is difficult to visually differentiate between them with readily available imaging systems [179]. In addition, a double reporter system is often required to establish reporter strains; therefore, easily identifiable, spectrally distinct colors, such as red, had to be developed. Over the past few years, a number of RFPs that emit orange, red and far-red fluorescence have been discovered from anthozoans (corals), and are available for a wide range of biological applications [171,180,181]. The first RFP isolated from *Discocoma sp.* was DsRed1 [182]. Hadjantonakis et al. [183] tried to generate a DsRed1 transgenic mouse but

failed to establish this line, which indicated that DsRed1 was not developmentally neutral or that constitutive transgene expression may not be sustained. Because DsRed1 has slow maturation times and poor solubility, improvements were made for DsRed1 to generate the mutant DsRed S197Y [184]. DsRed S197Y is brighter and essentially free from the secondary fluorescence peak, which makes it an ideal reporter for double labeling with GFP. A further improved DsRed variant, DsRed.T3, was produced through random mutagenesis [185]. Vintersten et al. [186] generated an Z/RED ES cell line and the corresponding transgenic reporter mouse, which expresses  $\beta$ -geo before Cre recombination and DsRed.T3 after Cre excision. These transgenic reporter mice developed normally and DsRed.T3 expression was inherited by their offspring at expected Mendelian ratios. As DsRed.T3 can form multimers, a series of monomeric RFP were generated subsequently. Campbell et al. [187] generated the first actual monomeric RFP, monomeric RFP 1 (mRFP1), which was later used for examining the expression of native mRFP1 in ES cells and its germline transmission [188]. They found that mRFP1 expression in a wide range of tissues is compatible with normal development and fertility in mRFP1 transgenic mice. Now, many monomeric RFPs improved from DsRed or other fluorescent proteins are available and are also widely applied in biology [171] and transgenic reporter strains. Two examples are monomeric cherry (mCherry) and tandem dimer Tomato (tdTomato). mCherry, which is brighter, matures faster, and has higher photostability than mRFP1, has been already used to generate ubiquitous mCherry transgenic reporter lines [189–193]. tdTomato exhibits a short maturation time, greater brightness and folds equivalently to a monomer, which may minimize toxicity when used in transgenic reporter strains [194].

#### **1.4.2 Random reporter strains**

Reporter animal lines can be generated through two main ways to introduce exogenous genes into animal genome: random transgenesis and targeted transgenesis by homologous recombination.

In mice, a series of random reporter mice have been generated by random transgenesis. Exogenous DNA with a promoter-cDNA cassette is either introduced into mouse ES cells via

transfection or micro-injected directly into zygotes [66,183]. Choosing an appropriate promoter is one of the crucial factors for the successful random transgenesis. The most commonly used promoter for ubiquitous expression of a transgene is the CAG promoter [195]; but some studies showed that the CAG promoter might cause non-ubiquitous or sometimes even silencing of transgenes [196,197]. Other promoters, such as the human ubiquitin C (UBC) promoter [190,198] and the *ROSA26* promoter [199], are also used for inducing widespread expression of transgenes. Since both UBC and the *ROSA26* promoter are derived from endogenous genes, the expression activities are lower than the CAG promoter [200]. But the UBC promoter and *ROSA26* promoter with genomic insulators show a more ubiquitous expression of the transgene than the CAG promoter according to recent publications [197,201].

### **1.4.3 Mouse Cre reporter strains**

Along with the wide application of the Cre/loxP system in experimental genetics, it has now become possible to generate conditional genome alterations that are spatially and temporally restricted or activated by combining this system with random transgenesis technologies [202,203]. Double reporter system was developed based on the Cre/loxP system. In the double reporter system, a first reporter gene flanked by two loxP sites with the same direction can be expressed prior to Cre recombination, then a second reporter gene after Cre recombination. A series of double reporter constructs have been widely used for generating double reporter mice, such as CAG-CAT-Z (chloramphenicol acetyltransferase/lacZ) [204], Z/EG (lacZ/EGFP) [205], Z/AP (lacZ/ human alkaline phosphatase) [206] *et al.* Those Cre random reporter mice are capable of monitoring Cre activity in diverse tissues and cell types. However, when used in the random integration method, those reporter strains showed some drawbacks. Firstly, the expression patterns of reporter lines vary due to different copy numbers and positional effects of the integration sites [207] and the inserted gene can be subject to gene-silencing effects in later offspring [134]. Secondly, it is not easy to choose a suitable reporter line for one's research among the many transgenic lines that have been established in different laboratories and assessed under different standards [208]. Furthermore, reporter mice that show high expression of the fluorescent reporter are often

infertile or not viable [209]. In order to overcome these issues, the ubiquitously expressed *ROSA26* locus was used to generate genetically modified reporter strains [210].

#### 1.4.4 *ROSA26* locus

Friedrich *et al.* [211] introduced several promoter trap constructs containing fusion lacZ-neo gene ( $\beta$ -geo) into mouse ES cells by electroporation or retroviral infection. Embryos from gene-trap line *ROSA $\beta$ -geo* (reverse orientation splice acceptor  $\beta$ -geo) 26 showed ubiquitous  $\beta$ -galactosidase ( $\beta$ -gal) expression during embryonic development. Zambrowicz *et al.* [210] later reported that in that mouse line the gene-trap vector was integrated into a gene with unknown function. This gene was subsequently named *ROSA26*. In mouse the *Rosa26* gene is located on chromosome 6 between *THUMPD3* and *SETD5* genes. It has 3 non-coding transcripts (NR\_027008.1, NR\_027009.1 and NR\_027010.1). *ROSA26* transcripts 1 and 2 contain 2 exons and 1 intron, while transcripts 3 is tail-to-tail overlapping (3' to 3') with *THUMPD3* gene containing 3 exons (Figure 1.10). The mouse *ROSA26* locus shows ubiquitous transcriptional activity and loss of this gene is not lethal [210]. The ubiquitous transcriptional activity of this locus indicates that the genomic region is not affected by chromatin configurations which may cause transcriptional repression of exogenous transgenes. Therefore, this locus is widely used as a permissive site for targeted placement of transgenes in mice [212,213], with no effect on animal viability or fertility. In mice, transgenes have been introduced into the *XbaI* site in the first intron of the *ROSA26* forward transcript where the presence of a splice acceptor allows the transgene expression to be driven by the ubiquitously expressed endogenous promoter [200]. Irion [214] and Kobayashi [215] demonstrated ubiquitous expression of red-fluorescent protein cDNA, after integration into the human and rat homolog of the mouse *ROSA26* locus through homologous recombination, indicating that the human and rat *ROSA26* locus conserve properties of its orthologue in mouse.

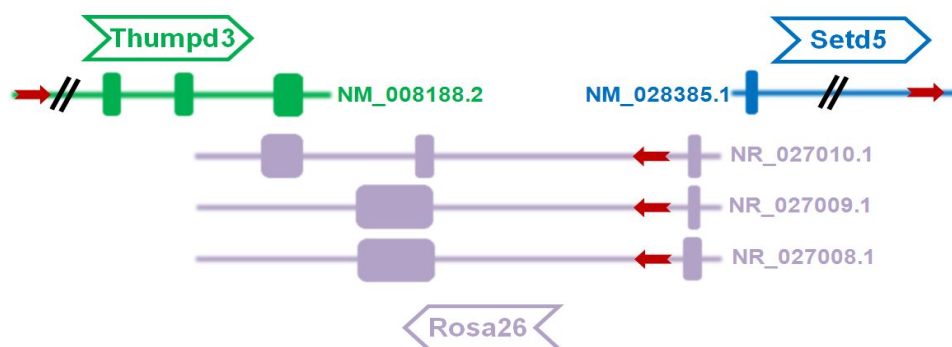


**Figure 1.10: Mouse *Rosa26* genomic locus and its adjacent genes (*Thumpd3* and *Setd5*) on chromosome 6.** The red arrowheads indicate the transcriptional orientation of *Rosa26*, *Thumpd3* and *Setd5* and genes are shown with exons and introns. Mouse *Rosa26* has three transcripts (Accession number: NR\_027008.1, NR\_027009.1 and NR\_027010.1) and the transcript NR\_027010.1 contains three exons and two introns. The third exon of NR\_027010.1 is tail-to-tail overlapping (3' to 3') with *Thumpd3* gene.

#### 1.4.5 ROSA26 reporter strains

The mouse *Rosa26* locus is widely used as a permissive site for targeted placement of transgenes. A series of reporter genes have been inserted into the *Rosa26* locus to generate reporter mouse lines with precisely designed genome modifications through homologous recombination in ES cells (Figure 1.11). Soriano [212] constructed the *Rosa26* targeting vector which comprises a splice acceptor sequence (SA), a PGK promoter, a neo expression cassette flanked by two loxP sites with the same direction, followed by a triple polyadenylation sequence to prevent neo cassette transcriptional read-through, a lacZ gene and a polyadenylation sequence. This *Rosa26* reporter construct was then linearized and inserted into a unique *Xba*I site approximately 300 bp 5'-stream of the original gene-trap integration site in intron 1 of the mouse *Rosa26* locus. Thus, a reporter mouse line for monitoring Cre recombinase activity at desired time points at the *Rosa26* locus was successfully established. However, the endogenous *ROSA26* promoter is weaker than exogenous artificial promoters (e.g. CAG promoter) [200,213], causing hardly detectable reporter signals in tissues and cells. Therefore, a stronger promoter, such as the CAG promoter, is often used in knock-in reporter lines in order to enhance expression activity at the *ROSA26* locus (Figure 1.11) [216–218]. The CAG promoter was shown to yield the highest expression levels at approximately 8-10 fold the level of the endogenous *ROSA26* promoter [200]. A series reporter genes driven by the CAG promoter were targeted into the mouse *Rosa26* locus to generate *ROSA26* reporter

lines, such as a multifunctional teal-fluorescent *Rosa26* reporter mouse line [219], which strongly expresses mTFP1 (bright teal fluorescent protein) after Cre and Flp mediated recombination; a global double-fluorescent Cre reporter mouse [194], which expresses membrane-targeted tandem dimer Tomato (mT) before Cre mediated excision and membrane-targeted green fluorescent protein (mG) after Cre recombination. All of those *ROSA26* reporter strains can be applied in live cell imaging, lineage tracing, monitoring Cre activity, analysis of cell morphology and so on.

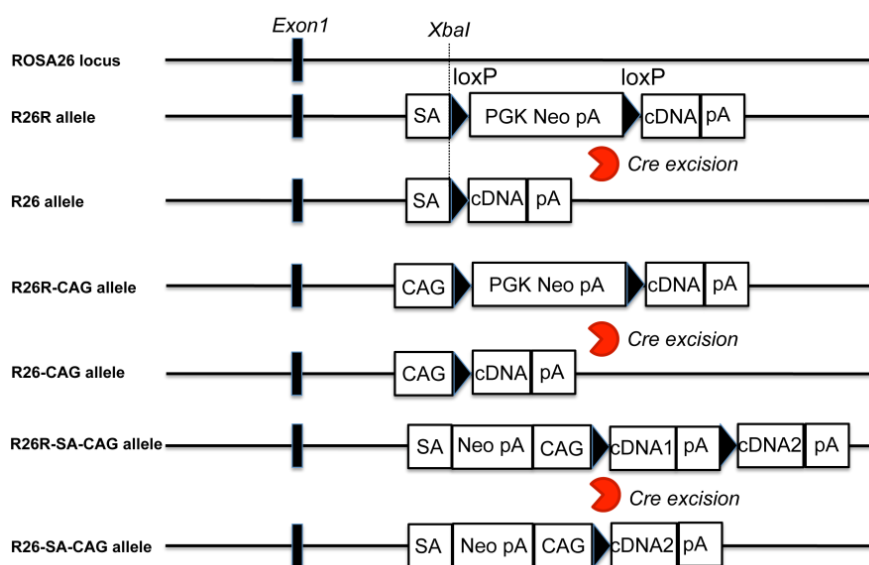


**Figure 1.11: Strategies of targeting reporter genes into the *ROSA26* locus.** From top to bottom: the wild type *ROSA26* locus with the indicated targeting site; the structure of the targeted R26R allele before and after Cre excision of the loxP flanked selection marker with stop cassette; the structure of the targeted R26R-CAG allele before and after Cre excision of the loxP flanked selection marker with stop cassette, where the CAG promoter is inserted in front of the loxP-flanked selection marker with stop cassette; the structure of R26R-SA-CAG allele before and after Cre excision of the loxP flanked cDNA with stop cassette. loxP sequences are indicated by arrowheads and the *ROSA26* exon 1 is shown as a black rectangles.

## 1.5 Functions of reporter animal lines

### 1.5.1 Live cell imaging

Live cell imaging is a powerful tool that can be used to understand embryonic development, the dynamic behaviors of cells driving, the morphogenesis of tissues and organs et al. [208,220]. Reporter animal lines labeled with fluorescent proteins fused to different subcellular

localization signals allow for the observation of real-time states of cells and molecules in specific organelles of living organisms (Figure 1.12).

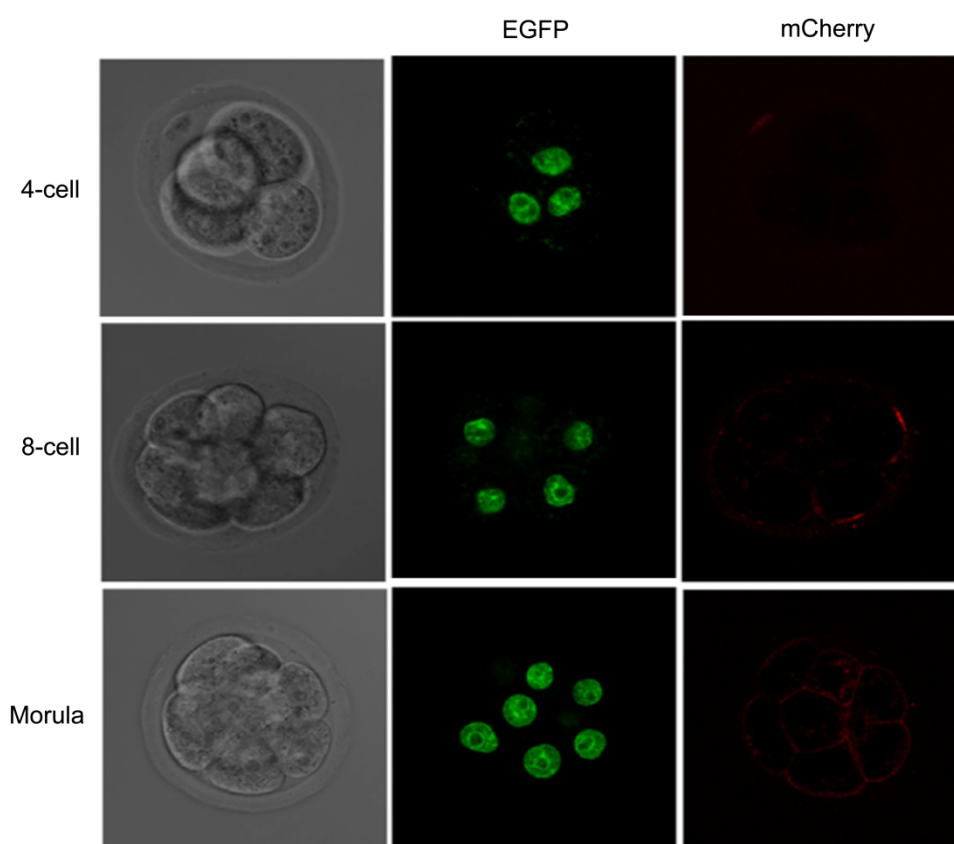


**Figure 1.12: Live imaging of homozygous Rosa26GR (GR stands for green nucleus-red membrane) pre-implantation embryos at different stages.** The chromatin-associated H2B-EGFP and plasma membrane-bound mCherry-GPI targeted into the *Rosa26* locus allow live cell imaging.

Reporter lines, that mark plasma membrane, Golgi apparatus, nucleus, mitochondria, microtubules, actin filament and focal adhesion, have been reported suitable for live imaging [208]. More specifically, Lyn, Ras, GAP43, and Display were used to target fluorescent proteins to the plasma membrane, which provides information on membrane dynamics and cell morphology [221–224]. Mouse  $\beta$ -1,4-galactosyltransferase 1 was used to target fluorescent proteins to the Golgi apparatus because it is known to localize at both trans- and cis-Golgi [225]. Histone H2B was used to target fluorescent proteins to the nucleus [226]. Mouse cytochrome c oxidase subunit (Cox8a) was used to target fluorescent proteins to the mitochondria [227]. Mouse  $\alpha$ -tubulin 2 and human microtubule-binding protein EMTB were used to target fluorescent proteins to microtubules [228]. Actin and moesin were used to target fluorescent proteins to actin filaments [229,230]. Paxillin was used to target fluorescent



proteins to the focal adhesions [231]. The establishment of these reporter animals has enabled scientists to get more detailed information by observing the behavior of each organelle, thus it is beneficial for investigate cell behaviors involving cell division, cell movement, cell death and morphological changes.

### **1.5.2 Cell lineage tracing**

Lineage tracing is the identification of all progeny of a single cell with the help of a transmittable mark that has been introduced into a single cell [232]. Lineage tracing is now widely used in stem cell research since it provides information about how the cell behaves in the context of intact tissue or organ. It is also a powerful method for understanding tissue developemnt, signals regulating cell-fate decisions and diseases. Usually, Cre reporter animal lines are used for genetic lineage tracing. In one animal line, Cre recombinase is expressed under the control of a tissue- or cell- specific promoter. This line can be crossed with reporter lines in which a reporter gene is blocked by a loxP-stop-loxP sequence. In the offspring which carries both constructs, Cre recombinase specifically activates the reporter gene in certain tissue or cells, by ablating the stop cassette. Therefore, the labeled Cre recombined tissues or cells can be monitored and traced easily. For example, the Sox9 promoter can drive the Cre recombinase expression specifically in hair follicle bulge stem cells. Thus in the Sox9-Cre animal lines, the reporter gene can be activated to trace the origin of bulge stem cells and their progeny during epidermal morphogenesis, indicating that Sox9 activated cells can give rise to all epidermal lineages [233]. Subsequently, double Cre-reporter lines were also established for lineage tracing because double-fluorescent marker system would allow for visualization of recombined and nonrecombined cells, simplifying mosaic analysis especially in live tissues. Mandar et al. [194] reported a membrane-targeted tdTomato/membrane-targeted EGFP (mT/mG) double-fluorescent Cre reporter mouse that expresses mT prior to Cre recombination and mG after Cre-mediated recombination. Later, multicolor reporters animal lines, such as 'Brainbow' mouse, were generated as a useful tool for lineage tracing [234]. In the 'Brainbow' mouse, Cre/loxP recombination leads to a stochastic distribution of expression between three or more fluorescent proteins (XFPs). For Brainbow-1, the Cre recombinase can mediate excision between pairs of incompatible loxP

sites, alternated to create mutually exclusive recombination events. In Brainbow-2, the fluorescent proteins were positioned in a tandem way and the Cre recombinase is able to invert DNA fragments delimited by two loxP sites in opposite directions, causing generation of several recombination outcomes. The various expression of multiple copies of those fluorescent genes generates mixtures of fluorescent proteins, allowing the labelling of individual cells with as many as 90 distinguishable colours. The Brainbow-2 has also been combined with the *ROSA26* locus to generate *ROSA26* reporter animal lines, such as the Rosa26-Confettie mouse which was produced by placing the CAG promoter, a loxP-flanked neo cassette and the Brainbow-2 cassette at the mouse *Rosa26* locus [217]. In these mice Cre-mediated recombination occurs at high frequencies in small intestinal crypts. For *Lgr5* stem cells, multicolored cells were initially observed, later on each crypt became labeled with a single color as it became populated by cells derived from a single clone. It was shown that murine intestinal crypts homeostasis is maintained by symmetrically dividing *Lgr5* stem cells through neutral competition [217]. For all these applications, it has to be ensured that the fluorescent protein can be easily visualized after tissue preparation. In order to achieve this, some fluorescent antibodies were used for fixed, paraffin-embedded or unfixed and frozen sections [235,236]. A series of imaging devices have also been applied for detecting fluorescence, such as two or multiphoton fluorescence microscopes, which allow in-depth scanning and optimal fluorophore separation of the multicolor fluorescence [232].

### **1.5.3 Cell cycle indicator**

Visualizing the progress of the cell cycle in cells plays a valuable role in understanding developmental processes, such as cell differentiation, growth, pattern formation, morphogenesis, cell migration and cell death [220]. In order to visualize the cell cycle in live cells, a fluorescent ubiquitylation-based probe, named the fluorescent ubiquitylation-based cell cycle indicator (Fucci) was produced by fusing monomeric Kusabira Orange 2 (mKO2) [237] and monomeric Azami Green (mAG) [238] to the ubiquitylation domains of human Cdt1 [hCdt1(30/120)] and Geminin [hGem(1/110)], respectively [201]. Those two chimeric proteins, mKO2-hCdt1(30/120) and mAG-hGem(1/110), are able to accumulate reciprocally in the nuclei during different stages of the cell cycle, labeling the nuclei of  $G_1$  phase cells in orange

and the nuclei of S, G<sub>2</sub> and M phase in green (Figure 1.13). Therefore, they function as G<sub>1</sub> and S/G<sub>2</sub>/M probes, respectively. By using those cell cycle probes, two mouse lines, CAG-mKO2-hCdt1(30/120) and CAG-mAG-hGem(1/110), were generated by random transgenesis for visualizing the cell cycle in live embryos or animals. Then the CAG-Fucci mouse line, in which both CAG-mKO2-hCdt1(30/120) and CAG-mAG-hGem(1/110) were present, was obtained by crossing these two transgenic lines. These CAG-Fucci mice have been successfully applied to monitor the cell cycle in the head region of embryonic day 13 embryos which demonstrated regional differences in cell proliferation activities in the neural tissue. However, the CAG-Fucci expression was too weak to analyze the cell cycle in some tissues, such as extraembryonic tissues in early post-implantation embryos [201]. Subsequently, a new Fucci probe Fucci2 was created, which used a red monomeric fluorescent protein (mCherry) and *Aequorea* green fluorescent protein (mVenus) to improve the imaging quality. Two Fucci2 reporter mouse lines were generated. One is the R26p-Fucci2 reporter line, in which the *Rosa26* promoter (R26p) bidirectionally drives mCherry-hCdt1(30/120) and mVenus-hGem(1/110) expression. For another Fucci2 reporter line, one *Rosa26* allele harbors mCherry-hCdt1(30/120) and the other allele harbors mVenus-hGem(1/110). Both reporter lines demonstrated the dynamic changes in cell cycle behavior during development and will therefore be a valuable tool for examining a variety of developmental processes, behaviors of adult stem or progenitor cells and pathogenetic processes, such as oncogenesis in tumor-prone mice [201].

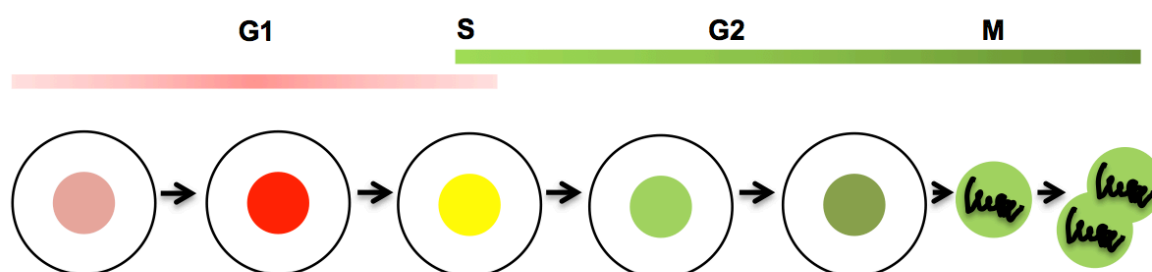


**Figure 1.13:** A fluorescent ubiquitylation-based cell cycle indicator (Fucci) probe labels individual G<sub>1</sub> phase nuclei in red and S/G<sub>2</sub>/M phase nuclei in green.

#### 1.5.4 For immunological research and cancers

The immune system plays a vital role in organisms and has the capacity to recognize and destroy malignant cells and pathogens [239]. Reporter animal lines, such as cytokine reporter strains, immune cell populations labeled reporter strains and so on, are also extending into this field to facilitate the immunological studies. In the immune system, cytokines are soluble messenger molecules having important regulatory function [240]. Cytokine reporter strains have been established by placing reporter genes under the control of elements from cytokine genes, enabling easy identification of their cellular sources. For example, IL-4, which is the hallmark cytokine for Th2 cells, plays an important role in immunity against extracellular pathogens. A bicistronic IL-4 reporter mouse was generated by inserting an internal ribosome entry site-green fluorescent protein (IRES-GFP) into the 3' untranslated region of the IL-4 gene [241]. This reporter line faithfully showed IL-4 expression under Th2 polarizing conditions [242–247] and it also labeled other constitutive IL-4 producers, like basophils, natural killer (NK) T cells, eosinophils and mast cells [242,246,247]. A series of other cytokine reporter lines, such as IL-2 [248,249], IL-7 [250,251], IL-10 [252–254], IL-17F [255–257], IFN- $\gamma$  [247], have been applied in immunological research. Reporter strains can also be used for visualization of immune responses to cancer [239]. One of the reporter lines was created by using the T cell specific human CD2 promoter to drive reporter genes, facilitating the studies on T cell localization. This reporter line was subsequently crossed with CD8<sup>+</sup> [258] or CD4<sup>+</sup> [259] T cell receptor transgenic mice, generating dual transgenic lines with expression of reporter gene in antigen-specific CD8<sup>+</sup> T cells or CD4<sup>+</sup> T cells. These dual transgenic strains allow longitudinal tracking of antigen-specific T cells *in vivo*, and they have been successfully used to follow responses to model antigens. The kinetics of T cell localization to transplantable tumors can be directly evaluated by challenging the reporter mouse with transplantable tumors expressing the model antigen. The ongoing development of reporter strains is opening an avenue for noninvasive and longitudinal studies of immune cell localization and function in cancer. Also, reporter transgenes have become a common approach to investigate diverse aspects of tumor biology *in vivo* [260].

## 1.6 Aim of this project

This project had three goals. The first aim was to generate a *ROSA26* dual, Cre-inducible reporter porcine model that can be applied in a wide range of fields, such as the studies of cellular differentiation, organogenesis, developmental biology, cancer initial cell lineage tracing, cell fate as well as transplantation. The second aim was to generate PDX-1-Cre transgenic pigs which are able to express Cre recombinase specifically in the pancreas. The last aim was to generate transgenic pigs containing an LSL-KRAS<sup>G12D</sup> allele that can be activated to express mutated KRAS<sup>G12D</sup> after Cre recombination.

In order to achieve the first goal, the following measures were adopted. Firstly, the location of the porcine *ROSA26* gene and its gene structure had to be indentified properly. Then the site in the porcine *ROSA26* intron 1 similar to that frequently used in mouse *Rosa26* was chosen as a preferential target site. The targeting vectors were constructed based on a promoter-trap approach and porcine mesenchymal stem cells were used for gene targeting. The dual, Cre-inducible reporter system was achieved by combining a loxP flanked first reporter gene with a second reporter marker. Functionality of the Cre-inducible system could be tested both in *in vitro* and *in vivo*. Afterwards, correctly targeted cells were used for somatic cell nuclear transfer (SCNT) to generate gene targeted pigs. Then, transgenic piglets and foetuses were analysed for correct transgenesis, *ROSA26* gene expression patterns and functionality of the double fluorescent system. Testing of the double fluorescent system *in vitro* was conducted by transducing Cre recombinase into targeted cells or somatic cells from transgenic piglets or foetuses. There are two approaches to check the double fluorescent system *in vivo*. One strategy is to cross *ROSA26* dual reporter pigs with pigs expressing Cre recombinase under the control of cell or tissue specific promoter (e.g. PDX-1). Another method is to re-target Cre recombinase under the control of a tissue specific promoter into kidney fibroblasts from *ROSA26* dual reporter foetuses or piglets. Via SCNT and embroy transfer (ET), genetically modified animals had to be analysed. To achieve the second aim, a targeting vector containing an IRES-Cre cassette had to be inserted after the stop codon of the endogenous PDX-1 locus with the help of TALENs. Regarding the third aim, a targeting vector containing

LoxP-stop-LoxP- KRAS<sup>G12D</sup> (LSL- KRAS<sup>G12D</sup>) had to be targeted in the KRAS locus. Finally, a porcine model of pancreatic cancer containing PDX-1-Cre, LSL-Trp53<sup>R172H</sup>, LSL-KRAS<sup>G12D</sup>, ROSA26<sup>mT/mG</sup> alleles can be generated through intercrossing.

## 2 Material and methods

### 2.1 Material

#### 2.1.1 Chemicals

Acetic acid	Fluka Laborchemikalien GmbH, Seelze, Germany
Alcian blue	Sigma, Steinheim, Germany
Ammonium persulfate (APS)	Carl Roth GmbH, Karlsruhe, Germany
Blocking solution for Southern Blot	Roche Diagnostic GmbH, Mannheim, Germany
Biozym LE Agarose	Biozym, Oldendorf, Germany
Boric Acid	Fluka Laborchemikalien GmbH, Seelze, Germany
Bovine Serum Albumin, pH 7.0	PAA, Pasching, Austria
Bromphenol blue	Sigma, Steinheim, Germany
Chloroform	Sigma, Steinheim, Germany
CDP Star	Roche Diagnostic GmbH, Mannheim, Germany
Dimethyl sulfoxide (DMSO)	Sigma-Aldrich Chemie GmbH, Steinheim
DIG Easy Hyb Granules	Roche Diagnostic GmbH, Mannheim, Germany
Digoxigenin-11-2'-deoxy -uridine-5'-triphosphate	Roche Diagnostic GmbH, Mannheim, Germany
Ethylene diamine tetracetic acid (EDTA)	Sigma, Steinheim, Germany
Ethanol	Riedel-de-Haen, Seelze, Germany
Ethidiumbromid solution	Sigma, Steinheim, Germany
Formalin	Sigma, Steinheim, Germany
Formamide (deionized)	Sigma, Steinheim, Germany
GenAgarose L.E.	Genaxxon Bioscience GmbH, Biberach, Germany
Glacial acetic acid	Fluka Laborchemikalien GmbH, Seelze, Germany
Glutaraldehyde	Fluka Laborchemikalien GmbH, Seelze, Germany
Glycerol	Carl Roth GmbH, Karlsruhe, Germany

Glycine	Carl Roth GmbH, Karlsruhe, Germany
Hydrochloric acid 37%	Merck KGaA, Darmstadt
Isopropanol (2-Propanol)	Carl Roth GmbH, Karlsruhe, Germany
Kanamycin (Kana)	Sigma-Aldrich Chemie GmbH, Steinheim, Germany
Magnesium chloride-hexahydrate	Merck KGaA, Darmstadt, Germany
Methanol	Sigma, Steinheim, Germany
NP40 (Igepal CA-630)	Sigma-Aldrich, Steinheim, Germany
Potassium chloride	Sigma-Aldrich, Steinheim, Germany
Saccharose	Sigma, Steinheim, Germany
Sodium chloride	J.T. Baker, Deventer, Holland
Sodium citrate tribasic dehydrate	Sigma, Steinheim, Germany
Sodium thiosulfate	Sigma, Steinheim, Germany
Sodium acetate	Roth, Karlsruhe, Germany
Sodium dodecyl sulfate (SDS)	Sigma, Steinheim, Germany
Sodium hydroxide pellets	Riedel-de Haen Laborchemikalien GmbH, Germany
Sucrose	Sigma, Steinheim, Germany
TEMED	Roth, Karlsruhe, Germany
Trizma base (Tris base)	Sigma, Steinheim, Germany
Tris hydrochloride (Tris HCl)	Sigma, Steinheim, Germany
Trypan blue solution (0.4%)	Sigma-Aldrich Chemie GmbH, Steinheim, Germany
Trizol	Invitrogen, Karlsruhe, Germany
Tween 20	Sigma, Steinheim, Germany

### 2.1.2 Enzymes

Antarctic Phosphatase	New England Biolabs, Frankfurt, Germany
DNA polymerase I, large (Klenow) fragment	New England Biolabs, Frankfurt, Germany
GoTaq DNA polymerase	Promega GmbH, Mannheim, Germany
PCR Extender System	5Prime GmbH, Hamburg, Germany
Proteinase K	Sigma-Aldrich Chemie GmbH, Steinheim, Germany



Restriction endonucleases (including corresponding buffers and 100x BSA)	New England Biolabs, Frankfurt, Germany
RNase A solution	Sigma-Aldrich Chemie GmbH, Steinheim, Germany
T4 DNA Ligase	New England Biolabs, Frankfurt, Germany

### 2.1.3 Kits

Amaxa Human MSC Nucleofector Kit	Lonza, Cologne, Germany
Mammalian Genomic DNA Miniprep Kit	Sigma-Aldrich Chemie GmbH, Steinheim, Germany
NucleoBond Xtra Plasmid Purification	Macherey-Nagel GmbH and Co. KG, Dueren, Germany
pGEM-T Easy Vector System	Promega, Mannheim, Germany
Turbo DNA-free	Ambion, huntingdon, UK
innuSPEED Tissue RNA Kit	analytikjena, Biometra, Yena, Germany
SurePrep™ TrueTotal™ RNA Purification Kit	Fisher BioReagents, Canada
ProtoScript™ M-MuLV Taq RT-PCR Kit	New England Biolabs GmbH, Frankfurt, Germany
Nanofection Kit	PAA, Pasching, Austria
Wizard SV Gel and PCR Clean-up System	Promega, Mannheim, Germany

### 2.1.4 Media, solutions, cells and supplements for molecularbiology and microbiology

#### 2.1.4.1 Bacterial growth media

Difco LB Agar, Miller	Becon, Dickinson, Erembodegem-Aalst, Belgium
-----------------------	--

#### 2.1.4.2 Solutions and supplements for molecular biology and microbiology

dNTPs	Biomers, Ulm, Germany
100 bp Ladder	New England Biolabs, Frankfurt, Germany
1 kb Ladder	New England Biolabs, Frankfurt, Germany

$\beta$ -Glycerol phosphate	Sigma-Aldrich Chemie GmbH, Steinheim, Germany
X-Gal (5-Bromo-4-chloro-3-indolyl- $\beta$ -D-galactopyranoside)	Sigma-Aldrich Chemie GmbH, Steinheim, Germany
Gel loading buffer (5 $\times$ )	5 ml Glycerol 4 ml EDTA (0.5 M) point of a spatula Bromphenol blue filled up with ddH <sub>2</sub> O to 10 ml
Miniprep solution I	5 mM sucrose TRIS (pH 8.0) 10 mM EDTA
Miniprep solution II	1% SDS 0.2 N NaOH
Miniprep solution III	3 M sodium acetate (pH 5.3)
TAE buffer (50 $\times$ )	2 M Trisbase 50 mM EDTA (0.5 M) 57.1 ml Glacial acetic acid filled up with ddH <sub>2</sub> O to 1L autoclaved
TBE buffer (10 $\times$ )	0.9 M Tris 20 mM EDTA (0.5 M) 0.9 M boric acid filled up with ddH <sub>2</sub> O to 1L autoclaved
RNase Away	Roth, Karlsruhe, Germany
X-Gal solution	100 mg X-Gal 1 ml N,N-Dimethylformamid (DMF)

### 2.1.4.3 Antibiotics for microbiology

Ampicillin	Sigma-Aldrich, Steinheim, Germany
------------	-----------------------------------

Kanamycin Sigma-Aldrich, Steinheim, Germany

#### 2.1.4.4 Bacterial strains

*E. Coli* DH10B ElectroMAX Invitrogen, Karlsruhe, Germany  
 Genotype:  $F^-mcrA \Delta(mrr-hsdRMS-mcrBC)$   
 $\Phi80lacZ\Delta M15 \Delta lacx74 recA1 endA1 araD139$   
 $\Delta(ara, leu)7697 galU galK \lambda^- rpsL nupG$

#### 2.1.5 Media, solutions, supplements and cell lines for mammalian cell culture

##### 2.1.5.1 Culture media

Advanced Dulbecco's Modified Gibco BRL, Paisley, Scotland

##### 2.1.5.2 Solutions and supplements for cell culture

Accutase	PAA, Pasching, Austria
$\beta$ -Mercaptoethanol	Sigma-Aldrich, Steinheim, Germany
Cell Culture Water, EP-grade	PAA, Pasching, Austria
Chicken serum	PAA, Pasching, Austria
Dulbecco's PBS, w/o Ca & Mg	PAA, Pasching, Austria
Dimethyl sulfoxide (DMSO)	Sigma-Aldrich, Steinheim, Germany
Fetal calf serum (FCS)	PAA, Pasching, Austria
GlutaMAX	Gibco BRL, Paisley, Scotland
Hypoosmolar Buffer	Eppendorf, Hamburg, Germany
Human Fibroblast Growth Factor (FGF-2)	Genaxxon, Biberach, Germany
HEPES	Invitrogen, Karlsruhe, Germany
Hank's buffered salt solution (HBSS), w/o Phenol red, with Ca and Mg	PAA, Pasching, Austria
Nanofectin solution	PAA, Pasching, Austria
Non-essential amino acids (NEAA)	PAA, Pasching, Austria
Nucleofector solution	Lonza, Cologne, Germany
Sodium pyruvate	PAA, Pasching, Austria

Trypsin-EDTA PAA, Pasching, Austria

### 2.1.5.3 Antibiotics and antimycotics

Amphotericin B solution PAA, Pasching, Austria

Blasticidin S InvivoGen, San Diego, USA

G418 PAA, Pasching, Austria

Penicillin/Streptomycin solution PAA, Pasching, Austria

### 2.1.5.4 Mammalian cell lines

poMSC-071210 Porcine mesenchymal stem cell line isolated from bone marrow by Dr. Krzysztof Flisikowski (TUM, Germany); sex: male; breed: DL×DL (Deutsche Landrasse); isolated: 7<sup>th</sup> Dec. 2010.

poMSC-110111 Porcine mesenchymal stem cell line isolated from adipose by Dr. Tatiana Flisikowska (TUM, Germany); sex: male; breed: DL; isolated: 11<sup>st</sup> Jan. 2011.

### 2.1.6 Primers

All primers were synthesized by Eurofins MWG Operon (Ebersberg, Germany).

Primers	Primer sequences (5'-3')
ROSA26 SAR	CAAACCTCTTCGCGGTCTTTC
ROSA26 targF	TCTGCTGCCTCCTTTTCCTA
R26endoR	GTTTGCACAGGAAACCCAAG
ROSA26 BSR	AGCAATTCACGAATCCAAC
R26Ex1F1	CGCCTAGAGAAGAGGCTGTG
R26Ex2R	TATGCTTAGCAGCTTCCTC
GAPDHF	TCCCACGGCACAGTCAA
GAPDHR	GCAGGTCAGGTCCACAA
BSprobF	ATGGCCAAGCCTTTGTCTC
BSprobR	GATTTAGCCCTCCCACACAT
NeoprobF	GGTTGAGGACAAACTCTTCG
NeoprobR	CAGCAGCAGACCATTTTCAA
mTR	GTACAGCTCGTCCATGCCGTA
mTF	ACATGGCCGTCATCAAAGAG

---

mCF	CCTGTCCCCTCAGTTCATGT
R26LR	CTTGCCCCACGACAAGATCA
R26Ex1F2	AGAAGAGGCTGTGCTCTGG
3'RACE adapter	GCGAGCACAGAATTAATACGACTCACTATAGGT12VN
3'RACE outer primer	GCTGATGGCGATGAATGAACACTG
3'RACE inner primer	CGCGGATCCGAACACTGCGTTTGCTGGCTTTGATG
PDX-1targF	ATGTCAGCTCTGTATCGGCG
PDX-1IRESR	CACACCGGCCTTATTCCAAG
PDX-1neoF	TGGGAAGACAATAGCAGGCA
PDX-1RAR	AAGCCCACTAAGTCCAGGTC
KRAStargF2	ACGCGGGGAATGAGGAAT
KRASendoR1	TGCTGTGGCTGTGGAGTAAG
SAR	GAAAGACCGCGAAGAGTTTG
KRASmutatedF	AGACCCCTATCCTGGGAATG
KRASmutatedR	TTCACATTTTCACCCCTCTGCT
R26E4R2	CTGCTGTGGCTGTGGTGTAG

---

### 2.1.7 Consumable Supplies

0.5 ml, 1.5 ml and 2.0 ml EP tubes	Brand, Wertheim, Germany
14 ml Polypropylene round bottom tube	Becton, Dickinson and Company, Sparks, USA
15 and 50 ml centrifugation Tubes	Greiner bio-one, Frickenhausen, Germany
Cell culture flasks (25, 75, 150 cm <sup>2</sup> )	Corning Inc., New York, USA
Cell culture plates (6-, 12-, 24-, 48-well)	Corning Inc., New York, USA
CryoTubes	Nunc, Wiesbaden-Biebrich, Germany
Disposable inoculating tube (10 µl)	Cole-Parmer Instrument Company, Illinois, USA
Electroporation Cuvettes, 2 mm	peqlab, Erlangen, Germany
Electroporation Cuvettes, 4 mm	peqlab, Erlangen, Germany
Glass transfer pipettes	Brand, Wertheim, Germany
Glassware (bottles, flasks)	Marienfeld GmbH, Lauda-Königshofen, Germany
Hybond-N+, positively charged	Amersham Bioscience, Freiburg,
nylon transfer membrane, 0.45 µm pore size	Germany

Immobilon-P Transfer Membrane, PVDF membrane, 0.45 µm pore size	Millipore Corporation, Billerica, USA
Petri dish (10 cm)	Brand, Wertheim, Germany
Photometer Cuvettes	Eppendorf, Hamburg, Germany
Pipette tips	Brand, Wertheim, Germany
Plugged pipette tips (2, 20, 200 and 1000 µl)	Mettler Toledo GmbH, Dreieich, Germany
Rotilabo® Blotting paper (1 mm)	Carl Roth GmbH, Karlsruhe, Germany
Sterile plastic pipettes 1-25 ml	Corning Inc., New York, USA
Syringes (BD Discardit™)	Becton Dickinson GmbH, Sparks, USA
Sterile syringe filter (0.2 µm)	Sartorius stedim biotech, Goettingen, Germany

### 2.1.8 Cloning vectors and plasmids

pBluescriptII SK+	Stratagene, La Jolla, USA
pCAGGS-Cherry	Laboratory stock
pGEM-T Easy	Promega, Mannheim, Germany
pJET1.2/blunt	Invitrogen, Karlsruhe, Germany
pSL1180	Amersham Bioscience, Piscataway, New Jersey, USA
pGEM-T + rosaF9R9 (reverse)	Livestock Biotechnology, TU Munich, Germany

### 2.1.9 Laboratory equipment

Agarose Gel Electrophoresis apparatus: Classic CSSU78 and CSSU1214	Thermo Electron GmbH, Dreieich, Germany
Amaxa Nucleofector	Lonza, Cologne, Germany
Axiovert 25	Zeiss AG, Oberkochen, Germany
Accu-Jet	Brand, Diethenhofen
Bio Imaging System Gene Genius	Syngene, Cambridge, UK

---

BioPhotometer 6131	Eppendorf, Hamburg, Germany
Cell counting chamber	Neubauer, Marienfeld, Lauda-K <sup>^</sup> nigshofen
Countess <sup>®</sup> automated cell counter	Invitrogen, USA
Digital Graphic Printer UP-D895MD	Syngene, Cambridge, UK
Digital camera for microscope	Carl Zeiss Jena GmbH, Jena
Fluorescence microscope Axiovert 135	Carl Zeiss Jena GmbH, Jena
Forma orbital shaker	Thermo Electron Corporation, Dreieich, Germany
Glassware (bottles, flasks)	Marienfeld GmbH, Lauda-Königshofen, Germany
Incubator	Binder GmbH, Tuttlingen, Germany
Ice maker	Eurfrigor, Lainate (MI), Italy
Laboratory centrifuges 4K15C, 1-15	Sigma, Osterode, Germany
Microwave MDA MW12M706-AU	MHA, Barsbüttel, Germany
Mr. Frosty	Nalgene, Rochester, USA
Membrapure high-purity water system	Membrapure, Bodenheim, Germany
MJ Research PTC Thermal Cycler	GMI Inc., Ramsey, USA
Nano Drop Lite	Thermo Scientific, USA
Pipetman P20, P200, P1000	Gilson, Bad Camberg, Germany
Pipetman Ultra U2	Gilson, Bad Camberg, Germany
Pipetus red dot	Hirschmann Laborgeräte, Eberstadt, Germany
Power supply EC105	Thermo Electron GmbH, Dreieich, Germany
Power PAC 300	Bio-Rad Laboratories GmbH, Munich, Germany
Precision Balances 440-33N	Kern, Balingen-Frommern, Germany
Safety Cabinets HERAsafe Type HSP	Heraeus Instruments, Munich, Germany
Shaker, Forma orbital shaker	Thermo Electron GmbH, Dreieich, Germany
Steri-Cycle CO <sub>2</sub> incubator	Thermo Electron GmbH, Dreieich, Germany
UV-Photometer DU-640	Beckman Coulter GmbH, Krefeld
Varifuge 3.0 R	Heraeus Instruments, Hanau
Vortex Mixer	VELP Scientifica srl, Milano, Italy

Water bath: Haake C10-K15	Thermo Fisher Scientific, Karlsruhe, Germany
+4°C fridge	Beko Technologies, Dresden, Germany
-20°C freezer	Liebherr International, Bulle, Switzerland
-80°C freezer	Thermo Electron GmbH, Dreieich, Germany

### 2.1.10 Softwares

AxioVision	Zeiss AG, Oberkochen, Germany
ClusterW	<a href="http://www.ebi.ac.uk/clusterw/index.html">http://www.ebi.ac.uk/clusterw/index.html</a>
Enzyme and Double Digests Finder	<a href="http://www.neb.com">http://www.neb.com</a>
Finch TV	<a href="http://www.geospiza.com/finchtv">www.geospiza.com/finchtv</a>
GenBank	<a href="http://www.ncbi.nlm.nih.gov">http://www.ncbi.nlm.nih.gov</a>
primer3 (version 0.4.0)	<a href="http://fokker.wi.mit.edu/primer3/input.htm">http://fokker.wi.mit.edu/primer3/input.htm</a>
Vector NTI Advance 10, ContigExpress and Alingx	Invitrogen, Karlsruhe, Germany

## 2.2 Methods

### 2.2.1 Molecular biology methods

#### 2.2.1.1 Isolation of nucleic acids

##### Isolation plasmid DNA from *E.coli* (*Escherichia coli*)

Each single bacterial colony was picked by toothpick and transferred into 15 ml falcon which contains 5 ml corresponding antibiotic LB medium and incubated overnight at 37°C in an orbital shaker at 220 rpm. Depending on the required amount for plasmid DNA, different protocols of isolating plasmid DNA from *E.coli* were performed.

**Miniprep:** Miniprep was applied to obtain small amounts of plasmid DNA. 2 ml of 5 ml overnight cultured bacterial cells liquid were transferred into a 2 ml Ep tube and centrifuged for 1 minute at 14,000 rpm. The supernatant was discarded and the cell pellet was resuspended in 100 µl of miniprep solution I by vortexing. Then 200 µl of miniprep solution II were added and mixed by inverting the tube several times. After incubation at room



temperature for 3 minutes, 150µl of miniprep solution III were applied. Afterwards, the tube was inverted again for mixing and incubated on ice for 30 minutes. Subsequently, the mixture was centrifuged for 5 minutes at 14,000 rpm in order to remove proteins, and the supernatant was transferred into a new 1.5 ml Ep tube and precipitated with 1 ml of 95% EtOH by vortexing. Then, the plasmid DNA was collected by centrifugation at 14,000 rpm for 15 minutes and the ethanol removed. The pellet was washed by 500 µl of 80% EtOH and followed with 500 µl of 95% EtOH. After each washing steps, centrifugation was conducted at 14,000 rpm for 10 minutes. Finally, after removal of EtOH, the plasmid DNA pellet was air dried at room temperature and resuspended in 50 µl of ddH<sub>2</sub>O supplemented with RNase.

**Midiprep:** For medium-scale plasmid DNA isolation, 100 ml LB medium containing the appropriate antibiotic were inoculated with bacteria and bacterial pellets were harvested by centrifugation in two 50 ml facons. The plasmid DNA isolation was performed by using NucleoBond xtra Midi kit according to the manufacturer's manual.

**Maxiprep:** For large-scale plasmid DNA isolation, preparation was performed with 300ml over night culture. The plasmid DNA isolation was conducted with the NucleoBond xtra Maxi kit according to the manufacturer's manual.

### **Genomic DNA isolation from mammalian cells**

**Igepal solution method:** Genomic DNA isolations from trypsinized porcine MSCs or KDNF were carried out for screening PCR of positive targeting event. About 100 µl of harvested cell suspension were centrifuged in a PCR tube at 14,000 rpm for 5 minutes and then the supernatant was removed completely. The cell pellet was resuspended in 50 µl Igepal lysis buffer (50 mM KCl, 1.5 mM MgCl<sub>2</sub>, 10 mM Tris pH 8.0, 0.5% NP40, 0.5% Tween 20) containing 0.25 µl of freshly added proteinase K (20 mg/ml) and incubated for 1 h at 60°C followed by proteinase K heat inactivated step at 95°C for 15 min. Afterwards, the cell lysate was centrifuged at 14,000 rpm for 10 minutes and 5 µl of the supernatant were used for screening PCR.

**DNA kit method:** In order to get high pure mammalian cells genomic DNA, DNA was isolated

by using the GenElute Mammalian Genomic DNA Miniprep Kit according to the manufacturer's protocol. Genomic DNA was eluted in 100  $\mu$ l of elution buffer and measured the concentration.

**Phenol-chloroform method:** To get higher amount of genomic DNA, such as for the southern blot, this classical DNA isolation method was applied. Trypsinized porcine MSCs or KDNF were centrifuged at 300 g for 5 minutes in order to get cell pellets. The cell pellets were then resuspended in 500  $\mu$ l cell lysis buffer (0,1M Tris, 5mM EDTA, 0,2% SDS, 0,2M NaCl, 100 $\mu$ g/ml Proteinase K) and incubated at 37°C overnight. Afterwards, 500  $\mu$ l Phenol-chloroform-isoamyl alcohol mixture were added and incubated at room temperature for 15 minutes. Subsequently, the mixture was centrifuged for 15 minutes at 14,000 rpm, and the supernatant was transferred into a new 1.5 ml Ep tube and added 500  $\mu$ l Chloroform. After vortexing the tube several times, the mixture was centrifuged for 10 minutes at 14,000 rpm, and the supernatant was transferred into another new 1.5 ml Ep and added 350 $\mu$ l Isopropanol. Then, the mixture was centrifuged at 14,000 rpm for 5 minutes to get the pellet and the supernatant was completely removed. The pellet was washed by 1 ml 70% EtOH and centrifuged for 10 minutes at 14,000 rpm. Finally, after removal of EtOH, the genomic DNA pellet was air dried at room temperature and dissolved in 50  $\mu$ l TE-buffer. Isolated DNA was stored at 4 °C.

### **Total RNA isolation**

#### **For mammalian cells**

Trypsinized porcine MSCs or KDNF were centrifuged at 300 g for 5 minutes in order to get cell pellets for RNA isolation. Total RNA isolation was performed using the SurePrep™ TrueTotal™ RNA Purification Kit (Fisher) according to the manufacturer's manual. Additionally, to remove DNA from RNA preparation, the TURBO DNA-free kit was used according to the supplier's instructions. RNA was then stored at -80°C.

#### **For tissues**

Up to 20 mg tissues were homogenized by using SpeedMill plus (analytikjena) for 30 seconds

twice and then the total RNA isolation was performed by InnuSPEED Tissue RNA kit (analytikjenaBiometra) according to supplier's protocol.

### **Photometric determination of nucleic acids concentration**

The concentration of nucleic acids was determined photometrically by using the BioPhotometer (Eppendorf). DNA and RNA samples were diluted from 1:35 to 1:100 depending on the original concentration and optical density (OD) was measured at 260nm after blanking by same amount of water. DNA and RNA concentrations were calculated according to the following formulas:

$$\text{DNA } [\mu\text{g}/\mu\text{l}] = (\text{OD}_{260} \times 50 \times \text{dilution factor})/1000$$

$$\text{RNA } [\mu\text{g}/\mu\text{l}] = (\text{OD}_{260} \times 40 \times \text{dilution factor})/1000$$

### **Nano Drop Lite determination of nucleic acids concentration**

By using Nano Drop Lite for nucleic acids concentration measurement, 1  $\mu\text{l}$   $\text{H}_2\text{O}$  was used as a blank, and then 1  $\mu\text{l}$  DNA or RNA was loaded on the Nano drop. The program of dsDNA (factor: 50) and RNA (factor: 40) has to be chosen, and the concentration of each sample is showed on the screen.

#### **2.2.1.2 DNA manipulation**

##### **Restriction digestion**

Restriction digestion of DNA was carried out using 3 units of enzyme per microgram DNA in the final volume of 50-100  $\mu\text{l}$ . Generally, for restriction patterns analysis, 1 to 3  $\mu\text{g}$  DNA were digested and for different preparative purposes up to 40  $\mu\text{g}$  were used. All digestions were performed using applicable NEB buffer and at the specific temperature according to the manufacturer's instructions. As the same principle, double or triple digestions performed in the appropriate buffer with highest activity for two or three enzymes were also applied in this study. Table 2.1 shows the standard reaction system for the restriction digestion.

**Table 2.1: Standard restriction enzyme reactions**

Components	Amount
DNA	1-3 $\mu\text{g}$
10 $\times$ NEB buffer	0.1 times of final volume
100 $\times$ BSA (if required)	0.01 times of final volume
Restriction enzyme	2-5 U/ $\mu\text{g}$ DNA
Nuclease-free water	Up to final volume (50-100 $\mu\text{l}$ )

**Klenow reaction for DNA fragments blunting**

For some restriction digest products, overhangs of DNA fragments had to be removed or filled in with DNA Polymerase I, Large (Klenow) Fragment for the further ligation steps. The enzyme forms blunt ends by 3' overhangs removal and 5' overhangs filling in. Table 2.2 shows the standard reaction system. The reaction can be stopped by adding EDTA to a final concentration of 10mM and heating at 75°C for 20 minutes.

**Table 2.2: Standard Klenow reaction**

Components	Amount
DNA	up to 5 $\mu\text{g}$
T4 ligase buffer	1 $\times$
dNTPs	0.1 mM
Klenow enzyme	1 $\mu\text{l}$
T4 ligase	1 $\mu\text{l}$
Nuclease-free water	Up to 25 $\mu\text{l}$

**Dephosphorylation of DNA fragments**

In order to avoid religation of linearized plasmid, which had compatible DNA ends after restriction digestion, *Antarctic Phosphatase* or *Calf Intestine Alkaline Phosphatase* (CIP) were used for removing 5' phosphate groups from DNA. The reaction system was conducted according to the supplier's instructions. After dephosphorylation, the enzyme was heat inactivated or removed by using the *Wizard SV Gel and PCR Clean-Up System*.

**Ligation**

In cloning experiments, it's often required to ligase two DNA fragments with compatible ends

together by using T4 DNA ligase, which can mediate the formation of phosphodiester groups between the 3'-OH and 5' phosphate group. The reaction was prepared according to the manufacturer's protocol and the ligation mix was incubated at room temperature for 1 to 2 hours or stored at 16°C overnight for the purpose of higher ligation efficiency. Afterwards, this ligation mix can be transformed in *E. coli*.

### **Agarose gel electrophoresis**

In order to separate DNA fragments with different size, such as analyzing the restriction pattern of plasmids and PCR product, agarose gel electrophoresis was performed. Depending on different size of DNA fragments, 0.8-1.5% agarose gels were prepared by melting appropriate amount of agarose in 1×TAE or 1×TBE buffer and adding 0.5 µg/ml ethidium bromide. Usually, TAE gel and buffer were used when DNA fragments need to be isolated from the gel. Before loading samples into the gel, samples were mixed with the corresponding volume of 5×DNA loading buffer and loaded to the gel together with 1 kb or 100 bp DNA ladders in different lanes. After loading the samples and corresponding ladders, gels were run for 45 minutes to 2 hours at 80 to 120 V based on the sizes of DNA fragments. Visualisation of DNA under UV light (366 nm) and photography were carried out by using the *Bio Imaging System Gene Genius*.

### **Purification of DNA fragments from agarose gels**

In order to cut and isolate the aimed bands from gels, DNA fragments were visualized by putting the gel on a UV table. Correct DNA bands were cut out from the gel with a sharp and clean scalpel and then transferred into 1.5 ml Ep tubes. The DNA was purified from the gel by using Wizard SV Gel and PCR Clean-Up System according to the manufacturer's protocol. The DNA was eluted in 50 µl nuclease free water and stored at -20°C.

### **Precipitation of DNA with sodium chloride and ethanol**

To get sterile DNA for transfection experiments in tissue culture, precipitation of DNA was done according to the following protocol. 0.1 volume of 3 M NaAC and 2 volume of 100% ethanol (precooled to -20°C) were added to the DNA solution and incubated over night at

-20°C. Then, the mixture was centrifuged for 10 minutes at 14,000 rpm and the supernatant was discarded after centrifugation. The pellet was washed with 1 ml 70% sterile ethanol and centrifuged for 5 minutes at 14,000 rpm. Afterwards, the ethanol was removed and the pellet air dried under a laminar flow hood. At last, the DNA was dissolved in 50 to 100 µl low Tris-EDTA solution and the concentration was then measured for the further studies.

### 2.2.1.3 Polymerase Chain Reaction (PCR)

Polymerase chain reaction (PCR) was conducted for specific amplification of desired DNA fragments from plasmids or genomic DNA. All primers were supplied by Eurofins MWG company and diluted in ddH<sub>2</sub>O to the stored solution with the concentration of 100 µM. Then the stored solution of primers were diluted into 10 µM for PCRs. GoTaq DNA polymerase, PCR Extender System (5 Prime) and Phire polymerase were used for PCRs by using corresponding supplier's protocols. Table 2.3 describes the components of the PCR master mix and cycling conditions by using different polymerases.

**Table 2.3: Components of PCR reaction master mix and cycling conditions**

Components	Final concentration	Steps	Degree	Time	Cycle
<b>Go Taq PCR</b>					
		Initial			
5×Green buffer	1×	denaturation	95	2 min	1
dNTPs	200 µM each	Denaturation	95	1 min	
Forward primer	20 pmol	Annealing	56-65	30 sec	35-40
Reverse primer	20 pmol	Elongation	72	1 min/Kb	
GoTaq	1.25 U	Final elongation	72	5 min	1
DNA	100 ng	Storage	8	forever	
H <sub>2</sub> O	up to 50µl				
<b>5Prime PCR</b>					
		Initial			
10×Buffer	1×	denaturation	94	2 min	1
dNTPs	200 µM each	Denaturation	94	20 sec	
Forward primer	20 pmol	Annealing	60-65	20 sec	35-40
Reverse primer	20 pmol	Elongation	72	1 min/Kb	
Polymerase	2 U	Final elongation	72	5 min	1
DNA	100 ng	Storage	8	forever	
H <sub>2</sub> O	up to 50µl				
<b>Phire PCR</b>					
		Initial			
5×Buffer	1×	denaturation	98	30 sec	1

Phire PCR		Initial			
5×Buffer	1×	denaturation	98	30 sec	1
dNTPs	200 µM each	Denaturation	98	5 sec	
Forward primer	20 pmol	Annealing	60	5 sec	35-40
Reverse primer	20 pmol	Elongation	72	15 sec/Kb	
Polymerase	0.5 µl	Final elongation	72	1 min	1
DNA	100 ng	Storage	8	forever	
H <sub>2</sub> O	up to 50µl				

#### 2.2.1.4 Reverse transcriptase polymerase chain reaction (RT-PCR)

RT-PCR reactions were performed with the ProtoScript™ M-MuLV*Taq* RT-PCR Kit (NEB) according to the supplier's manual. The procedure is shown in Table 2.4. To exclude contamination with genomic DNA, PCR controls were carried out by using only GoTaq polymerase without the synthesized cDNA under the same conditions for tested samples.

**Table 2.4: RT-PCR reaction master mix set ups and conditions**

Components	Final concentration	Used volumes
Total RNA	500 ng-2 µg	Up to 10 µl
Random Primer Mix (60 µM)	6 µM	2 µl
dNTP mix (2.5 mM)	0,5 mM	4 µl
Nuclease free H <sub>2</sub> O	-	up to 16 µl
70°C for 5 min, immediately chill on ice, then add followed components		
10×RT Buffer	1×	2 µl
Murine RNase inhibitor	1 U/µl	1 µl
M-MuLV Reverse Transcriptase	0,5 U/µl	1 µl
Total volume		20µl
	25 °C 5 min	
	42 °C 1 h	
	90 °C 10 min	

#### 2.2.1.5 Sequencing of DNA

Sequencing was carried out by MWG Eurofins Operon (Ebersberg, Germany). All of samples and primers were prepared according to the company's guidelines.

#### 2.2.1.6 Southern blot analysis

Southern blot hybridisation was carried out for analysis the gene targeted structures.

### **Preparation of DIG labelled probes**

For the detection of DNA on the membrane, DIG-labeled probe was amplified with digoxigenin-11-2'-deoxy-uridine-5'-triphosphate (20  $\mu$ M) and primers by GoTaq PCR. A control PCR reaction without DIG labeled UTPs was set up to compare the fragment shift of the DIG-labeled probe after agarose gel electrophoresis. The DIG-labeled probe was slightly larger than the control because of the higher molecular weight of DIG-labeled dUTPs. Then the DIG-labeled fragment was cut out from the gel and purified by using Wizard SV Gel and PCR Clean-Up System. The probe was stored at -20°C for the next research.

### **Southern blot**

For Southern blot analysis, 10  $\mu$ g genomic DNA were digested with 40 U restriction enzymes for 4 h at 37°C and then separated by agarose gel electrophoresis on a 1% TAE gel without ethidium bromide in order to avoid a high background. All samples were mixed with 5 $\times$ DNA loading buffer and loaded into the gel. In order to compare the fragment sizes of samples and the progress of separation, 6  $\mu$ l of 1 kb NEB ladder and 3  $\mu$ l of DIG labeled molecular weight marker VII were loaded into the gel as well. The gel was run at 40 V for 16 hours. Afterwards, the gel lane with 1 kb NEB ladder was cut off and stained with ethidium bromide for 20 minutes. By using the Bio Imaging System Gene Genius, the 1 kb NEB ladder was visualized. Compared with the ladder bands, the gel parts with DNA fragments which were unnecessary to retain were cut off from the gel to minimize the gel area for blotting. The gel was then incubated in 250 mM HCl for 10 minutes for DNA depurination and rinsed with water. Denaturation step was carried out by soaking the gel in denaturation solution at Room temperature for 15 minutes. After rinsing the gel with water, the gel was neutralized in neutralisation solution (0.5 M Tris-HCl (pH 7.5), 1.5 M sodium chloride) twice for 15 minutes at room temperature. Subsequently, the gel was equilibrated in 20 $\times$ SSC (3.0 M sodium chloride, 0.3 M sodium citrate, adjust with 1.0 M HCl to pH 7.0) for 10 min. All steps were performed with gentle shaking. The capillary blot was assembled according to the manual. After transferring the DNA onto the membrane, the membrane was washed by 2 $\times$ SSC and baked at 120°C for 30 min to link the DNA to the membrane. Then the membrane was incubated



with DIG Easy Hyb for 1 hour in a rotating hybridization glass tube at the properly hybridized temperature. In parallel, 7.5  $\mu$ l DIG-labeled probe (1.5  $\mu$ l probe per 1 ml hybridization buffer) were diluted in ddH<sub>2</sub>O to the final volume of 50  $\mu$ l and denatured for 5 min at 95°C. After cooling down the probe on ice, the hybridization solution was prepared by adding this denatured probe into 5 ml 37°C pre-warmed DIG Easy Hyb and the mixture was mixed thoroughly. The pre-hybridization solution was then removed from the hybridization glass tube and replaced by hybridization solution. To improve hybridization efficiency, hybridization took place over night at the properly hybridized temperature.

When hybridization finished, the membrane was washed with low stringency buffer (2 $\times$ SSC, 0.1% SDS) twice at room temperature for 15 minutes with gentle shaking. Afterwards, the membrane was incubated twice in 68°C pre-heated high stringency buffer (0.5 $\times$ SSC, 0.1% SDS) for 15 minutes at 68°C with gentle shaking. Subsequently, the membrane was soaked with washing buffer (0.1 M maleic acid, 0.15 M sodium chloride (adjusted with sodium hydroxide to pH 7.5), 0.3% Tween 20) for 2 minutes and blocking solution (0.1 M maleic acid, 0.15 M sodium chloride (adjusted with sodium hydroxide to pH 7.5), 1 $\times$ blocking solution) for 1 hour at room temperature with gentle shaking. After removing the blocking solution, the membrane was incubated in the antibody solution (Blocking solution, anti-Digoxigenin-AP, Fab fragments 1:1000) for 30 minutes at room temperature under shaking. Then the membrane was washed twice with washing buffer for 15 minutes at room temperature and equilibrated in detection buffer (0.1 M Tris-HCl, 0.1 M NaCl, pH 9.5) for 3 min at Room temperature. The membrane was put into an open plastic wrap and the CDP star solution which was diluted 1:100 in the detection buffer were dropwise added onto the membrane. After 5 minutes of incubation at room temperature, excess liquid in the plastic wrap was carefully squeezed off and the plastic wrap was sealed around the membrane. Developing and detection of the chemiluminescence was carried out by exposure of membrane to Lumi-Film-X-ray film for 15 to 60 minutes.

## **2.2.2 Microbiology methods**

### **2.2.2.1 Cultivation of *E.coli***

*E. coli* were grown over night at 37°C on either agar plates or in LB medium in an orbital shaker at 220 rpm. Based on different antibiotic resistance genes on plasmid DNA, agar plates and LB medium were supplemented with the appropriate antibiotic: such as 100 µg/ml ampicillin or 30 µg/ml kanamycin. Toward blue-white screening, agar plates were coated with 20 µl X-Gal (40 mg/ml in DMF) and 40 µl IPTG (100 mM in H<sub>2</sub>O) per plate prior to plating of bacteria. For Miniprep, 5 ml LB medium containing corresponding antibiotic were inoculated with a bacterial colony picked by a sterile toothpick. For liquid culture of 100 ml LB medium were inoculated with either 200 µl of an overnight culture or 100 µl aliquot of a glycerol stock solution.

#### **2.2.2.2 Transformation of *E.coli***

For transformation of electro-competent *DH10B E. coli*, a 50 µl aliquot of competent bacterial cells was thawed on ice and mixed with 1 µl of ligation solution. Then, the mixture was pipette into a pre-cooled 2 mm electroporation cuvette avoiding bubbles and pulsed for 5 ms at 2500 V in the electroporator. Cells were immediately incubated in 1 ml of LB medium (without antibiotics) and incubated at 37°C in an orbital shaker for 1 hour at 220 rpm. Afterwards, 100 µl to 300 µl of cell suspension were plated on agar plates containing corresponding antibiotics for selection and the plates were incubated at 37°C over night in an incubator.

#### **2.2.2.3 Storage of *E.coli***

For short period storage, agar plates with *E. coli* colonies can be stored at 4°C in the fridge. For long term storage of correct bacterial colonies, 750 µl of bacterial liquid were mixed with 250 µl sterile 99% glycerol and stored at -80°C.

### **2.2.3 Tissue culture methods**

#### **2.2.3.1 General cell culture**

All cells were cultivated with the corresponding medium in a humidified Steri-Cycle CO<sub>2</sub> incubator at standard conditions of 5% CO<sub>2</sub> and 37°C. The cell culture work was performed in the sterile class II laminar flow hood using plugged pipette tips and autoclaved material.

Generally, cultured cells were kept on observing in terms of cell morphology, confluence and viability under a microscope and medium was changed every other day. The amount of PBS, medium, detachment solution and growth area are showed in the table 2.5.

**Table 2.5: Cell culture vessels and cultural conditions**

Cell culture vessel	PBS (ml)	Medium (ml)	Detachment solution (ml)	Growth area (cm <sup>2</sup> )
24 well plate	0.1	0.5	0.1	$2.5 \times 10^5$
12 well plate	0.3	1	0.3	$5 \times 10^5$
6 well plate	0.5	2	0.5	$1.2 \times 10^6$
T-25 flask	1	5	1	$3.1 \times 10^6$
T-75 flask	5	15	5	$9.4 \times 10^6$
T-150 flask	15	25	15	$1.9 \times 10^7$

In order to avoid cells growing to more than 90% confluence, cultured cells had to be passaged regularly. Therefore, old medium was discarded and culture vessels were washed with appropriate amount of PBS. The cells were splitted by adding Accutase or Tripsion and incubated at 37°C for 3 to 5 minutes until cells completely detached. After gentle shaking of the culture vessel, cells were resuspended in suitable amount of fresh medium and pipette up and down several times for mixing. Then, after transferring a required volume of cells into a new dish containing pre-warmed medium, the dish was moved forward and backward to distribute evenly. The dish was migrated into the incubator for cultivation. Sometimes, an exact amount of cells required for the cell culture work, the cell numbers had to be determined by using either improved Neubauer counting chamber or counting machine.

### 2.2.3.2 Freezing and thawing of cells

During cell culture, it's often required to keep cells available for analysis over a prolonged range of time. Therefore, cells have to be frozen down according to the requirment of experiments and freezing cells can also avoid cell senescence and genetic drift. In addition, whenever we need to continue culture cells, cells can be thawed with appropriate method. The details protocol of freezing and thawing cells are described below.

For freezing of cells, the desired amount of cells was detached by Acutase and centrifuged at 300 g for 5 minutes to obtain cell pellet. Then the cell pellet was resuspended with freezing medium (10% DMSO, 50% FCS, 40% medium) and transferred into several 2 ml cryovials. Then those cryovials were immediately stored in Mr Frosty and transferred into -80°C. After 2 days, the cells were stored in the vapour above the liquid nitrogen in the tank.

Thawing of cells had to be conducted as quickly as possible due to the cytotoxicity of DMSO. Cells were thawed in a water bath at 37°C and then transferred into a 15 ml falcon containing 10 ml of pre-warmed medium immediately. The cells were centrifuged at 300 g for 5 minutes to get the cell pellet. Cell pellet was resuspended in suitable amount of fresh medium and transferred everything into a new culture vessel. At last, the cells were stored in the incubator without disturbing for at least 6 hours.

### **2.2.3.3 Isolation of porcine cells**

In the cell culture work, it is necessary to isolate various porcine cells according to the requirements of research. Therefore, pigs were slaughtered and desired tissues for cell isolation were kept at 37°C during transport to the laboratory. All required equipment and tissues were thoroughly cleaned with 80% ethanol before cell isolation. For the primary cell culture, the medium containing 100 µg/ml Penicillin/Streptomycin and 100 µg/ml Amphotericin B was used for the first 3 days in order to reduce the risk of contamination. After this period, antibiotic-free medium was applied and cells were culture according to the standard method described above.

### **Isolation and cultivation of porcine mesenchymal stem cells (poMSCs)**

Mesenchymal stem cells (MSCs) were isolated either from fat or bone marrow. For MSCs isolation from adipose tissues, 6 g of fat was minced into small pieces using scalpel. Minced tissues were then transferred into a 100 ml sterile glass flask containing 10 ml of a collagenase I solution (0.1% in PBS) and incubated at 37°C for 45 minutes with uninterrupted stirring. Subsequently, the mixture was filtered through a 100 µm filter into a new 50 ml falcon and an equal amount of pre-warmed medium was added into the falcon. Then the tube was

centrifuged at 600 g for 10 minutes and the cell pellet was resuspended in suitable amount of fresh medium containing antibiotic. Cells suspension liquid was pipetted up and down, seeded into two T-25 flasks and cultured.

Isolation of porcine bone marrow MSCs was performed from femur and tibia. The epiphyses of bone were opened by a saw and bone marrow was flushed with pre-warmed heparin solution (1000U heparin/ ml HBSS) into a 100 mm petri dish. A maximum amount of 20 ml of the cell suspension was loaded into 25 ml of lymphocyte separation medium LSM 1077 and centrifuged for 20 min at 1000g. The centrifuge acceleration and brake were switched to soft mode in order to prevent gradient disturbance. After centrifugation, mononuclear cells from the interphase were transferred into 20 ml HBSS for washing. Then the cell suspension were centrifuged at 600 g for 10 minutes and the cell pellets were resuspended in MSC medium containing antibiotics. The medium containing cells was transferred into two T-25 flasks and cultured in the incubator.

#### **Isolation and cultivation of porcine fetal fibroblasts (poFFs)**

In order to get porcine fetuses for the isolation of poFFs, sows were slaughtered at 28-30 days after fertilization and the uterus containing the embryos were excised. The uterus was opened carefully by sterile scissors and the amniotic sacs with the embryos were transferred into 100 mm<sup>2</sup> dishes which were containing pre-warmed PBS. The embryos were removed from the amniotic sacs carefully under the sterilized hoods. For each of the embryos, a foreleg was cut for genomic DNA isolation and a rare leg was separated for poFFs isolation. The rest bodies of embryo were transferred to the 50 ml tubes for fixation by 4% paraformaldehyde. The rare legs were then washed with 80% ethanol and PBS twice and digested in 0.5ml Trypsin-EDTA (1×) solution containing 2% chicken serum at 37 °C for 30 minutes with gentle vortexing. Subsequently, the digested mixture was transferred into a new 15 ml falcon containing 10 ml pre-warmed porcine fetal fibroblast medium (DMEM with 4.5 g/l glucose, 2 mM GlutaMAX, 1×NEAA, 1×sodium pyruvate, 10% FCS, 5 ng/ml FGF-2) and centrifuged at 300 g for 5 minutes. The cell pellets were resuspended by poFFs medium supplemented with 100 µg/ml Penicillin/Streptomycin and 100 µg/ml Amphotericin B and transferred into two

collagen deposited T-25 flasks for culturing in the incubator. After three days, the poFFs medium without Penicillin/Streptomycin and Amphotericin B was used instead. The poFFs medium was changed every 2 or 3 days after rinsing the cells once by PBS. Cells were passaged regularly by using Accutase to avoid more than 90% confluence of the cells growing.

### **Isolation and cultivation of porcine kidney fibroblasts**

For the isolation of porcine kidney fibroblasts, the tissues were minced and digested with collagenase II at 37°C for 30 minutes under gentle vortexing. Subsequently, the digested mixture was transferred into a new 15 ml falcon containing 10 ml pre-warmed porcine fibroblast medium (DMEM with 4.5 g/l glucose, 2 mM GlutaMAX, 1×NEAA, 1×sodium pyruvate, 10% FCS, 5 ng/ml FGF-2) and centrifuged at 600 g for 10 minutes. The cell pellets were washed by HBSS, spun down again and resuspended in fresh culture medium containing antibiotics. Cells were then seeded into two collagen deposited T25 flasks and passaged regularly by using Accutase to avoid more than 90 % confluence of the cells growing.

#### **2.2.3.4 Transfection of mammalian cells**

##### **Electroporation**

For transfection by using electroporation, cells were washed by PBS and detached with Accutase.  $1 \times 10^6$  cells were pelleted by centrifugation at 320 g for 5 minutes and resuspended in 800µl prewarmed (37°C) hypoosmolar electroporation buffer. 10 µg sterile DNA (dissolved in low-TE buffer) were added and the cell suspension was transferred to a 4 mm electroporation cuvette avoiding bubbles. Cells were pulsed at 1,200 V for 85 µs and incubated at room temperature for 5 minutes. Then, all liquid in the electroporation cuvette was equally splitted into two T-25 flasks containing fresh prewarmed medium. After 48 h, the medium containing appropriate concentration of G418 or blasticidin S for selection was replaced.

##### **Nucleofection**

Nucleofection of porcine MSCs was performed using the Amaxa Human MSC Nucleofector Kit (Lonza) according to the supplier's protocol.  $5 \times 10^5$  cells were pelleted by centrifugation at 320 g for 5 minutes and resuspended in 100  $\mu$ l nucleofection solution. 2  $\mu$ g sterile DNA (dissolved in low-TE buffer) were added and cell suspension was transferred to a nucleofection cuvette. The cells were pulsed by using the program "C-17" of the Amaxa Nucleofector. Subsequently, 500  $\mu$ l of fresh pre-warmed medium were added to the cuvette and all liquid was transferred to a T-25 flask containing prewarmed medium. After 48 h, the medium containing appropriate concentration of G418 or blasticidin S for selection was replaced.

### **Nanofection**

Nanofection was carried out by using the Nanofection kit (PAA) according to the manufacturer's manual. One day before transfection,  $3 \times 10^5$  cells were seeded in a 6-well plate. For each well, 3  $\mu$ g sterile DNA (dissolved in low-TE buffer) were mixed with 100  $\mu$ l Diluent in a sterile tube and 9.6  $\mu$ l Nanofectin were added to 100  $\mu$ l Diluent in a second sterile tube. Then, the nanofectin solution was transferred to the first sterile tube containing DNA and incubated at room temperature for 20 minutes. Meanwhile, cells were washed with PBS and 2 ml fresh pre-warmed medium were added to each well. The final mixture was added dropwise to the cells of each well. After 2-4 hours, the medium was changed because of the toxic side-effects of Nanofectin to cells.

### **Stemfect RNA transfection**

RNA transfection was performed using Stemfect RNA Transfection Kit by Stemgent®. Cells were harvested using Accutase and  $3 \times 10^5$  cells were seeded in 1 well of a 6 well plate (12 well plate) and incubated at 37°C until 90% confluency. 1-2 hours prior transfection the medium was aspirated and 2 ml (1 ml) of new medium was added. The Stemfect RNA Transfection Reagent and the Stemfect Transfection Buffer was warmed to room temperature, while the mRNA was thawed on ice. 60  $\mu$ l (25  $\mu$ l) of Stemfect Transfection Buffer was added in 2 sterilized tubes. To the first tube 4  $\mu$ l (2  $\mu$ l) of Stemfect RNA Transfection Reagent and to the second tube 300-500 ng of RNA was added. Then the first tube was mixed with the second tube and incubated for 20-25 min at room temperature. The entire mRNA transfection

complex was added dropwise to the cells and to ensure an even distribution within the well the plate was gently rocked crosswise. Cells were incubated at 37°C and medium was changed every 2 days.

### **2.2.3.5 Selection of transfected cells and picking clones**

After 48 hours after transfection, cells cultured in the T-25 flasks were splitted 1:3 to the 15 cm dishes containing corresponding medium with 500 µg/ml G418 or 8 µg/ml blasticidin S. The selective medium was changed every other day and obvious single cell colonies were formed roughly after 10-15 days for selection. The visible colonies were picked by either filter paper or plastic rings. For using the method of filter paper, the cells were washed with PBS and the Accutase soaked filter papers were placed on the top of each colony for 2 minutes. Filter papers were transferred to 24-well plates with pre-warmed fresh medium supplemented with G418 or blasticidin S. The filter papers were removed after 48 hours. For using rings method, after cells washing with PBS, the rings touched with suitable amount of glue were surrounded each colony. 100 µl Accutase were added directly to the colonies for 2 minutes and 100 µl pre-warmed medium were applied. Finally, the 200 µl cell suspension was transferred to 24-well plates with pre-warmed fresh medium supplemented with G418 or blasticidin S. After cells reaching 80-90% confluence, cells were passaged and checked the targeted events by screening PCR.

### **2.2.3.6 PCR and RT-PCR from cell culture**

#### **Screening PCR from cell culture**

To screen the correct gene targeting of single-cell colonies, cells cultured in the 24-well were washed once with PBS, detached with 100 µl Trypsin-EDTA per well and mixed with 100 µl pre-warmed MSCs medium. 100 µl of this cell suspension were aliquoted into a new 24-well plate for continued culturing, whereas the residual 100 µl of the cell suspension were pipetted into a PCR tube for genomic DNA isolation by using IPGAL method (see 2.2.1.1). Each screening PCR was performed by using 6 µl aliquot of the genomic DNA solution.

#### **RT-PCR from cell culture**



Cells were detached with suitable amount of Accutase and the RNA isolation was carried out by using the SurePrep™ TrueTotal™ RNA Purification Kit (Fisher) according to the supplier's protocol (see 2.2.1.1).

#### **2.2.3.7 $\beta$ -Galactosidase staining of eukaryotic cells**

$5 \times 10^5$  cells were seeded in 6-well plates one day before  $\beta$ -Galactosidase staining. After aspiration of medium, cells were rinsed with PBS once and fixed with 2 ml of fixation solution (2% Formaldehyde and 0.2% Glutaraldehyde in PBS) for 5 to 10 minutes at room temperature. The fixation solution was aspirated and the cells were washed with PBS 3 to 5 times. Subsequently, the staining solution (1 mg/ml X-Gal) was added in the 6-wells and the cells were stained in the staining solution at 37°C for 20 hours in the bacterial incubator. After staining, the cells were washed with PBS in order to remove staining solution and kept the cells in PBS to avoid drying.

#### **2.2.3.8 Cell preparation for somatic cell nuclear transfer (SCNT)**

The gene-targeted clones were thawed and induced to cell cycle synchronization by serum starvation. Two days before the somatic cell nuclear transfer, MSC medium was replaced with starvation MSC medium which contained only 0.5% FCS and were lack of FGF.

#### **2.2.3.9 Cre transduction**

Cre protein was produced in vitro with the vector pTriEx-HTNC (Addgene plasmid 13763) according to the method described by Peitz et al [261] and Müntz et al [262].  $4 \times 10^4$  cells were seeded in a 24 well dish and cultured with 5  $\mu$ M purified Cre recombinase in culture medium containing 0.5% serum for 8 hours. Afterwards, medium was replaced with standard medium and culture continued.

#### **2.2.3.10 Cryosection**

Around 1 cm<sup>3</sup> tissues of brain, skin, bladder, spleen, liver, colon, heart, lung from TGROSA transgenic fetuses were embedded into the OCT embedding compound, frozen down on the dry ice and stored in -80°C for a long period. The embedded tissue probes were sliced into 5  $\mu$ m sections by the cryosection machine and detected the fluorescence under microscope.

### **2.2.3.11 Whole animal Tomato fluorescence**

Tomato fluorescence was revealed in foetuses and piglets using a hand held flashlight with excitation light source UFP-MDS-G2/B/HB, photographs were taken using camera filter FS/CEF-4R2 (Biological Laboratory Equipment Maintenance And Service Ltd., Hungary).

## 3 Results

### 3.1 Identification of porcine *ROSA26* gene

To identify *ROSA26* locus in the porcine genome, the nucleotide sequence of the promoter region and exon 1 of *Rosa26* in mouse (NR\_027008.1) were used as a reference sequence to align with the NCBI *Sus scrofa* 10.2 porcine genome assembly. A highly conserved genomic region on porcine chromosome 13 (NW\_003611693: 29648-30716), which shares 85%, 86% and 91% similarity with the promoter region of mouse, rat, human *ROSA26* promoter and exon 1 respectively, was identified. Then, the forward primer binding on identified porcine *ROSA26* exon1 region was used for the 3' RACE (rapid amplification of cDNA end) and an 800 bp fragment was amplified (Figure 3.1). Alignment of the 3'RACE amplified fragment for porcine *ROSA26* gene with the porcine genomic sequence (NW\_003611693) indicated that exon 2 has a size of 112 bp, exon 3 is 118 bp and exon 4 is 480 bp in size. The sequence of porcine *ROSA26* gene was submitted into the NCBI and got the accession number: KF768776. The 3' *ROSA26* cDNA sequence overlaps the 3' region of an adjacent gene *THUMPD3*. The primers located in porcine *ROSA26* exon 1 and 2, and primers binding on *ROSA26* exon 1 and 4 were used to investigate the expression pattern of porcine *ROSA26* gene in wild type pig. The RT-PCR results showed similar levels of expression in all porcine tissues examined (Figure 3.2).

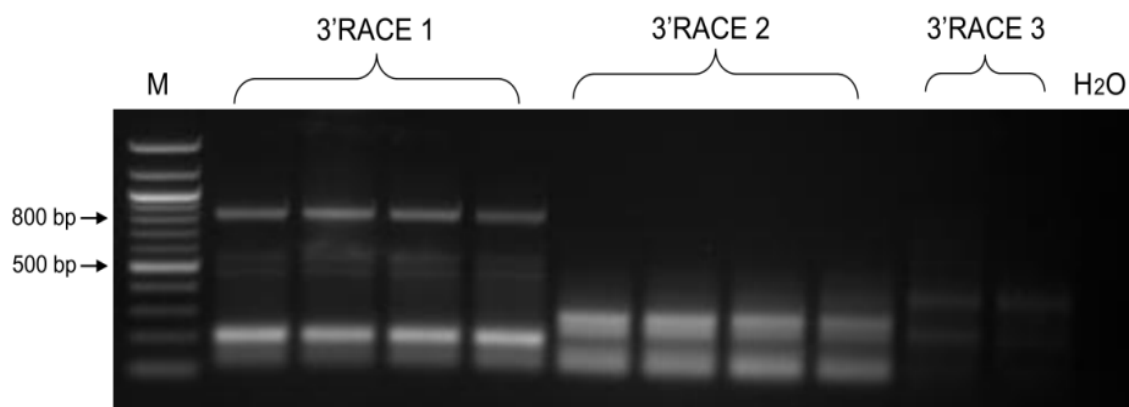


**Figure 3.1: PCR of porcine *ROSA26* 3'RACE.** 3'RACE 1, 2 and 3 indicate the *ROSA26* 3'RACE results by using three different forward primers and correct 800 bp fragments were amplified by using the forward primer 1. H<sub>2</sub>O was used as a negative control. Kidney RNA isolated from a wild type pig was reverse transcribed to cDNA which was used as the template for performing 3'RACE. M, NEB 100 bp ladder.

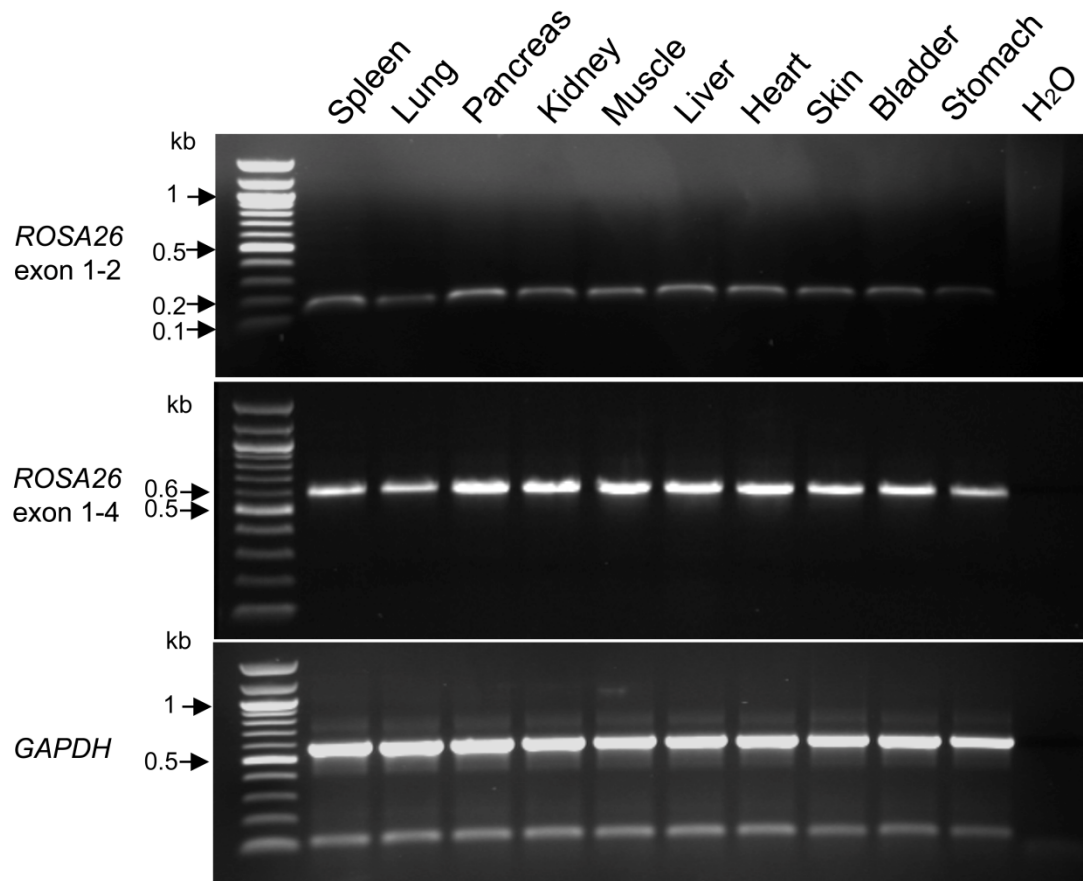


**Figure 3.2: Expression of porcine *ROSA26* in different adult wild type tissues detected by RT-PCR.** The primers anneal in exon 1 and exon 2 and amplify a correctly spliced product of 168 bp (top). The primers anneal in exon 1 and exon 4 and amplify a correctly spliced product of 621 bp (middle). *GAPDH* expression was used as a control for RNA quality (below).

## 3.2 Construction of *ROSA26* gene targeting constructs

### 3.2.1 Construction of the GCROSA targeting vector

The DNA sequence on porcine chromosome 13 (NCBI accession number NW\_003611693) was used to generate the promoter trap *ROSA26* gene targeting vector which was named GCROSA (Figure 3.3). GCROSA comprised: a 2.166 kb 5' short arm of homology corresponding to a region of *ROSA26* intron 1 from position 32043 to 34208

(NW\_003611693); a 159 bp adenoviral splicing acceptor; a 7.739 kb floxed  $\beta$ -geo cassette (loxP-beta-geo-loxP); a 1.681 kb mCherry-poly A cassette; a 4.675 kb 3' homology long arm. The 7.739 kb floxed  $\beta$ -geo cassette (loxP- $\beta$ -geo-loxP) of targeting vector comprised: a 34 bp loxP site; a 3.707 kb promoterless  $\beta$ -geo cassette; three polyadenylation signals derived from SV40, bovine growth hormone and cytomegalo virus (CMV); a 3.053 kb HPRT Stuffer sequence; a second loxP site.

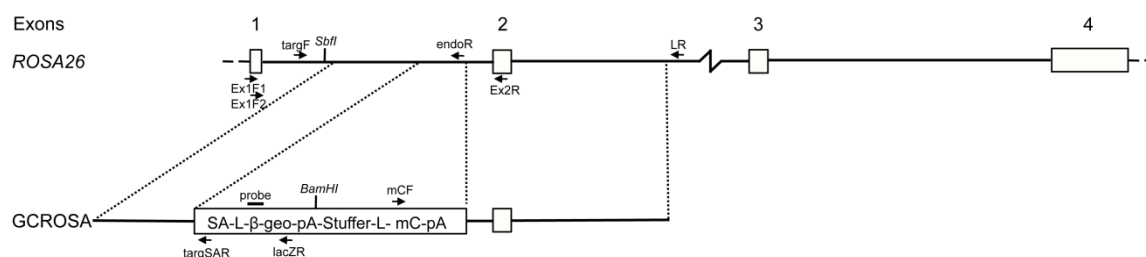


**Figure 3.3: Schematic diagram of wild type porcine *ROSA26* gene and the GCROSA26 targeting vector.** Top. Porcine *ROSA26* gene. Exon numbers are indicated. Below. GCROSA targeting vector. PCR and RT-PCR primers used to identify targeted cell clones and detect mRNA are indicated. *SbfI* and *BamHI* restriction sites and the hybridisation probe used for Southern analysis are also shown.

### 3.2.2 Construction of the TGROSA targeting vector

The DNA sequence on porcine chromosome 13 (NCBI accession number NW\_003611693) was used to generate the promoter trap *ROSA26* gene targeting vector which was named TGROSA (Figure 3.4). TGROSA comprised: a 2.110 kb 5' short arm of homology corresponding to a region of *ROSA26* intron 1 from position 32043 to 34152 (NW\_003611693); a 159 bp adenoviral splice acceptor; a 426 bp promoterless blasticidin resistance gene (*bsr*) followed by two polyadenylation signals derived from SV40 and the bovine growth hormone gene; a 1.715 kb CAG promoter; a 2.440 kb membrane-targeted tdTomato (mTomato) gene flanked by two loxP sites; a 1.099 kb membrane-targeted EGFP (mEGFP) gene; and a 4.647 kb 3' long arm of homology. The mTomato and mEGFP cassette was derived from Addgene (plasmid no. 17787).

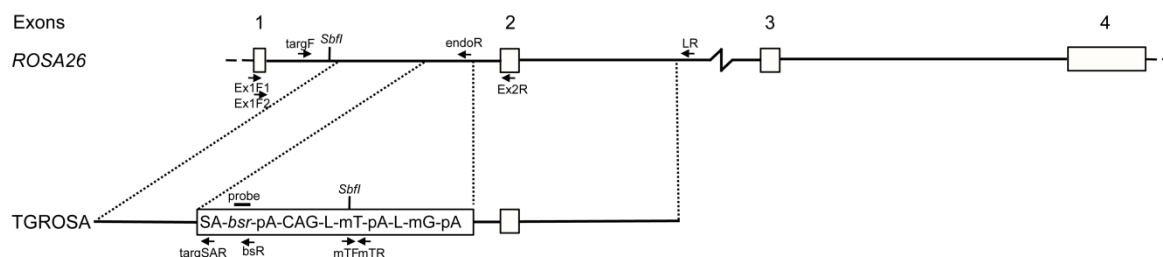


**Figure 3.4: Schematic of wild type porcine *ROSA26* gene and the TGROSA targeting vector.** Top. Porcine *ROSA26* gene. Exon numbers are indicated. Below. TGROSA targeting vector. PCR and RT-PCR primers used to identify targeted cell clones and detect mRNA are indicated. *SbfI* restriction sites and the hybridisation probe used for Southern analysis are also shown.

### 3.2.3 Linearization of targeting vectors

Uncut plasmid DNA has three conformations: supercoiled, open circular and linear. If the plasmid is cut once by a restriction enzyme, the supercoiled and open circular conformations are reduced to a linear conformation. It has been reported that linearized plasmids enhance the homologous recombination frequency about 10-fold in mammalian somatic cells [263]. Therefore, before transfection, GCROSA and TGROSA targeting vectors were linearized with the *NotI* and *MluI* respectively (Figure 3.5). After linearization of targeting vectors, the DNA of targeting vectors was precipitate by using NaAC/ethanol method.

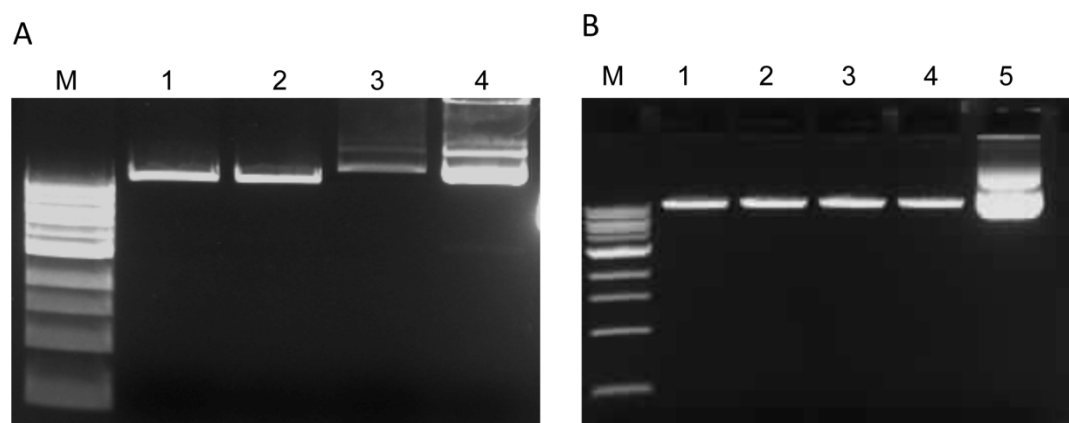


**Figure 3.5: Linearization of targeting vectors.** A. Lane 1-2, linearised GCROSA targeting vector; lane 3-4, undigested GCROSA targeting vector as a control. B. Lane 1-4, linearised TGROSA targeting vector; lane 5, undigested TGROSA targeting vector as a control. M, NEB 1 kb ladder.

## 3.3 Porcine *ROSA26* gene targeting

Mesenchymal stem cells (MSCs) were isolated from adipose tissue and bone marrow of pure

German landrace male pig. The characterization of MSCs was confirmed via differentiation assay. MSCs capable of differentiation into osteogenic, adipogenic and chondrogenic lineages were used for cell targeting (MSCs were obtained from Chair of Livestock Biotechnology, TUM).

### 3.3.1 Transfection and selection of MSC clones

For the GCROSA targeting vector, the MSCs isolated from bone marrow were used for transfection, and MSCs derived from adipose tissues were used for the transfection of TGROSA targeting vector. Electroporation was used for the transfection of the two targeting vectors. The GCROSA and TGROSA targeting vectors contain promoterless G418 and *bsr* resistance marker respectively. The promoterless selection markers targeted into the porcine *ROSA26* intron 1 can be driven by the endogenous *ROSA26* promoter. This promoter trap approach can improve the efficiency of gene targeting. For the GCROSA targeting, the clones were picked after around 10-15 days of selection. Regarding TGROSA targeting, the clones were checked under fluorescence microscope, and only clones with mTomato expression were picked because it is a sign of intact cassette integration.

### 3.3.2 PCR screening for gene targeting events

After picking the clones, single-cell clones were expanded and screened by PCR. The 2.6 kb DNA fragments were amplified by using forward primer, which hybridizes to a point in the *ROSA26* intron 1 outside of the 5' homologous arm of targeting vector and reverse primer, which hybridizes to the splice acceptor. In order to assess the DNA quality and detect the existence of single or double *ROSA26* targeted allele in screened samples, endogenous PCRs were performed for each sample. The 3.2 kb endogenous fragment were amplified by using the same forward primer as above and another reverse primer, which hybridizes the *ROSA26* intron 1 that has been deleted on the targeted allele. Twenty-four of fifty (48%) GCROSA transfectants and sixteen of thirty-eight (42%) TGROSA transfectants were identified as targeted according to the targeting PCR results. Representative screening results are shown in Figure 3.6 and 3.7. All of the screened clones were amplified correct

endogenous fragment, indicating only one *ROSA26* allele was targeted and sufficient DNA was present in screened samples (Figure 3.6 and 3.7).

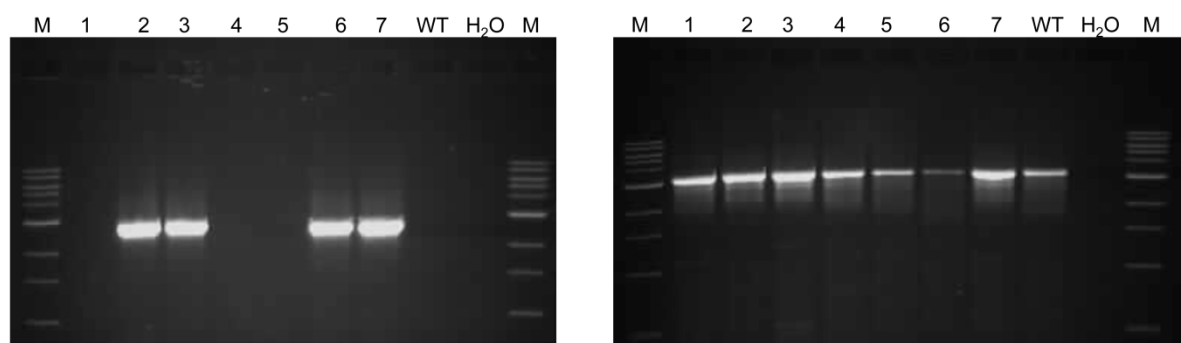


**Figure 3.6: PCR screening of GCROSA targeting events.** A part of results of targeting PCR (left) and endogenous PCR (right) for G418 resistant single-cell clones. The size of positive targeting PCR product is 2.6 kb and the length of endogenous PCR fragment is 3.2 kb. WT (wild type DNA) and H<sub>2</sub>O were used as negative control. M, NEB 1 kb ladder.

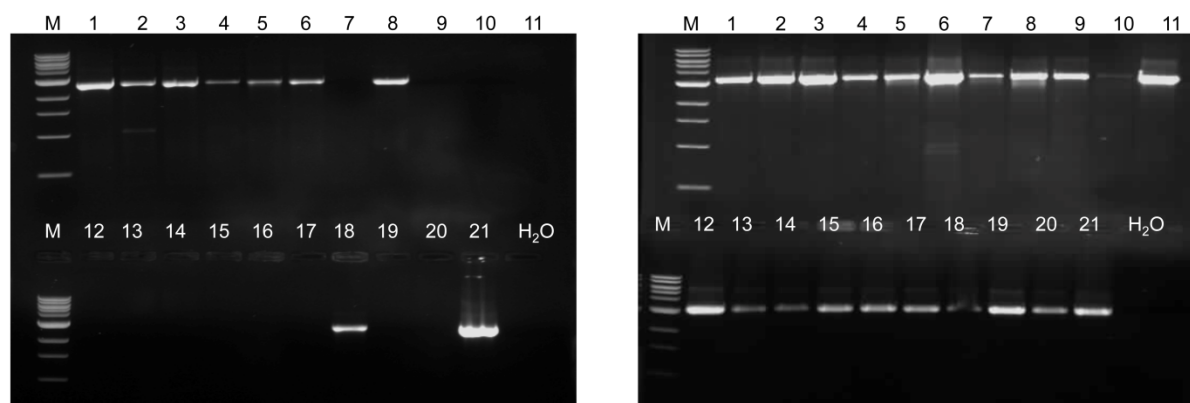


**Figure 3.7: PCR screening of TGROSA targeting events.** Selected results of targeting PCR (left) and endogenous PCR (right) for *bsr* resistant single-cell clones. The size of positive targeting PCR product is 2.6 kb and the length of endogenous PCR fragment is 3.2 kb. WT (wild type DNA) and H<sub>2</sub>O were used as negative control. M, NEB 1 kb ladder.

### 3.3.3 RT-PCR analyses of *ROSA26* targeted clones

The cell clones positive for targeting PCR were chosen to isolate RNA and analyse on the RNA level. GCROSA transfectants with correctly targeted cassette in the *ROSA26* intron 1 are able to express mRNA from the *ROSA26* exon 1 spliced to the  $\beta$ -geo cassette. For TGROSA transfected clones with correctly targeted cassette in the *ROSA26* intron 1 can express mRNA from the *ROSA26* exon 1 spliced to the blasticidin selectable gene (*bsr*). The RT-PCR screening was established using forward primer that hybridizes in *ROSA26* exon 1



and reverse primer hybridizing in the  $\beta$ -geo cassette or blasticidin selectable gene (*bsr*) respectively. Figure 3.8 A shows the RT-PCR screening of GCROSA targeted clones, and the four tested clones indicated the correct 750 bp fragment. For TGROSA targeted clones, RT-PCR results (Figure 3.8 B) showed correct 500 bp fragment for six out of seven screened clones. Wild type cDNA were used as negative control and no fragments were amplified as predicted.

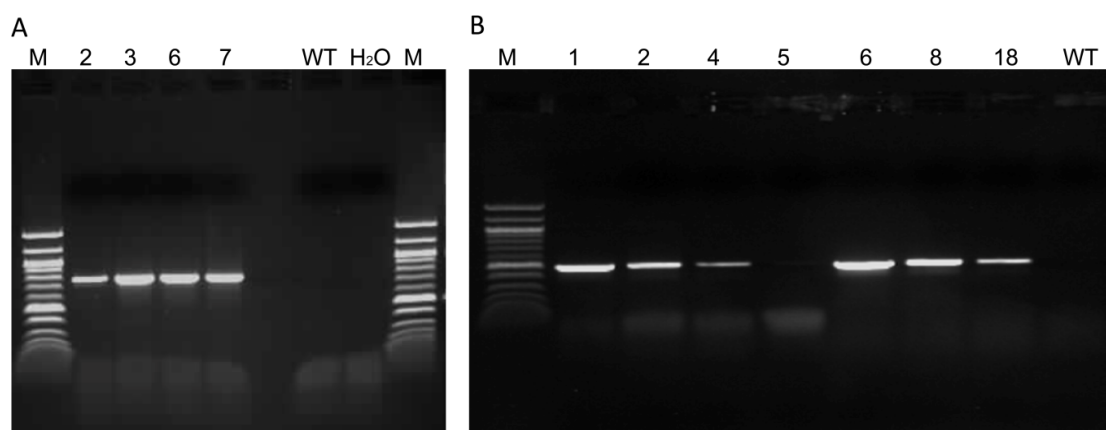


**Figure 3.8: RT-PCR screening of GCROSA (A) and TGROSA (B) targeted MSCs clones.** A: Selected results of RT-PCR detection of GCROSA targeted *ROSA26* RNA from exon1 splice to  $\beta$ -geo. Amplified fragment size: 750 bp. B: Selected results of RT-PCR detection of TGROSA targeted *ROSA26* RNA from exon1 splice to *bsr*. Amplified fragment size: 500 bp. WT (wild type cDNA) and H<sub>2</sub>O were used as negative control. M: NEB 100 bp ladder.

### 3.3.4 Southern blot analyses of *ROSA26* targeted clones

Southern blot was performed for the positive clones to confirm the structure of the targeted *ROSA26* alleles and to exclude random integrants. For this, two different probes were used: the  $\beta$ -geo probe for GCROSA and the *bsr* probe for TGROSA targeted MSC clones. Southern blot analysis of selected GCROSA MSC clones 2, 3, 6 and 12 showed expected 5644 bp fragment, while clone 7 indicated random integration due to an unpredicted fragment at 8.5 kb (Figure 3.9). For selected TGROSA targeted MSC clones, southern blot results demonstrated correct 5783 bp fragment in MSC clones 1, 2, 4, 6 and 18, confirming right *ROSA26* targeted structure for those clones, while clones 5, 8 and 9 showed no fragment, indicating incorrect targeted structure in these clones (Figure 3.10).

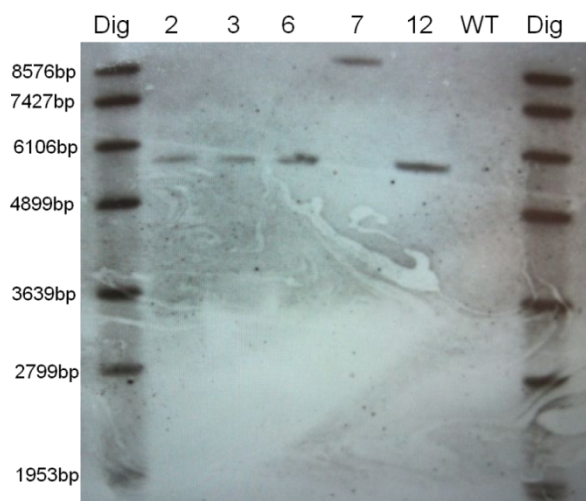


**Figure 3.9: Selective results of southern blot analysis for GCROSA targeted cell clones.** Lanes show *SbfI* and *BamHI* double digested genomic DNA from five GCROSA targeted MSC clones 2, 3, 6, 7, 12 and wild type DNA. The probe binds on the  $\beta$ -geo cassette and the 5644 bp diagnostic fragment detected by the  $\beta$ -geo probe is shown.

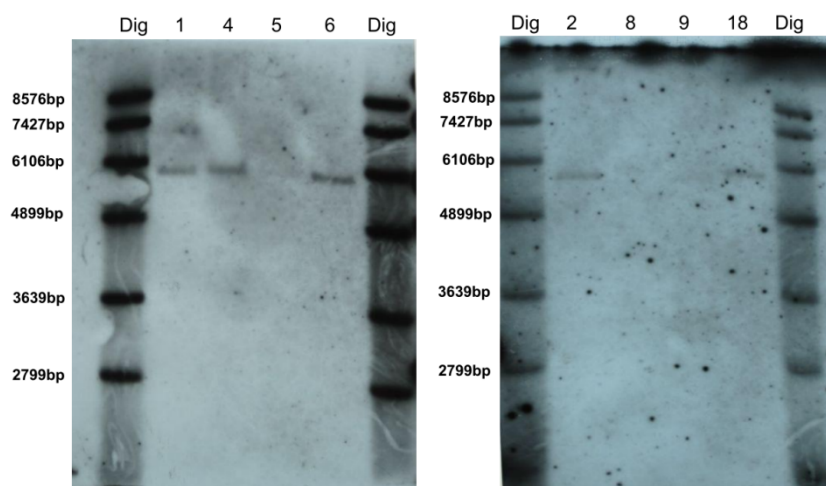


**Figure 3.10: Selective results of southern blot analysis for TGROSA targeted cell clones.** Lanes show *SbfI* digested genomic DNA from eight TGROSA targeted MSC clones 1, 2, 4, 5, 6, 8, 9 and 18. The probe binds on the *bsr* cassette and the 5783 bp diagnostic fragment detected by the *bsr* probe is shown.

### 3.3.5 lacZ staining and activation of mCherry for GCROSA targeted MSC cell clones

The correct GCROSA targeted allele leads to the  $\beta$ -geo expression prior to Cre excision and mCherry activated after Cre recombination (Figure 3.11). The lacZ staining was carried out to check the expression of  $\beta$ -geo of the GCROSA26 targeted MSC clones. The positive targeted clones were stained blue because the *ROSA26* promoter drives the lacZ gene that encodes

the bacterial enzyme  $\beta$ -galactosidase expression, which can cleave the substrate X-gal into blue precipitates. After lacZ staining, representative GCROSA targeted MSC clone was stained blue, indicating the expression of  $\beta$ -geo (Figure 3.12). GCROSA targeted MSC clone showed no mCherry fluorescence without processing Cre protein transduction, which indicate the polyadenylation cassette after  $\beta$ -geo was sufficient to block the expression of mCherry expression. After Cre protein transduction, the mCherry fluorescence gene was activated in GCROSA targeted MSC clone, which demonstrate that mCherry activation is Cre-dependent (Figure 3.12). MSCs transfected with CAG promoter directed  $\beta$ -geo/mCherry constructs were used as a control, which were produced by Simon Leuchs (Figure 3.12).

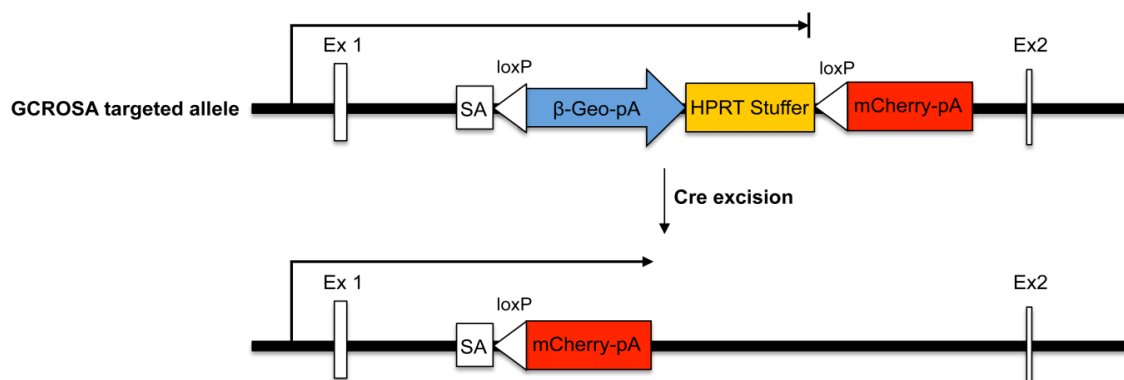


**Figure 3.11: Schematic overview of dual reporter system of GCROSA targeted allele.** Top. The GCROSA targeted allele leads to  $\beta$ -geo expression and blockade of mCherry expression before Cre excision. Below. Cre protein mediates excision of  $\beta$ -geo and activation mCherry gene expression. Ex1 and Ex2 indicate porcine *ROSA26* exon 1 and 2. SA, splice acceptor.

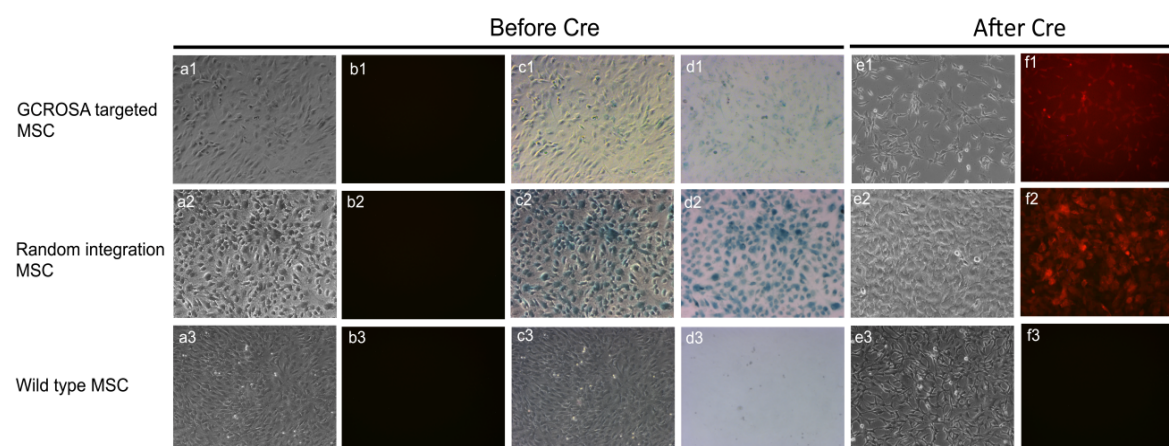


**Figure 3.12: lacZ staining and Cre protein mediated mCherry activation of reporter constructs.** a1-3, e1-e3, black and white channel. b1-b3, f1-f3, red fluorescence channel. c1-c3, non-filtered color channel. d1-d3, color channel with gray filter. Top panels, GCROSA targeted MSCs; middle panels, MSCs transfected with CAG promoter directed  $\beta$ -geo/mCherry constructs. Wild type MSCs were used

as negative control.

### 3.3.6 Activation of mEGFP expression for TGROSA targeted MSC clones

The correct TGROSA targeted allele leads to mTomato expression prior to Cre excision and mEGFP activated after Cre recombination (Figure 3.13). For TGROSA targeted MSC clones, only mTomato and no mEGFP expression was observed (Figure 3.14). This indicates that the polyadenylation cassette after mTomato cassette blocked the expression of mEGFP. To determine whether double reporter system functions effectively as a Cre reporter, the effects of Cre protein transduction into TGROSA targeted MSC cells was examined. After 8 hours of Cre transduction, both the mTomato fluorescence and mEGFP fluorescence could be detected for the TGROSA targeted cells. A steady decline in double-labeled cells was observed after about 8 days interval for loss of mTomato in nearly all mEGFP labeled cells. This demonstrates that mEGFP labeling is Cre-dependent (Figure 3.14).

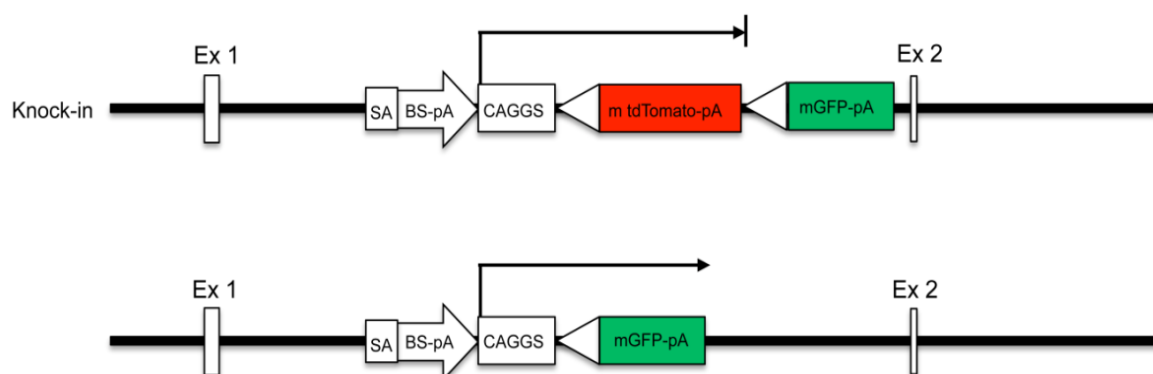


**Figure 3.13: Schematic overview of dual reporter system of TGROSA targeted allele.** Top. The TGROSA targeted allele leads to mTomato expression and blocking of mGFP expression before Cre excision. Below. Cre protein mediates losing of mTomato and activated mGFP expression. Ex1 and Ex2 indicate porcine *ROSA26* exon 1 and 2. SA, splice acceptor.

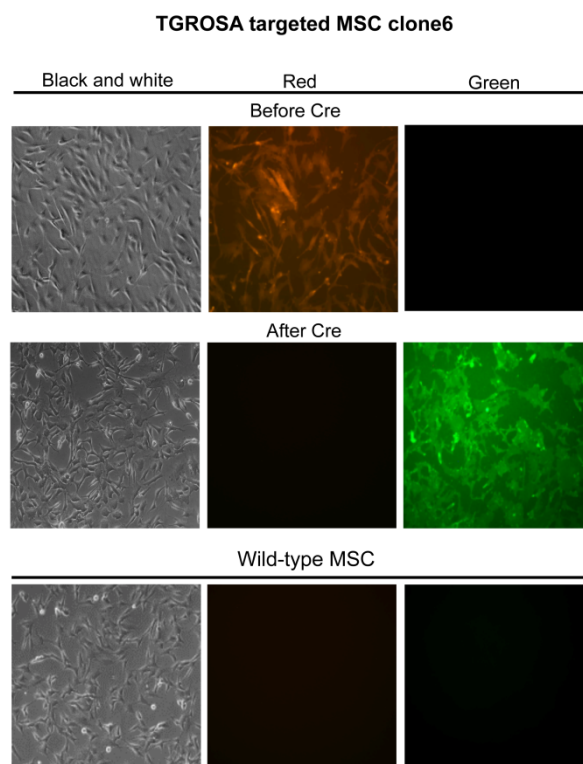


**Figure 3.14: Cre-induced loss of Tomato and activation of GFP fluorescence in TGROSA targeted MSC cell clones.** Fluorescence before, and eight days after Cre transduction as indicated. Wild-type MSCs are shown.

### 3.4 Generation of *ROSA26* targeted fetuses and pigs

In order to generate *ROSA26* gene targeted pigs, correctly GCROSA and TGROSA targeted MSC clones were used for nuclear transfer (NT). This part of work was conducted in the collaborative Institute of Molecular Animal Breeding and Biotechnology (Prof. Dr. Wolf, LMU). For each NT, three GCROSA targeted clones (2, 3 and 6) were mixed. Two rounds of nuclear transfer experiment were carried out and reconstructed embryos were transferred into 4 recipients. One pregnancy was established and two fully developed male piglets #132 and #133 were born. However, those two piglets showed macroglossia causing asphyxia and death after birth. To obtain TGROSA targeted pigs, three TGROSA targeted cell clones (4, 6 and 18) were pooled and used for nuclear transfer and pregnancies established. One pregnant sow was sacrificed and four fetuses explanted for analysis. Other pregnancies were allowed to continue to birth. One normal healthy piglet (#131) was unfortunately killed by the sow. Two normal healthy piglets (#258 and #265) were born, and when mature these will be mated and used to found a reporter pig line.

### 3.4.1 Analysis of GCROSA targeted piglets by PCR and southern blot

GCROSA targeted piglets were analysed by 5' and 3' terminal region PCR, indicating that genotype of pigs is identical to the original cell clones (Figure 3.15 A and B). The endogenous PCR shows one porcine *ROSA26* allele was targeted both in piglet #132 and #133, which is consistent with the original cell clones (Figure 3.15 C).

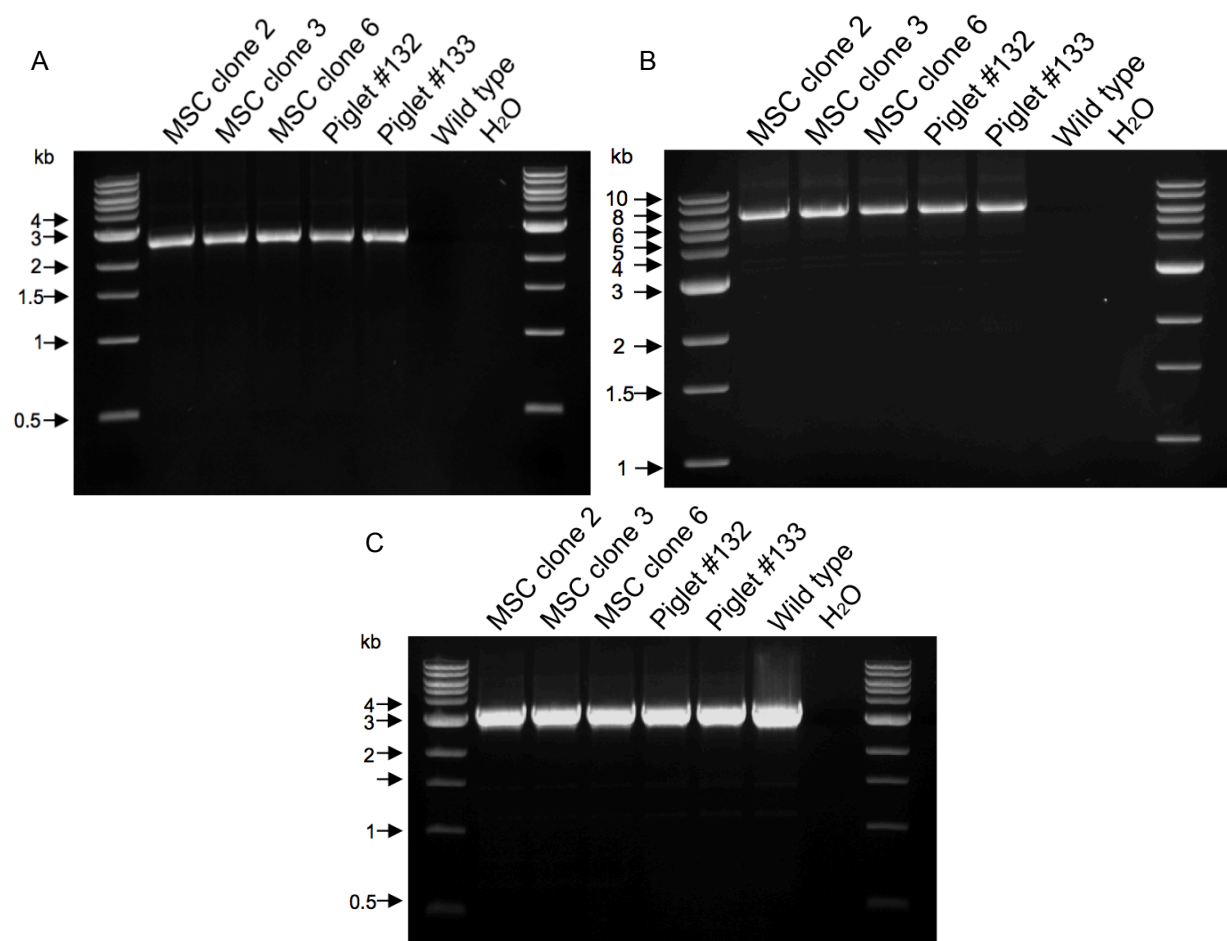


**Figure 3.15: PCR screening of GCROSA nuclear transfer derived piglet #132, #133 and original GCROSA targeted MSC clones 2, 3 and 6.** A, PCR detection of GCROSA targeted 5' terminal region. Amplified fragment size: 2616 bp. B, PCR detection of GCROSA targeted 3' terminal region. Amplified fragment size: 6331 bp. C, Endogenous PCR detection of wild type *ROSA26* allele. Amplified fragment size: 3206 bp.

The southern blot analysis was subsequently performed to confirm the structure of targeted allele for the GCROSA piglet #132 and #133. Figure 3.16 shows that a diagnostic 5644 bp fragment was detected both in piglet #132 and #133, like in the original MSC clone 2, 3 and 6.

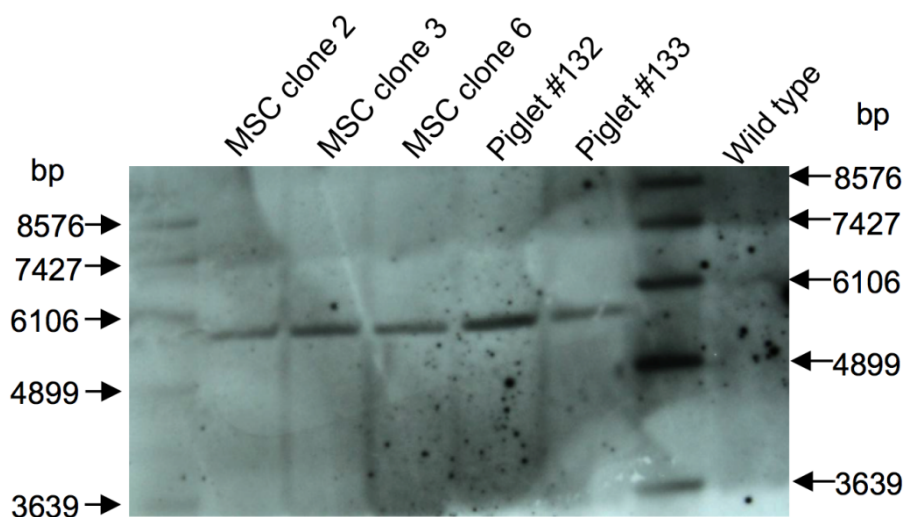


**Figure 3.16: Southern blot analysis of GCROSA targeted porcine *ROSA26*.** Lanes show *SbfI* and *BamHI* double digested genomic DNA from three GCROSA targeted MSC clones 2, 3 and 6, two newborn piglet #132 and #133, and a wild type piglet as indicated. The probe binds on the  $\beta$ -geo cassette and the 5644 bp diagnostic fragment detected by the  $\beta$ -geo probe is shown.

### 3.4.2 Analysis of GCROSA targeted piglets by RT-PCR

Tissues of spleen, lung, pancreas, kidney, muscle, liver, heart and skin were collected from the GCROSA targeted piglet #132, and total RNA was isolated from each tissues respectively. The RT-PCR was performed to check the presence of RNA transcribed from the *ROSA26* promoter extending from exon 1 spliced to the  $\beta$ -geo. RT-PCR results showed the presence of predicted amplified 750 bp fragment in all the tested tissues (Figure 3.17).

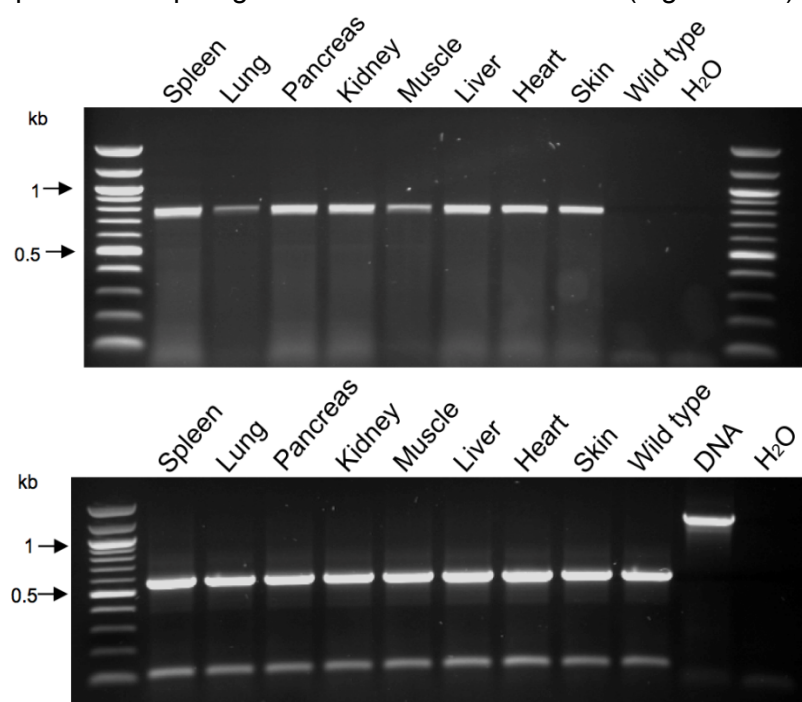


**Figure 3.17: RT-PCR screening of GCROSA nuclear transfer derived piglet #132.** Top: RT-PCR detection of targeted *ROSA26* RNA from exon1 splice to  $\beta$ -geo in different tissues derived from GCROSA piglet #132. Amplified fragment size: 750 bp. Below: RT-PCR performed for porcine housekeeping gene *GAPDH* in different tissues derived from GCROSA piglet #132. Wild type cDNA, DNA, and H<sub>2</sub>O were used as controls. Amplified fragment size: 575 bp.

### 3.4.3 lacZ staining and activation of mCherry for fibroblasts derived from GCROSA piglet

Kidney fibroblasts (pKDNF) isolated from GCROSA targeted piglet #132 showed no mCherry fluorescence detected before Cre recombination (lack of leakiness), and pKDNF were stained into light blue colour after lacZ staining (Figure 3.18). Cloned foetuses derived from MSCs transfected with CAG promoter directed  $\beta$ -geo/mCherry constructs were used as control, which were produced by Simon Leuchs. Fibroblasts isolated from CAG  $\beta$ -Geo/mCherry randomly integrated foetuses were stained dark blue and no mCherry fluorescence visible before Cre excision (Figure 3.18). After Cre protein transduction, fibroblasts from CAGGS  $\beta$ -Geo/mCherry randomly integrated foetuses showed stronger mCherry fluorescence than pKDNF isolated from piglet #132 (Figure 3.18).

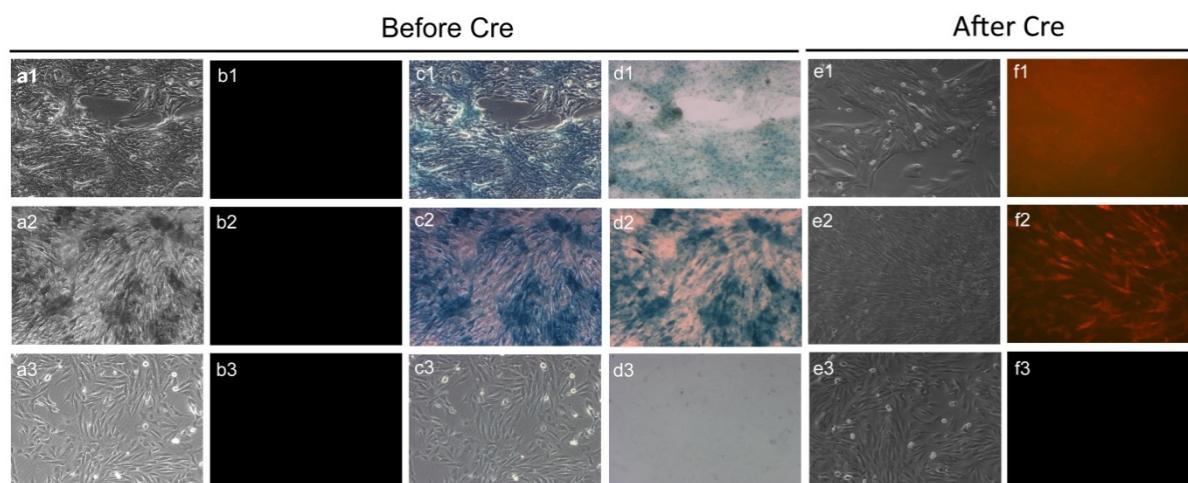
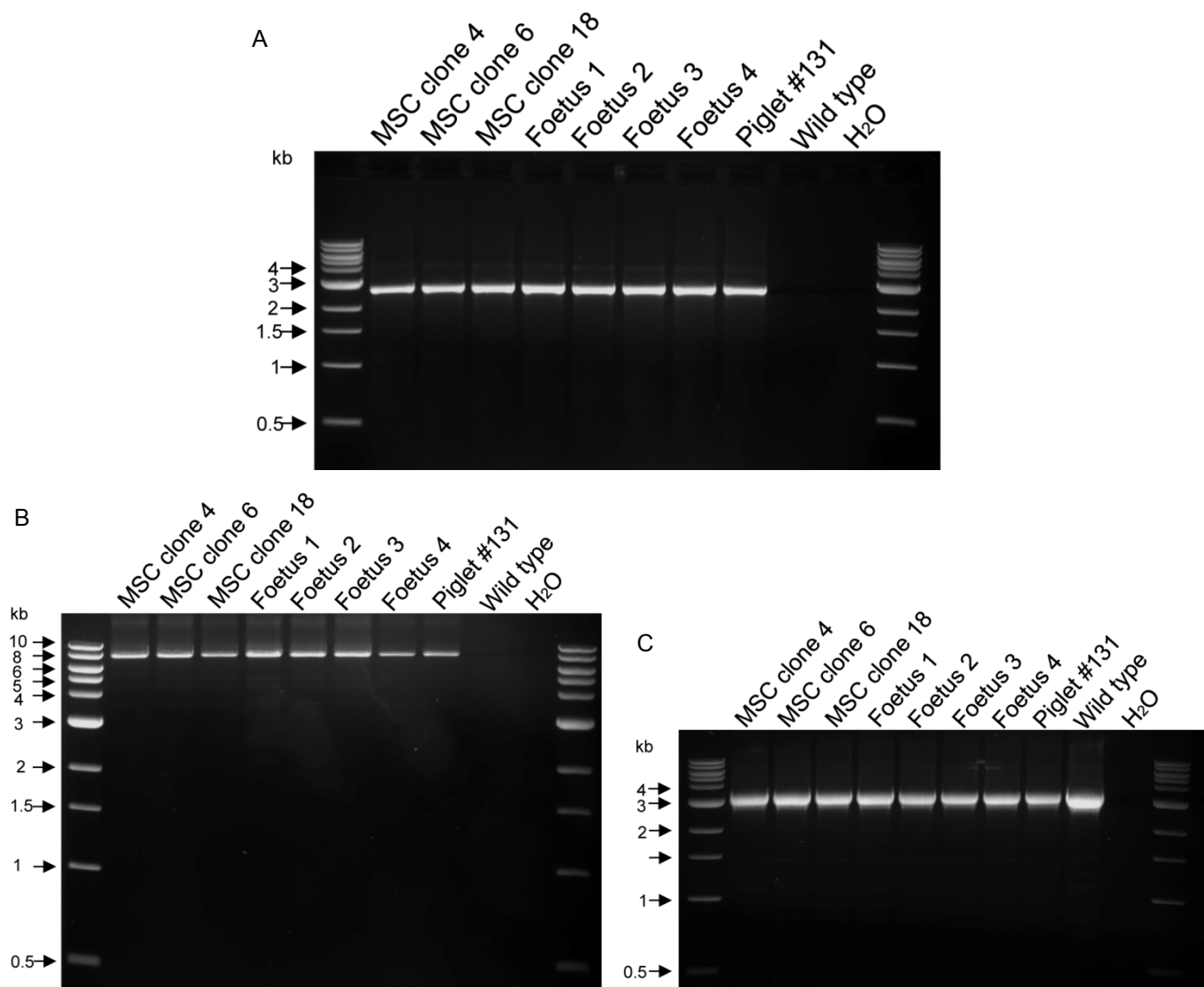


**Figure 3.18: lacZ staining and Cre protein mediated mCherry activation of reporter constructs.** a1-3, e1-e3, black and white channel. b1-b3, f1-f3, red fluorescence channel. c1-c3, non-filtered color channel. d1-d3, color channel with gray filter. Top panels, pKDNF isolated from GCROSA piglet #132; middle panels, pKDNF derived from CAG  $\beta$ -Geo/mCherry randomly integrated foetuses. Wild-type pKDNF were used as negative control.



### 3.4.4 Analysis of TGROSA fetuses and piglet by PCR and southern blot

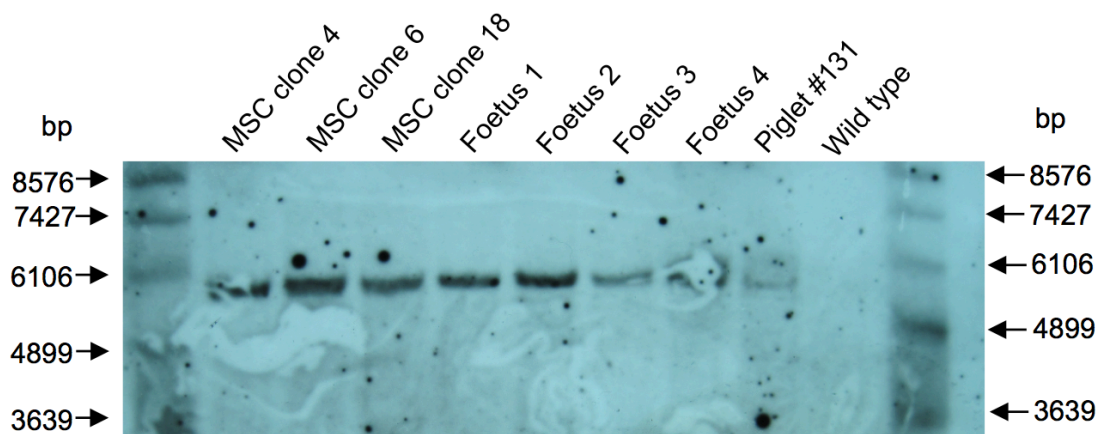
TGROSA targeted fetuses and piglets #131 were confirmed by PCR amplification across 5' and 3' junction regions, which showed that the genotype of piglets is identical to the original cell clones (Figure 3.19 A and B). The endogenous PCR showed only one porcine *ROSA26* allele to be targeted in fetuses and piglet #131, which is consistent with the original cell clones (Figure 3.19 C).



**Figure 3.19: PCR screening of TGROSA nuclear transfer derived fetuses, piglet #131 and original TGROSA targeted MSC clones 4, 6 and 18.** A, PCR detection of TGROSA targeted 5' terminal region. Amplified fragment size: 2630 bp. B, PCR detection of TGROSA targeted 3' terminal region. Amplified fragment size: 7868 bp. C, Endogenous PCR detection of wild type *ROSA26* allele. Amplified fragment size: 3206 bp.

The southern blot analysis was subsequently performed to confirm the structure of targeted

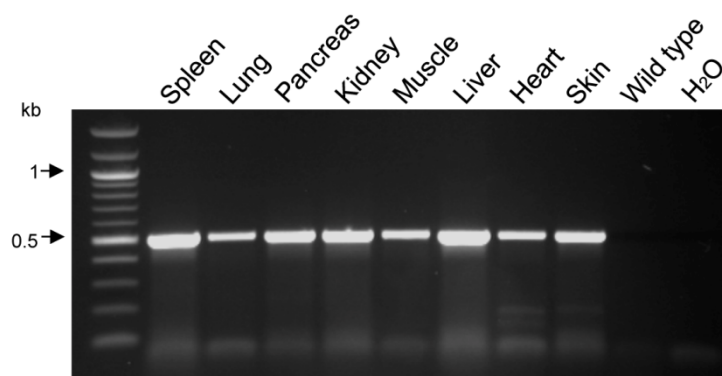
allele for the TGROSA targeted fetuses and piglet #131. Figure 3.20 showed that a diagnostic 5783 bp fragment was detected in TGROSA targeted fetuses and piglet #131, the same as in the original MSC clone 4, 6 and 18.



**Figure 3.20: Southern blot analysis of TGROSA targeted porcine *ROSA26*.** Lanes show *SbfI* digested genomic DNA from three TGROSA targeted MSC clones 4, 6 and 18, four fetuses, newborn piglet #131 and a wild type piglet as indicated. The probe binds on the  $\beta$ -geo cassette and the 5783 bp diagnostic fragment detected by the *bsr* probe is shown.

### 3.4.5 Analysis of TGROSA targeted piglets by RT-PCR

The pattern of reporter gene expression was further detected in TGROSA targeted piglet #131. Tissues of spleen, lung, pancreas, kidney, muscle, liver, heart and skin were tested by RT-PCR for the presence of RNA transcribed from the *ROSA26* promoter extending from exon 1 spliced to the blasticidin gene, and also for mTomato RNA transcribed from the CAG promoter. The results showed that both RNA species were present in all tested samples (Figure 3.21).



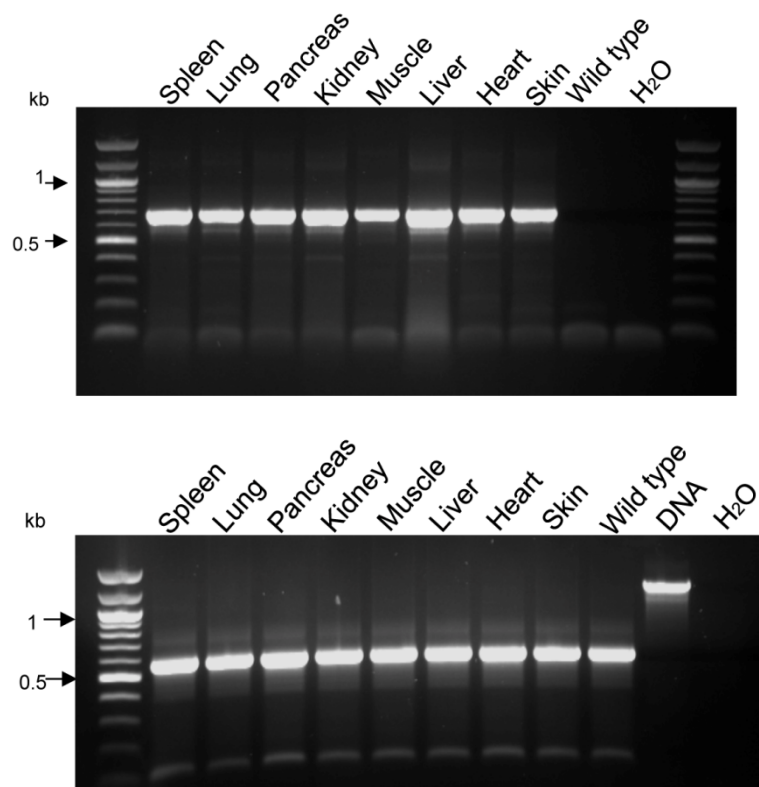


**Figure 3.21: RT-PCR screening of TGROSA piglet #131.** A: RT-PCR detection of targeted *ROSA26* RNA from exon1 splice to blasticidin selectable gene (*bsr*) in different tissues derived from TGROSA piglet #131. Amplified fragment size: 500 bp. Wild type piglet and H<sub>2</sub>O were used as controls. B: RT-PCR detection of mTomato RNA in different tissues. Amplified fragment size 686 bp. Wild type piglet and H<sub>2</sub>O were used as controls. C: RT-PCR performed for porcine housekeeping gene *GAPDH* in different tissues derived from TGROSA piglet #131. Amplified fragment size: 575 bp. Wild type piglet and H<sub>2</sub>O were used as controls.

### 3.4.6 mTomato fluorescence detection for TGROSA foetuses and live piglet #258

TGROSA targeted foetuses were also checked for mTomato fluorescence. Figure 3.22 shows four TGROSA targeted foetuses and four wild type foetuses of the same gestational age, and mTomato fluorescence was easily visualized for TGROSA targeted foetuses while no detectable fluorescence at all for wild type foetuses. Cryosections were further prepared and analysed from a series of foetal organs including bladder, brain, colon, heart, liver, lung, skin, pancreas and spleen. The results showed that mTomato fluorescence was evident in all organs from TGROSA foetuses and there were no mTomato expression in the organs isolated from the wild type animal (Figure 3.23). The live piglet #258 was identified by Tomato fluorescence as well (Figure 3.24).

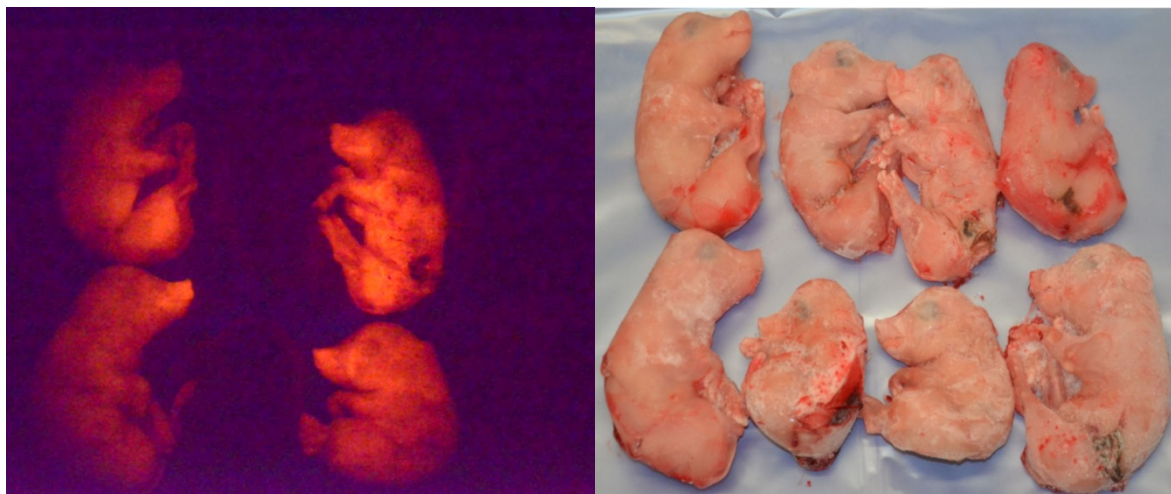


**Figure 3.22: TGROSA and wild-type fetuses at day 77.** mTomato fluorescence (left) and bright light (right).

		TGROSA foetus4			Wild-type foetus		
		Black and white	Red	Green	Black and white	Red	Green
Bladder	a				j		
	b				k		
Brain	c				l		
	d				m		
Colon	e				n		
	f				o		
Heart	g				p		
	h				q		
Liver	i				r		
Lung							
Skin							
Pancreas							
Spleen							

**Figure 3.23: Fluorescence microscopy of tissue cryosections.** Panels a-i, organs from a 77 day gene-targeted foetus<sup>4</sup> derived by nuclear transfer as indicated. Panels j-r, organs from a 77 day wild-type foetus. Each section is visualised through black and white, red (excitation=554nm, emission=581nm) and green (excitation=489nm, emission=509nm) channels as indicated.



**Figure 3.24: Nuclear transfer derived TGROSA piglet (left) and wild-type piglet (right).**

### 3.4.7 Activation of mGFP for fibroblasts derived from TGROSA foetus

To investigate the response of the dual reporter to Cre activity, kidney fibroblasts prepared from explanted foetuses were transduced with Cre protein. Prior to Cre transduction mEGFP fluorescence was not detected in pKDNF, indicating blockade by the floxed transcriptional termination cassette, while strong Tomato fluorescence was evident (Figure 3.25). After Cre transduction, EGFP fluorescence became evident and Tomato fluorescence steadily declined over a period of 8 days until it was absent from almost all cells (Figure 3.25).

#### TGROSA foetal kidney fibroblast

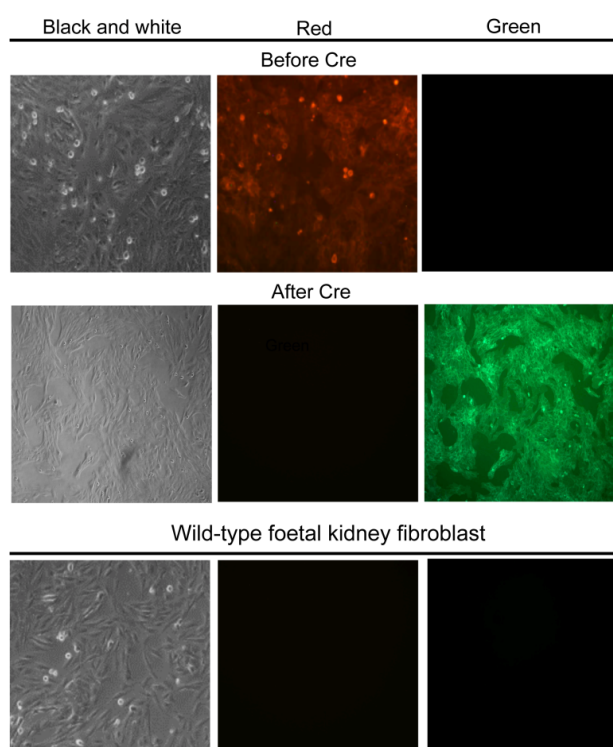


**Figure 3.25: Cre-induced loss of mTomato and activation of EGFP expression in kidney fibroblasts derived from four 77 day TGROSA targeted fetuses.** Fluorescence before, and 8 days after Cre transduction are indicated. Wild-type foetal kidney fibroblast are also shown.

### 3.5 Porcine PDX-1 gene targeting

In order to generate pigs expressing Cre recombinase under the control of PDX-1 promoter, an IRES-Cre cassette can be inserted after the stop codon of the endogenous PDX-1 locus with the help of TALENs. The targeting diagram is shown in Figure 3.26. For this, pKDNF isolated from TGROSA fetuses were used for PDX-1 gene re-targeting. The PDX-1-IRES-Cre vector and a pair of PDX-1 TALENs RNA were produced by Lena Glashauser.

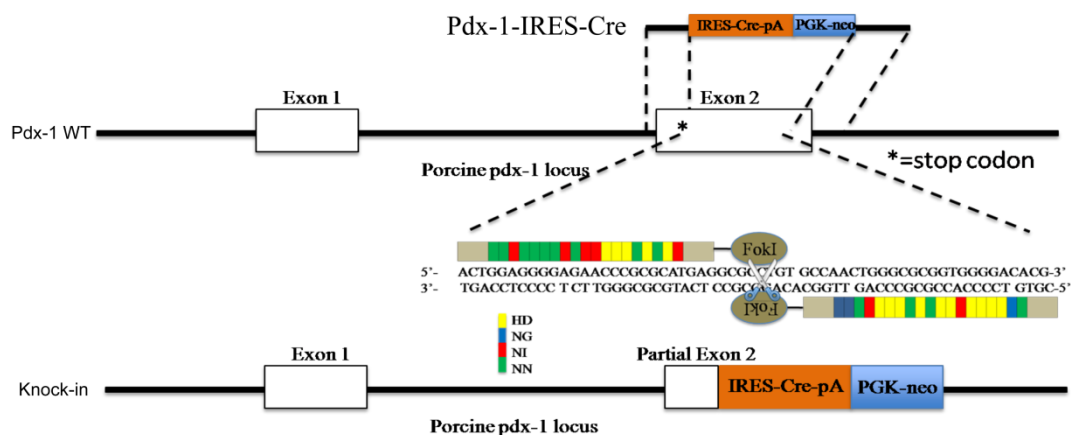


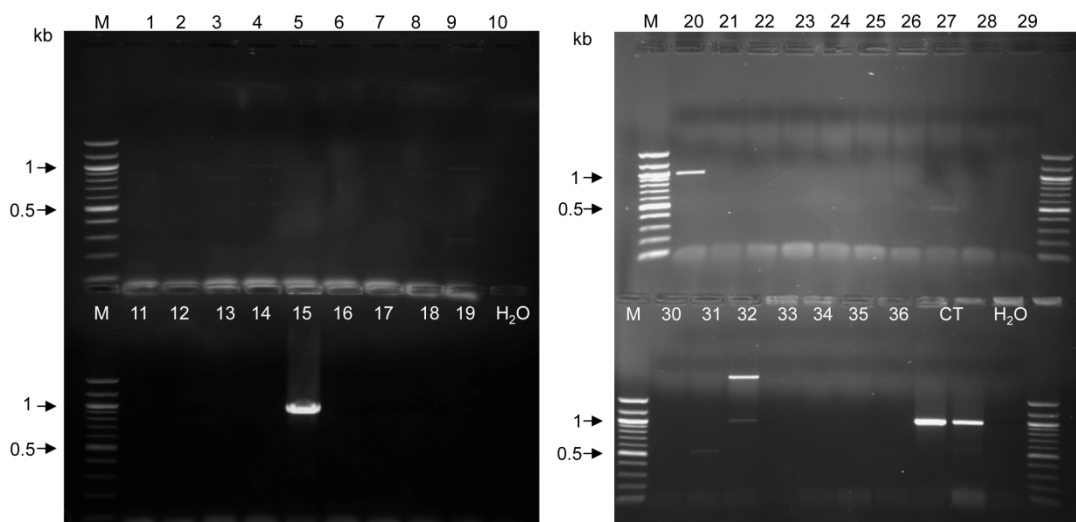
**Figure 3.26: Schematic overview depicting the targeting strategy for the PDX-1 gene.** Top: PDX-1-IRES-Cre vector containing IRES-Cre cassette and neo selection marker. Middle: Two exons and targeted site are shown for the wild type PDX-1 gene. Individual TALE repeats are shown by different colours, and their recognized DNA bases are according to the following code (NI=A, HD=C, NN=G, NG=T). Below: PDX-1 targeted allele.

#### 3.5.1 Transfection and selection of pKDNF clones

The PDX-1-IRES-Cre vector was linearized by *NotI* and co-transfected with a pair of PDX-1 TALENs RNA. After 10-15 days of selection in 400 µg/ml G418, the individual stable transfected cell clones were isolated. Samples of each clone was cryopreserved at an early stage and replicate samples cultured further for analyses.

### 3.5.2 PCR screening for gene targeting events

Single-cell clones were expanded and screened by targeting PCR. The 969 bp DNA fragments were amplified by using forward primer, which hybridizes outside of the 5' homologous arm of PDX-1-IRES-Cre vector in the intron 1 of PDX-1 gene and reverse primer, which hybridizes to the internal ribosome entry site (IRES) cassette. In order to assess the DNA quality and detect the existence of single or double PDX-1 targeted allele in screened samples, endogenous PCRs were performed for each sample. The 1100 bp endogenous fragment was amplified by using the same forward primer as above and another reverse primer, which hybridizes the exon 2 of PDX-1 gene that has been deleted on the targeted allele. Based on the targeting PCR results, two clones (15 and 20) out of fifty-five transfectants were identified as correctly targeted (Figure 3.27). Clone 15 and 20 were further analysed by 3' PCR across junction region using two different forward primers, both of which hybridizes on the neo selection marker and the reverse primer, which hybridizes outside of the 3' homologous arm of PDX-1-IRES-Cre vector. 1339 bp and 1579 bp fragments were amplified by using two pairs of primers in those two clones (Figure 3.28).



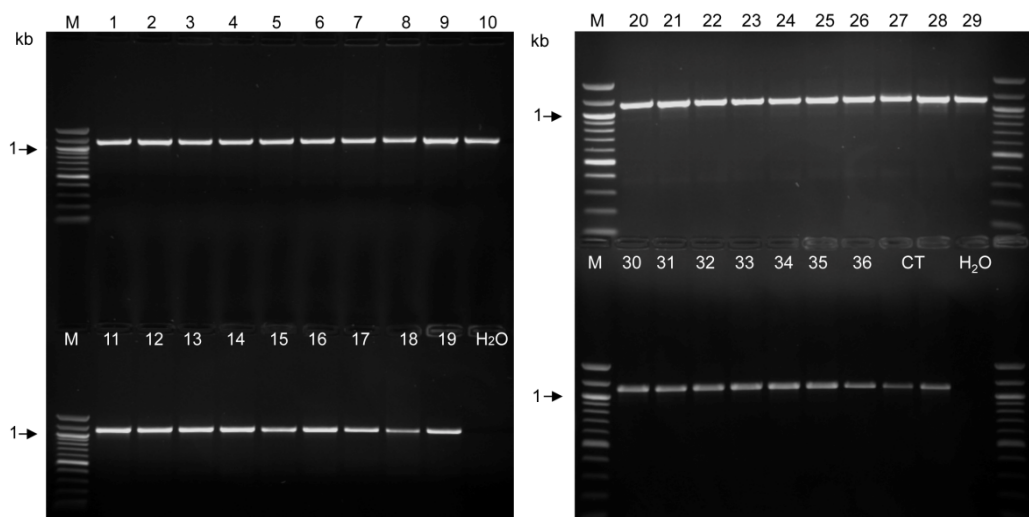


**Figure 3.27: PCR screening of PDX-1 targeting events.** A part of results of screening PCR (top) and endogenous PCR (below) for G418 resistant single-cell clones. The size of positive targeting PCR product is 969 bp and the length of endogenous PCR fragment is 1100 bp. H<sub>2</sub>O were used as negative control and clone 15 was used for positive control for later screening.

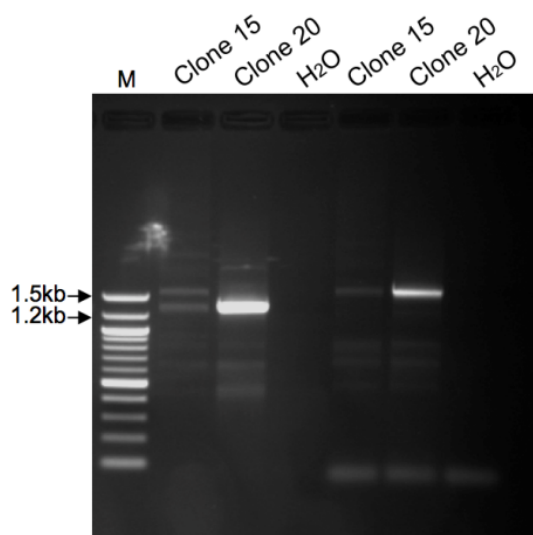


**Figure 3.28: 3' PCR across junction region for clone 15 and 20 using two different pair of primers.** Amplified fragment size: 1339 bp and 1579 bp.

### 3.5.3 Southern blot analysis of PDX-1 targeted clones

Clone 15 and 20 were further analyzed by Southern blot to confirm correct targeting. Southern blot analysis was performed by using a neo probe to distinguish between the PDX-1 targeted allele and random integrants. After genomic DNA digested by *XmnI*, *BamHI* and *XmaI*, the correct diagnostic fragments were expected at 3748 bp, 4102 bp and 5019 bp, respectively. The Southern blot results showed that a larger fragment for clone 15, and multiple fragments



for clone 20 (Figure 3.29). This indicated that clone 15 has random integration, while clone 20 has integrated several copies of the targeting vector due to off-target effects of the used PDX-1 TALENs.

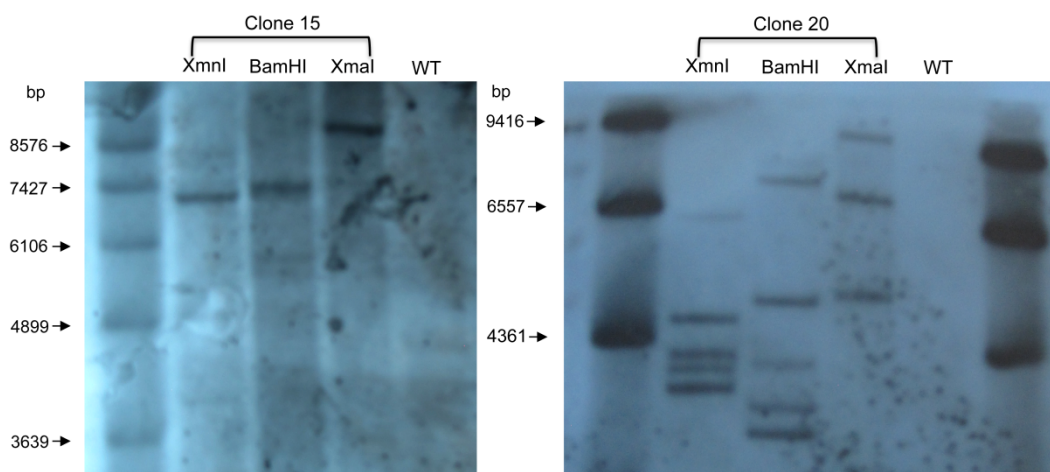


**Figure 3.29: Southern blot analysis of PDX-1 targeted clones 15 and 20.** Lanes show *XmnI*, *BamHI*, and *XmaI* digested genomic DNA from clone 15 (left) and 20 (right), and wild type cells as indicate as negative control. The probe binds on the neo cassette.

## 3.6 Porcine KRAS gene targeting

### 3.6.1 KRAS gene targeting vector

In order to generate pigs carrying a KRAS<sup>G12D</sup> mutant allele that can be activated by Cre recombination, a floxed transcriptional stop cassette (LSL) was inserted into intron 1 of porcine KRAS gene. The mutation KRAS<sup>G12D</sup> was inserted into exon 2 of KRAS. Targeting scheme of porcine KRAS gene is shown in Figure 3.30. KRAS gene targeting vector was generated by Alexander Tschukes. The vector comprised: a 3.090 kb 5' short arm of homology corresponding to a region of KRAS intron 1 from position 660 to 3749 (NC\_010447); a floxed transcriptional terminator signal (LSL cassette) consisting of 34 bp loxP site; a 159 bp adenoviral splice acceptor; a 1476 bp promoterless neomycin resistance gene (*neo*) followed by three polyadenylation signals derived from SV40, the bovine growth hormone gene and CMV; another 34 bp loxP site; a 9.195 kb 3' long arm of homology, which included also the engineered G to A point mutation within exon 2 that results in a glycine to aspartic acid substitution at codon 12 (G12D).

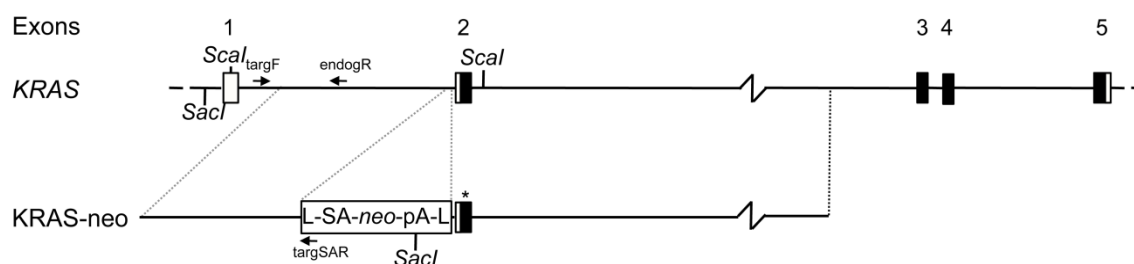


**Figure 3.30: Porcine KRAS gene targeting scheme.** Top. Porcine KRAS gene. Exon numbers are indicated, coding and non-coding regions are marked as black and white boxes. Below. KRAS-neo targeting vector. The transcription termination cassette and its insertion site in intron 1 is shown, the G to A substitution mutation in exon 2 is indicated by an asterisk. PCR primers used to identify targeted cell clones are indicated. *SacI* and *Scal* restriction sites are also shown.

### 3.6.2 Transfection and selection of pKDNF clones

The KRAS targeting vector was linearized by *NotI* and transfected by using electroporation. After 10-15 days selection in 400  $\mu\text{g/ml}$  G418, the individual stable transfected cell clones were isolated. Samples of each clone were cryopreserved at an early stage and replicate samples were cultured further for analysis.

### 3.6.3 PCR screening for gene targeting events

Single-cell clones were expanded and screened by PCR. The 3378 bp DNA fragment was amplified by using forward primer, which hybridizes outside of the 5' homologous arm of KRAS gene targeting vector and reverse primer, which hybridizes to the splice acceptor. The 1597 bp fragment was amplified by endogenous PCRs to assess the DNA quality. Thirteen clones were identified correctly targeted based on the screening PCR results (Figure 3.31).

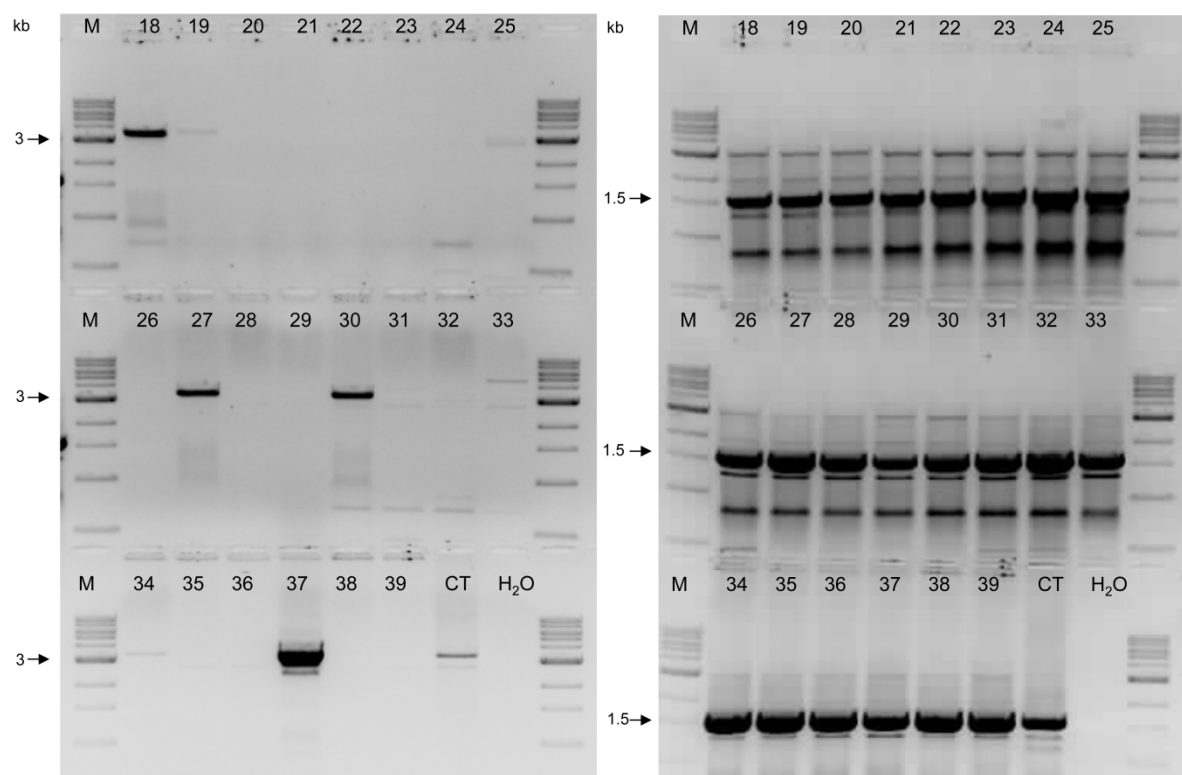


**Figure 3.31: PCR screening of KRAS targeting events.** A part of results of screening PCR (left) and endogenous PCR (right) for G418 resistant single-cell clones. The size of positive screening PCR product is 3378 bp and the length of endogenous PCR fragment is 1597 bp. H<sub>2</sub>O were used as negative control and positive control was also used. (Conducted by Marlene)

Those thirteen clones were further checked for the presence of mutation (G to A) within the exon 2 of KRAS. The 772 bp PCR fragment across exon 2 was amplified and then digested by the restricted enzyme *Bcl*I (Figure 3.32). If case of the mutation presence, the 772 bp PCR fragment can be digested into 257 bp, 190 bp, 134 bp, 114 bp and 77 bp, otherwise it can be digested into 391 bp, 190 bp, 114 bp and 77 bp. The clones 12, 14, 15, 19, 27, 30, 37, 54 and 57 were digested into 257 bp, 190 bp, 134 bp, 114 bp and 77 bp, indicating the presence of the G to A mutation within the exon 2 of KRAS gene (Figure 3.32).

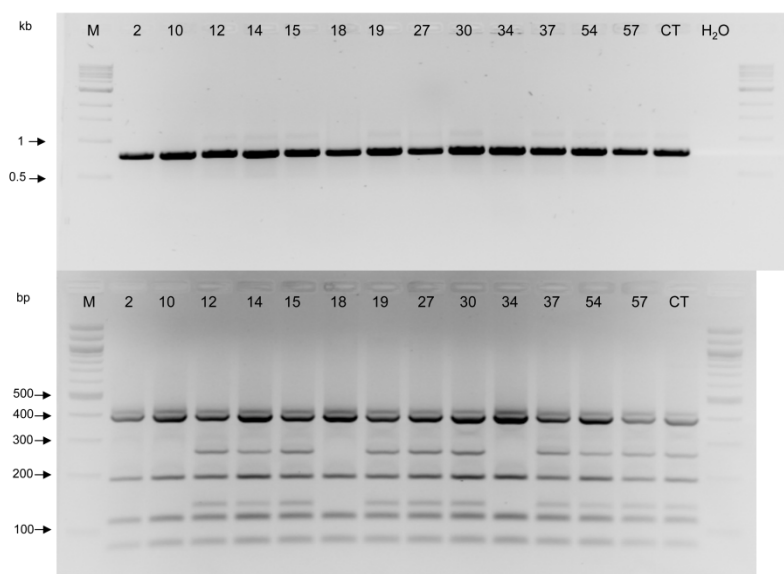


**Figure 3.32: Mutation screening PCR and its digestion fragments.** Top. 772 bp fragment amplified for thirteen screening PCR positive clones. Below. 772 bp PCR fragment digested by *BclI*. (Conducted by Marlene)

### 3.6.4 RT-PCR analyses of KRAS targeted clones

The clone 15, 19, 27, 30, 37 and 54 were further analysed for the mutation (G to A) on the RNA level. The 408 bp RT-PCR fragment was amplified by using forward primer, which hybridizes to the exon 2 of KRAS and reverse primer, which hybridizes to the exon 4 of KRAS. The reverse primer was then used for sequencing the 408 bp RT-PCR fragment sequencing in order to detect the mutation G to A. Before Cre transduction, the 408 bp RT-PCR fragment from six clones were mixed and sequenced (Figure 3.33). The G to A mutation within exon 2 was not detected for the pool of all of the clones, which indicate the lack of expression from the mutated KRAS allele (Figure 3.34). After Cre transduction, the 408 bp RT-PCR fragment from the six clones were sequenced separately (Figure 3.35). The KRAS mutation mRNA was detected in clone 15, 19, 27, 30 and 37, but not in clone 54 (Figure 3.36).

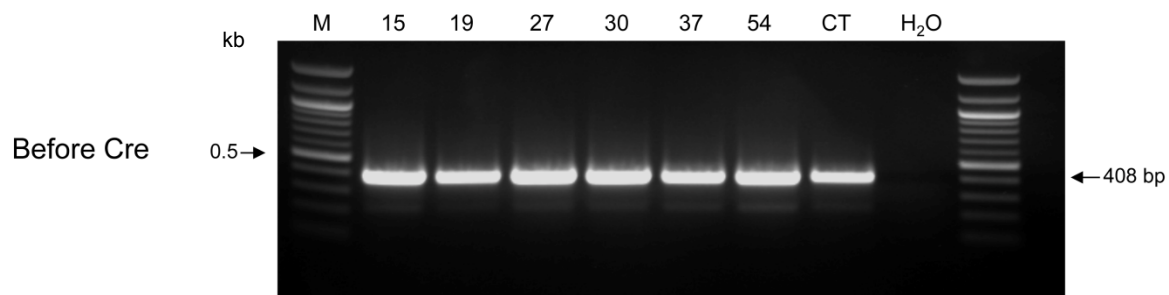


Figure 3.33: The 408 bp RT-PCR fragment amplified from six clones before Cre transduction.

Clones pool (before Cre)

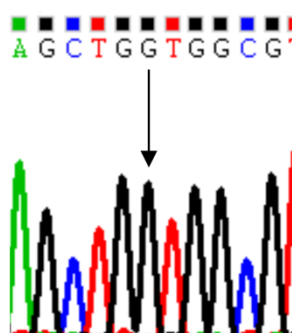


Figure 3.34: Sequencing of 408 bp RT-PCR fragment from the pool of six clones before Cre transduction. Arrow indicates mutation site.

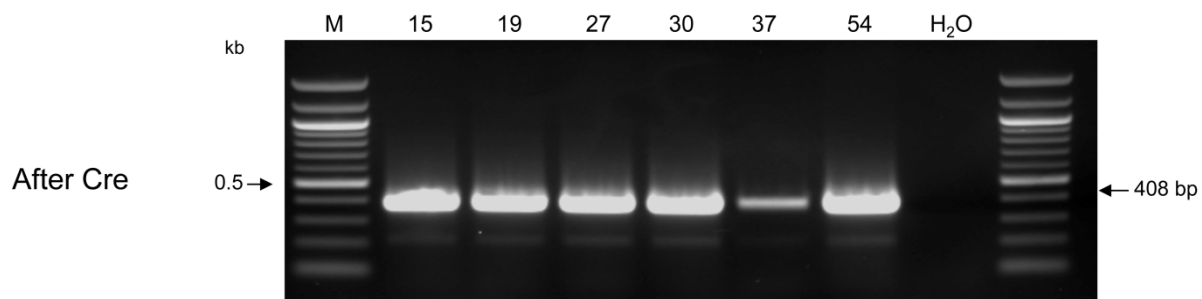


Figure 3.35: The 408 bp RT-PCR fragment amplified from six clones after Cre transduction.

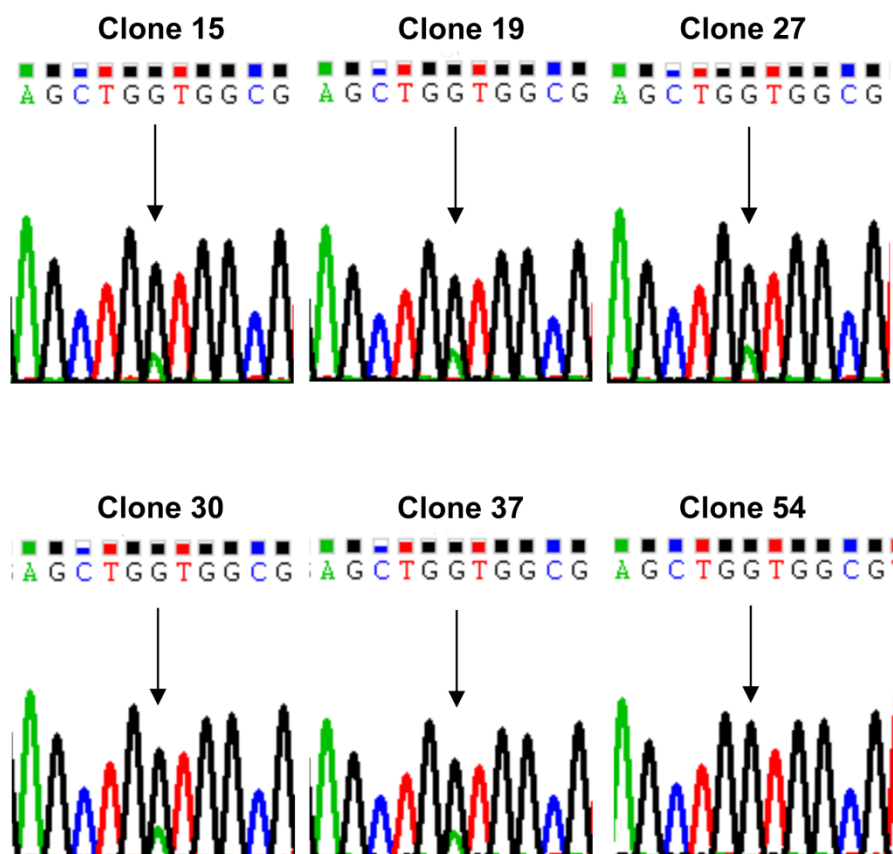
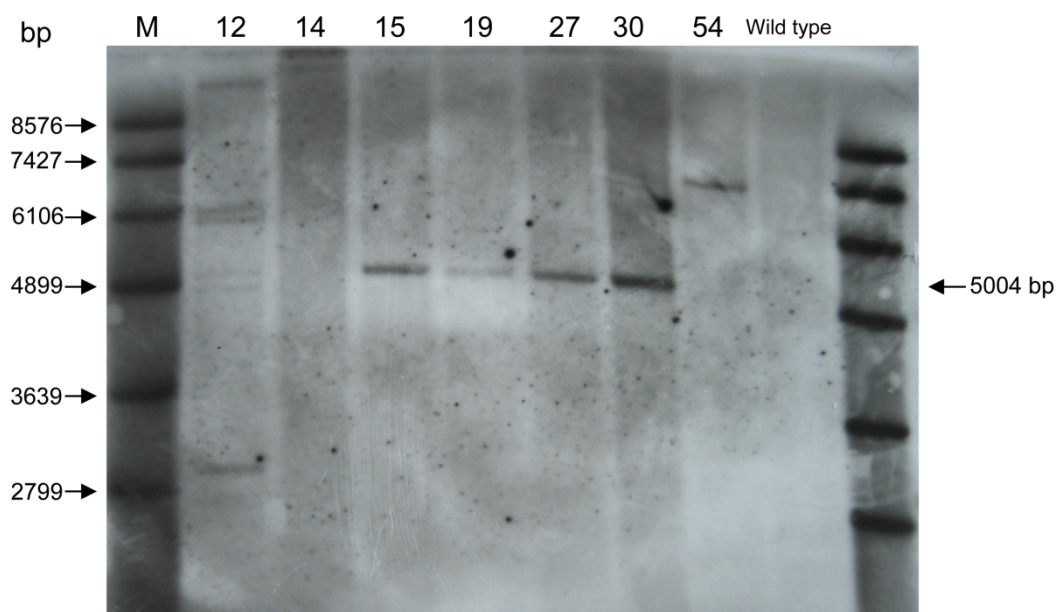


Figure 3.36: Sequencing of 408 bp RT-PCR fragment from each clone after Cre transduction. Arrows indicate mutation site.

### 3.6.5 Southern blot analyses of KRAS targeted clones

Southern blot analysis was performed by using a neo probe to detect the structure of KRAS targeted allele. A diagnostic 5004 bp fragment was detected in clone 15, 19, 27 and 30, confirming right KRAS targeted structure for those clones. Clone 12, 14 and 54 showed unexpected size of band, indicating random integration of KRAS targeting vector (Figure 3.37).



**Figure 3.37: Southern blot analyses of KRAS targeted structure.** Lanes show *SacI* digested genomic DNA from seven KRAS targeted pKDNF clones and wild type pKDNF cells. The probe binds on the neo cassette and the 5004 bp diagnostic fragment detected by a neo probe is shown.

## 4 Discussion

### 4.1 Gene targeting of porcine *ROSA26*

#### 4.1.1 Identification of the porcine *ROSA26* gene and its importance

It has been reported that transgenic mice generated by random transgenesis have limitations. For example, expression patterns vary among transgenic animals due to differences in copy number; unpredictability of expression and inheritance of the transgene due to positional effects of integration sites and promoter silencing [207,264]. In addition, if random reporter transgenic lines generated in different laboratories and assessed under different standards, it is difficult to evaluate whether they are suitable for one's research interest [265]. Furthermore, reporter lines that show high fluorescence are often infertile or not viable [209]. Therefore, it is vital to use an endogenous locus which is ubiquitously expressed and the loss of which is not lethal in order to overcome these issues. The *ROSA26* locus has been established as the preferred placement site for transgene expression because the expression of transgenes inserted into the *ROSA26* locus has been demonstrated at suitable levels in every tissue from embryonic to adult stages [176,212]. Moreover, animals with homozygous mutation at the *ROSA26* locus are viable and fertile [210]. Mouse, human and rat *ROSA26* loci have been characterized and widely used in genetic modification as they can be targeted with high efficiency by homologous recombination. The porcine *ROSA26* has not been characterized yet, therefore, it was of important to identify the *ROSA26* gene in pigs.

Mouse, rat and human *ROSA26* gene have been identified and characterized [210,214,215], which made identification of the porcine *ROSA26* possible. Here the porcine *ROSA26* gene was firstly identified by using the sequence of promoter and exon 1 regions of the mouse *Rosa26* to search the NCBI *Sus Scrofa* 10.2 porcine genome database. A highly conserved putative porcine *ROSA26* promoter and exon 1 region on chromosome 13 were identified. Based on this putative porcine *ROSA26* region, exon 2-4 were further identified with 3'RACE method. The results accord with the partial description published recently [266], although we



identified four rather than two exons. This suggests that the porcine *ROSA26* expresses multiple transcript variants, as found in other species [210]. In mouse and human, 3' *ROSA26* cDNA sequence overlaps the 3' region of the adjacent gene *THUMPD3*, and the putative porcine *ROSA26* was also found overlapping with *THUMPD3*. This supplies another evidence of the correctness of the identified porcine *ROSA26* gene.

In mouse, the *Rosa26* locus shows expression in a variety of adult tissues [210] and human *ROSA26* also gives this broad expression pattern in tested adult tissues, such as brain, pancreas, lung, kidney, bone marrow, skeletal muscle and three human ES cell lines [214]. Toshihiro et al. [215] reported that transcripts from the rat *ROSA26* locus are ubiquitously expressed as shown by the detected expression of rat *ROSA26* in brain, duodenum, kidney, pancreas, liver, lung, spleen and ESC. In pigs, the RT-PCR results showed the porcine *ROSA26* is expressed in a wide range of tissues, including spleen, lung, pancreas, kidney, muscle, liver, heart, skin, bladder and stomach. These data demonstrate the conservation of the *Rosa26/ROSA26* locus among mouse, human, rat and pig, which also supports the identity of the porcine *ROSA26* gene.

#### 4.1.2 Construction of the targeting vectors

For gene targeting into mouse, human and rat *ROSA26* locus, a promoter trap approach was adopted for the generation a series of targeting vectors [212,214,215]. The Promoter trap approach is based on the integration of a promoterless gene into the genome behind an endogenous trigger, which will initiate transcription of the transgene [211,267,268]. In this study, such promoter trap approach was also applied to the construction of GCROSA and TGROSA for targeting of the porcine *ROSA26*. In mouse *Rosa26* targeting, exogenous genes were placed into a unique *XbaI* site in the intron 1 region [212]; since a homologous site was identified in the porcine gene, we designed the short and the long homologous arms of the GCROSA and TGROSA targeting vectors to flank this site. A splice acceptor sequence was placed in front of the promoterless reporter gene or selectable marker in the constructs, as it can allow for the expression of the cassette when it integrates into an intron. In the GCROSA and TGROSA targeting vectors, the splice acceptor was added in front of the  $\beta$ -gal and *bsr*

selection marker. After targeting porcine *ROSA26* locus with those two vectors, both the RNA spliced from porcine *ROSA26* exon 1 to  $\beta$ -gal and to *bsr* were detected. Moreover, promoter trap constructs in which the ATG was omitted were significantly less efficient [267,269]. In the porcine *ROSA26* targeting vectors, the reporter genes, namely  $\beta$ -gal, mCherry, mTomato, mGFP, and *bsr* selection marker, include a Kozak sequence with an ATG codon as an initiator to allow for recognition and translation by the ribosome [270].

In addition, in order to obtain a double Cre recombinase reporter system, the first reporter genes on the targeting vectors were flanked by two loxP sites with the same direction on both porcine *ROSA26* targeting vectors. Thus, the Cre protein will excise the first floxed reporter gene, thereby allowing expression of the second reporter gene. This double reporter system has also been widely used in generating mouse Cre reporter lines [194,205,206,271]. In pigs, Li et al. [177] generated a reporter pig, which can express EGFP only after Cre-mediated excision of a loxP-flanked stop cassette. However, it is widely recognised that dual reporters are more useful and reliable indicators of Cre recombination, because one reporter gene is always active in any individual cell providing an internal control. Another group has recently generated a porcine *ROSA26* reporter porcine model by placing mTomato gene flanked by wild type loxP and loxP2272 into the *ROSA26* locus through recombinase-mediated cassette exchange (RMCE) [266]. Compared with wild type loxP, loxP2272 has two nucleotide mutation within the spacer region. loxP sites with same spacer region have efficient Cre recombination, while loxP sites whose spacer regions are different in even as little as one nucleotide have dramatically reduced recombination efficiency. This *ROSA26* reporter porcine model carrying mTomato gene flanked by wild type loxP and loxP2272, thus it can not be used for monitoring Cre recombinase activity. Therefore, in this study, GCROSA and TGROSA containing loxP- $\beta$ -gal-loxP-mCherry and loxP-mTomato-loxP-mGFP respectively were constructed in order to obtain *ROSA26* dual reporter pigs.

#### 4.1.3 Targeting efficiency of the *ROSA26* locus

Soriano et al [212] targeted the mouse *Rosa26* locus with a reporter construct containing a lacZ gene. After transfection and G418 selection, 8 of 23 (34.7%) G418 colonies were

confirmed to have correctly undergone homologous recombination. These results show the high rate of homologous recombination and successful targeting to the *ROSA26* locus in mouse. Kobayashi et al. [215] reported that on average about 30% of picked clones demonstrated correct targeting to rat *ROSA26* locus by using rat pluripotent stem cells (PSCs). This also shows the high targeting efficiency at rat *ROSA26* locus. Irion et al. [214] performed gene targeting to the human *ROSA26* locus, overall 2 targeted clones out of 88 clones were confirmed, with a targeting efficiency around 2.3%. Compared with the high targeting efficiency in mouse and rat *ROSA26* locus, these results indicate lower targeting frequencies in the human *ROSA26* locus. This might be related to locus-specific species differences in homologous recombination, but technical issues might also play a role. For example, the optimal transfection method, critical parameters for optimizing homologous recombination in the hES cells used remain to be further investigated.

In this study, it was shown that *ROSA26* targeting in porcine MSCs is quite efficient using targeting vectors without the help of site-specific nucleases. 24 of 50 (48%) GCROSA transfectants and 16 of 38 (42%) TGROSA transfectants were identified as targeted by screening PCR. In other work we also obtained efficient targeting (28% of cell clones analysed) when placing an atherosclerosis marker gene under the control of a tissue-specific promoter at the same site (unpublished). These findings contrast with those recently described by Li et al. [266], who reported poor targeting efficiency into the porcine *ROSA26* using a conventional vector, which could be due to the different location they used within the *ROSA26* intron 1. Efficient gene targeting is an important factor if, as in mice, porcine *ROSA26* is to be used as a 'general purpose' permissive locus for transgene placement. Reliable ubiquitous or tightly controlled transgene expression, free of position effect variation or silencing, is a basic requirement for many new biomedical applications where genetically modified pigs are playing an increasingly important role [272].

#### 4.1.4 Activity of the *ROSA26* promoter

Since the *ROSA26* locus has become the preferred placement site for transgene expression in mouse, rat, human and pig, it is important to analyse the endogenous *ROSA26* promoter

activity. Chen et al. [200] compared the activities of nine ubiquitous promoters (*ROSA26*, CAG, CMV, CMVd1, UbC, EF1 $\alpha$ , PGK, chicken  $\beta$ -actin and MC1) in mouse embryonic stem cells. Their results showed that the CAG promoter has the highest level of expression at about 9-10 fold the level of the mouse endogenous *ROSA26* promoter. Nyabi et al. [213] also reported that the CAG promoter is approximately 8-10 fold the level of the mouse *ROSA26* promoter. In this study, the GCROSA integrated into *ROSA26* intron 1 at a site equivalent to that frequently used in mouse *ROSA26*, under the control of the endogenous porcine *ROSA26* promoter. The results showed that expression of lacZ (before Cre recombination) and mCherry (after Cre recombination) directed by the porcine endogenous *ROSA26* promoter was weak. On the other hand, the TGROSA was inserted at the same site, higher expression of mTomato and mGFP genes were detected. This also indicates that the CAG promoter activity is higher than that of the porcine *ROSA26* promoter, consistent with findings with the mouse *Rosa26* promoter [200].

#### 4.1.5 Ubiquitously expression of genes placed in the *ROSA26* locus

Transgenes integrated into the mouse *Rosa26* locus are ubiquitously expressed and not subject to gene-silencing effects [210]. Muzumdar et al. [273] reported a global double-fluorescent Cre reporter mouse, in which the reporter gene was placed in the mouse *Rosa26* locus, was expressed in all tissues examined, such as brain, retina, heart, lung, rib, liver, spleen, kidney, bowel, ovary. Another *Rosa26* reporter mouse line also proved ubiquitous expression of mTFP1 (bright teal fluorescent protein) in brain, heart, liver, lung, kidney, stomach, spleen, tail, intestine, eye and embryo day 16.5 [274]. In human, insertion of RFP (red fluorescent protein) into the *ROSA26* locus allows ubiquitous expression of RFP in both undifferentiated and differentiated populations representative of the three germ layers [214]. Kobayashi et al. [215] identified the rat *ROSA26* locus and inserted tdTomato into the rat *ROSA26* locus to generate knock-in rat lines which showed ubiquitous expression of tdTomato.

In this study, a promoter trap vector, TGROSA, was constructed to place an mTomato, mGFP dual reporter cassette driven by the constitutive CAG promoter into the porcine *ROSA26*

locus, and TGROSA fetuses and live piglets were generated. Tomato fluorescence was evident in all foetal organs examined including bladder, brain, colon, heart, liver, lung, skin, pancreas and spleen. The live TGROSA piglet showed Tomato fluorescence throughout its body. Both RNA species (mTomato RNA and RNA transcribed from the *ROSA26* promoter) were detected in all the tissue samples from TGROSA piglet, such as spleen, lung, pancreas, kidney, muscle, liver, heart and skin. These results support ubiquitous expression of a transgene inserted into the porcine *ROSA26* locus, consistent with results from mouse, rat, and human. Thus, these results indicate that the porcine *ROSA26* locus conserves the properties of its orthologues in rat, mouse and human. The ubiquitous transcriptional activity of the *ROSA26* locus suggests that the genomic region is not affected by chromatin configurations which could cause transcriptional repression of inserted transgenes. Therefore, the *ROSA26* locus has become a reliable insertion site for exogenous transgenes in mouse, rat, human and pig.

#### 4.1.6 **Placing gene of interests into porcine *ROSA26* locus through RMCE**

Cre/loxP site-specific recombination system is a powerful and versatile tool that has been widely used to engineer the genome of experimental animals. Cre recombination happens efficiently between two loxP sites having the identical spacer region, while Cre recombination does not occur between two loxP sites with different spacer region [275]. Recombinase mediated cassette exchange (RMCE) is a site-specific recombination that enables the exchange of one chromosomally preinserted DNA cassette flanked by two different heterospecific loxP sites for another cassette on a replacement vector flanked by the same heterospecific loxP site [276]. So far, several heterospecific loxP sites, such as loxP511, loxP2272, and loxP5171, have been widely used in RMCE [277–279]. Among these heterospecific loxP sites, loxP2272 showed the highest recombination efficiency and resulted in a stable recombined structure [280]. Therefore, loxP2272 has been frequently used in RMCE. Irion et al. [214] generated a valuable human embryonic stem cell line having a loxP/loxP2272 homing site, which allows for efficient introduction of any gene of interest into the human *ROSA26* locus via RMCE. This technology has also been extended into pigs. Li et

al. [266] inserted loxP/loxP2272 sites along with EGFP into the porcine *ROSA26* locus, and later successfully replaced tdTomato with EGFP through RMCE. This demonstrated that RMCE is a feasible and efficient way to replace any gene of interest into the *ROSA26* locus. In a further step of this study, RMCE could be also used to place any gene into the porcine *ROSA26* locus.

## 4.2 Somatic cell nuclear transfer

### 4.2.1 Factors influencing efficiency of generating genetically modified pigs by SCNT

SCNT is widely used for the generation of genetically modified large animals, such as cattle [281], sheep [107], goat [282] and pig [55,283]. In the pig, although cloned pigs produced by SCNT have been reported more than ten years ago, the efficiency of cloning (live cloned piglet per reconstructed embryos transferred to recipients) is still very low, typically between 1 to 5% [284]. There are several factors that may contribute to this inefficiency. These include season, oocyte quality, donor cell type, type of genetic modification, number of cloning rounds, loss of somatic imprinting in the nuclei of the reconstructed embryo, and pre-selection of cloned embryos for early development [110,284].

Recipient sows have lower pregnancy rate after embryo transfer (ET) in winter [284]. It is not always guaranteed to maintain reconstructed embryos in an optimal temperature, therefore, low temperatures in winter might affect the developmental capability of the embryos. However, in winter, cloning efficiency is highest for performing SCNT and ET because the cloning efficiency is calculated only for the recipients generated offsprings.

Faast et al. [285] reported that using porcine bone marrow MSCs for SCNT can lead to higher blastocyst rates compared with fibroblasts isolated from the same animal. These results were also supported by Jin et al. [286] and Kumar et al. [287]. MSCs isolated from peripheral blood can be used for SCNT as well, and they can increase the number of SCNT embryos that develop to term [285]. So it seems like MSCs are superior to fibroblasts for SCNT in pigs

based on the previous research. Kurome et al. [284] analysed a large data set and showed there were no differences in the cloning efficiency among the different donor cell types. However, a higher pregnancy rate was observed when MSCs were used for SCNT. In this study, bone marrow MSCs were also used for SCNT, and piglet # 132 and 133 were generated from bone marrow MSCs clones. Nevertheless, cloned piglets # 132 and 133 showed enlarged tongues, a phenomenon that has also been observed in other offspring cloned from bone marrow derived mesenchymal stem cells [153]. MSCs derived from adipose tissue, on the other hand, showed a high proportion of viable offspring without malformations, such as cloned piglet # 258. On the other hand, Richter et al. [288] characterized primary porcine kidney fibroblast and demonstrated that these are a valuable cell source for the generation of genetically modified pigs via SCNT. One of the advantage of kidney fibroblast is that they can be cultured up to 71 passages while maintaining a stable karyotype, whereas porcine ear fibroblasts and fetal fibroblasts are difficult to be cultured for more than 20 passages. In addition, compared with porcine fetal fibroblasts and ear fibroblasts, kidney fibroblasts showed a higher proliferation rate and double higher blastocyst rate after SCNT [288]. Thus, in this study, porcine kidney fibroblasts derived from TGROSA foetuses were isolated and used for gene targeting.

Usually, genetic modification of donor cells takes a long time in *in vitro* culture for transfection and selection, which could cause cellular changes. This may lead to a decrease in cloning efficiency. Therefore, it is necessary to use donor cells with lower passage numbers (less than 8 passages for additive gene transfer and less than 10 passages for gene targeting) for SCNT [284]. Some studies have demonstrated that additional rounds of cloning cause a decrease in cloning efficiency [289–291]. Kurome et al. [284] also reported that additional rounds of cloning decreased cloning efficiency, thus the cloning efficiency in the first, second and third round are 4.4%, 3.5% and 2.9% respectively. The reduced cloning efficiency of multiple rounds of cloning might be due to altered gene expression patterns and accumulation of epigenetic errors after nuclear transfer [292].

*In vitro* culture of cloned embryos and selection of normal development embryos for ET also influences the cloning efficiency. The *in vitro* culture conditions for porcine embryos have

been substantially improved during the past years, which is helpful for improving the cloning efficiency. Kurome et al. [284] showed that using re-constructed embryos during the 2-cell to 4-cell stage for ET resulted in the highest percentage of offspring per re-constructed embryos transferred. Genetically modified animals generated by SCNT and ET often show anomalies. Common anomalies include reduced or increased birth weight, respiratory distress, cardiovascular abnormalities and enlargement of organs [293]. Many cloned offspring even die soon after birth. These phenotypic defects and unique pattern of mortality during the neonatal stage may be related to changes in the expression of imprinted genes. Examples include insulin-like growth factor II (IGF2) and H19, both of which play an important role in regulating growth during fetal development. And in fact, decreased expression of IGF2 has been detected in the liver, kidney, heart and muscle of unusually large cloned sheep fetuses [294]. In mice, imprinting errors have also been detected in overgrown foetus, while they were not observed in phenotypically normal foetuses [295]. Besides to the improper expression of some imprinted genes, dysregulation of non-imprinted genes has also been reported in cloned animals [296]. The abnormality has been noted after nuclear transfer in pigs [297]. In this study, cloned piglets # 132 and # 133 showed large tongue and died at birth, which might be a consequence of defective epigenetic reprogramming and related to the donor cell type.

#### **4.2.2 Cell cycle synchronization between donor cells and recipient oocytes**

Normal development of cloned embryos depends on maintaining correct ploidy and preventing DNA damage by coordinating the cell cycle between the recipient cytoplasm and the donor nucleus [298]. MII oocytes are often used as the recipient cytoplasm [299]. Because maturation/meiosis/mitosis-promoting factor (MPF) activity is maximal at MII stage [298], and in the MII oocyte, the donor nuclear envelope is broken down and premature chromosome condensation occurs because of the high activity of MPF [300]. When MII oocytes are used as recipients, one of the following strategies is adopted for embryo reconstruction by nuclear transfer. In the first strategy, nuclei in G0 or G1 phase are directly transferred into untreated enucleated MII oocytes [298], and reconstructed embryos are able to develop to offspring in many species [110,281,299,301]. The second is the transfer of nuclei in G1, S or G2 phase



into enucleated MII oocytes which are activated before nuclear transfer, thereby reducing MPF activity. This is applied when using blastomeres as donor nuclei, because it is difficult to synchronize embryonic nuclei, and most of blastomeres are in the S phase [302]. The last strategy is the transfer of G2/M phase nuclei into untreated enucleated MII oocytes, the reconstructed embryos can return to the normal ploidy when a polar body has been excluded after parthenogenetic activation, and the embryos are able to develop to offspring. This strategy has been reported with mouse embryonic stem cells [303] and bovine somatic cells [304] used as nuclear donors.

In this study, the first strategy was adopted. In order to arrest diploid cells in the G0/G1 phase, the genetically modified donor cells underwent serum starvation for 48 hours before SCNT. It has already been understood that most the serum starved cells used as nuclear donors are cell cycle arrested in G0/G1. Contact inhibition also reported as a method to arrest the cell cycle, but the contact-inhibited cells used as nuclear donors for embryo reconstruction contain both of cell-cycle arrested diploid cells (G0/G1) and unarrested diploid cells (G1) [110]. Therefore, in this study, the serum starvation method was used to arrest the cell cycle for donor cells.

### 4.3 TALENs and CRISPR/Cas9 for genome engineering

TALENs are a tool that has been used for a broad range of genetic modifications [305–308]. In this study, TALENs were also used for targeting the porcine PDX-1 locus. When co-transfecting cells with a pair of TALEN plasmids and donor plasmid, it is possible that the TALEN plasmids can integrate into the host genome. In order to avoid this, TALEN plasmids were *in vitro* transcribed into mRNA. Cells were then transfected with TALEN mRNA and the donor plasmid. Two out of 50 clones were positive based on the screening PCR. However, according to the southern blot result, one of the clones showed an unexpected band pattern in the southern blot with fragments larger than expected, indicating random integration of the donor plasmid. The other clone had the correct fragment together with some additional fragments, hinting at a mixed population with both correctly targeted cells and cells with random integration. Therefore, another transfection needs to be done.

So far, CRISPR/Cas9 system has widely used to target desired genomic sites in mammalian cells, bacteria, zebrafish and mice [118,309,310]. CRISPR/Cas9 RNA-based adaptive immune system was found in bacteria and archaea with the function of protecting hosts against invasion of viruses and plasmids [311–313]. The type II CRISPR system is the well characterized and used in genomic engineering [314–318], and it comprises of the nuclease Cas9, the crRNA array that encodes the guide RNAs and a trans-activating crRNA (tracrRNA). Cas9 nucleases displayed strong DNA strand cleavage activity because it contains the conserved HNH and RuvC nuclease domains [319]. Cas9 nuclease activity can be guided by two RNA elements: crRNA which contains a 20 base pairs of target sequence (spacer sequence) and tracrRNA [320]. The combination of crRNA and tracrRNA is able to direct Cas9 to spacer sequence via Watson-Crick complementary base pairing between the spacer sequence on the crRNA and the complementary sequence (protospacer) on the target DNA [321]. In this CRISPR/Cas9 system, three nucleotides (5' NGG) located at the 3' side of the protospacer is called the protospacer adjacent motif (PAM) which is required to ensure the cleavage specificity in target sequences [315]. Recent publications showed that the crRNA:tracrRNA complex can be further fused together to generate a chimeric, single-guide RNA (sgRNA) [315]. Cas9 can be guided by sgRNA to cleave double-strand DNA at desired site defined by the spacer sequence on sgRNA and a 5' NGG PAM. This indicated that Cas9/sgRNA complexes is a concise and versatile RNA-guided system for causing DSBs which could facilitate site-specific genome engineering.

The TALEN and CRISPR/Cas9 based methods for genome engineering share common features, but also differ in a few aspects. Both TALENs and CRISPR/Cas9 are able to cause DSBs, which can either generate indels via NHEJ, or allow for knock-in of an exogenous DNA with homologous sequences via the HR-directed DNA repair system. But compared with TALENs, the CRISPR/Cas9 system has some advantages, namely: ease of customization, higher targeting efficiency, and the ability of multiplex genome editing. So the CRISPR/Cas9 system can be changed to target any DNA sequences by simply exchanging a pair of 20 nucleotides oligos, whereas targeting a new DNA sequence with TALENs requires cloning a number of repetitive sequences encoding for the DNA binding domains into a

recipient vector. So it is more time-consuming to construct a new pair of TALENs, even though many protocols exist for TALEN construction.

Although the CRISPR/Cas9 system has several advantages over TALENs, there are some limitations as well. The 20 bp target sequence requires a PAM sequence in the 3'-terminal end, thereby limiting the number of available target sites. Another limitation is the high potential for off-target mutagenesis [117,322,323]. So far, several strategies have been reported to improve the specificity of RNA-guided Cas9, such as adding two guanine nucleotides before the 20 nucleotide complementarity region of the gRNA or truncation of the 3'-end of the gRNA (i.e. the tracrRNA domain where interaction with Cas9 is mediated). However, by using these altered gRNAs, CRISPR RNA-guided nucleases have also decreased on-target activities [323,324]. Double nicking by RNA-guided CRISPR Cas9 has reported as another approach to enhance the specificity. For this approach, two gRNAs can target adjacent sites on opposite DNA strands. Then each gRNA recruits a Cas9 nickase (Cas9 D10A) that nicks DNA instead of cleaving both strands. It has been reported that this approach can reduce off-target activity by 50- to 1500-fold in mouse cell lines [325]. However, the additional gRNA might lead to new off-target mutations because a single gRNA-directed Cas9 nickase can also induce indels at some sites [118,324,326]. Recently, Fu et al [327] reported that truncated gRNAs, with a target sequence of less than 20 nucleotides (e.g. gRNA with targeting segments of 17 nucleotides), can decrease undesired mutagenesis at some off-target sites by 5000-fold without sacrificing on-target genome editing efficiency. Therefore, such truncated gRNAs are a promising approach to minimize off-target effects of Cas9 nucleases. By using them, the CRISPR/Cas9 system could be used as an alternative way for targeting the porcine PDX-1 locus in the near future.

#### 4.4 PDX-1 gene targeted locus

The mouse, human, and rat pancreatic duodenal homeobox 1 (PDX-1) gene is located on chromosomes 5 [328], 13 [329,330], and 12 [331], respectively, and they comprise two exons. In pig, the PDX-1 gene is located on chromosome 11 and also has two exons. PDX-1 plays an important role in pancreas development and islet  $\beta$ -cell function [332]. Thomas et al. [333]

developed a transgenic mouse model expressing an antisense ribozyme specific for PDX-1 mRNA. In this transgenic mouse, the expression of the PDX-1 was decreased, which causes impaired glucose tolerance, elevated glycosylated hemoglobin levels, and decreased insulin/glucose ratios. Mice heterozygous for PDX-1 gene have also been shown to be glucose intolerant [334], and targeted disruption of the PDX-1 gene in mice results in pancreatic agenesis [335]. In humans, early-onset type-II diabetes mellitus (MODY4) is linked to heterozygosity for mutations in the PDX-1 gene, and mutation of PDX-1 gene also results in agenesis of the pancreas [336]. Therefore, in order to avoid inducing diabetes in the targeted pigs, the 3'-untranslated region of the PDX-1 gene (after the stop codon of the coding region) was targeted in this study. More specifically, an IRES linked to a Cre recombinase gene was inserted. The IRES was used in this study, because it allows ribosomes to internally bind at the initiation codon (AUG) without scanning the 5'-untranslated region of the transcript [337]. In addition, without IRES connecting two genes, the relative efficiency of expression of the second gene was even less than 1% that of expression of the first gene; while the presence of IRES dramatically increased second gene expression for more than 10 to 100 fold [338]. However, some studies have reported that the gene in the downstream of the IRES is often still expressed at a lower level than the gene located upstream [338]. Recently, the 2A peptide has become a popular alternative to the IRES. This 2A peptide can cause the ribosome to skip and begin to translate from the next codon, causing the expression of two independent proteins from a single transcription event [339]. Thus, the 2A peptide has already become a useful tool for the coexpression of two or more separate proteins from a single open reading fragment (ORF) [340]. In this study, the PDX-1 gene targeting site is after the stop codon, therefore, the IRES was used in stead of the 2A peptide. Thus, the PDX-1 gene and the Cre recombinase gene connected by an IRES sequence will be both expressed from the PDX-1 promoter.

## 4.5 Outlook

**Application of *ROSA26* dual Cre reporter pigs** The *ROSA26* dual Cre reporter pigs will be used to establish a reporter line to characterise and monitor Cre-driver pigs designed to

express Cre recombinase in specific cell types, at defined time points, or in response to drug induction, as widely used in mice [341]. For instance, *ROSA26* dual Cre reporter pigs can be crossed with the PDX-1-Cre porcine model (Cre recombinase driven by a pancreatic specific promoter) to visualize pancreatic cells expressing Cre recombinase and non-expressing cells, which will pave a useful way for studying the pancreas development and regeneration.

The dual reporter pigs can also be crossed with pigs carrying Cre-ER<sup>T</sup> or Cre-ER<sup>T2</sup> driven by various promoters, thereby allowing for monitoring of the spatial and temporal expression of the Cre recombinase. Cre-ER<sup>T</sup> or Cre-ER<sup>T2</sup> is fusion protein between the mutant estrogen ligand-binding domain (ER<sup>T</sup> or ER<sup>T2</sup>) and the Cre recombinase, the activity of which can be induced by 4-hydroxy-tamoxifen (OHT) [342]. One limitation of using OHT *in vivo* may be its toxicity [342], but Cre-ER<sup>T2</sup> is approximately 10 times more sensitive to OHT induction *in vivo* than Cre-ER<sup>T</sup> [343]. So, using Cre-ER<sup>T2</sup> instead of Cre-ER<sup>T</sup> can minimize the toxicity issue. The F1 generation of *ROSA26* dual Cre reporter pigs crossed with Cre-ER<sup>T2</sup> pigs is a useful tool to monitor Cre recombinase activity at defined time points by injection of OHT.

Combining the *ROSA26* dual Cre reporter pigs with porcine cancer models carrying inducible mutations in tumour suppressor genes and proto-oncogenes will provide a powerful tool to monitor tumor formation, neoplastic lesions and so on in real time. For example, so far, a triple transgenic LSL-Kras<sup>G12D/+</sup>; LSL-Trp53<sup>R172H/+</sup>; PDX-1-Cre mouse model of pancreatic cancer has proven to present pancreatic intraepithelial neoplasia (PanIN) and well differentiated infiltrating ductal adenocarcinoma of the pancreas (PDAC) [42,44]. However, such a triple transgenic porcine model is still missing. This study is an important contribution to the establishment of such a triple transgenic porcine model which can mimic the human pancreatic cancer at a more realistic scale [344]. For this, *ROSA26* reporter pigs then can be crossed with pancreatic cancer pigs to monitor and trace pancreatic neoplasia forming, cellular pathology of pancreatic neoplasia and PanIN lesions.

The *ROSA26* Cre reporter pig line can also be used to directly assess the pattern of Cre expression administered locally, for example by *in vivo* viral transduction, DNA transfection, or protein transduction [345,346].

Therefore, these *ROSA26* dual reporter pigs will be an important and useful resource that will help to investigate basic biological principles, developmental biology and new therapeutic approaches for cancers.

**Alternative way to generate transgenic pigs** In this study, the currently common strategy used to generate gene modified pigs was applied, which requires two steps. Firstly, gene modified porcine somatic cells are obtained with the help of site-specific nucleases (ZFNs, TALENs, CRISPR/Cas9 system) or using traditional targeting vectors. Secondly, the nuclei of gene modified porcine somatic cells are transferred into enucleated oocytes to generate gene engineered pigs. However, the technical challenges of SCNT and low efficiency of cloning have limited the application of porcine models. An alternative and promising way to generate transgenic pigs is direct injection of site-specific nucleases (such as Cas9 mRNA and sgRNA) into zygotes. This method only requires one step. Highly efficient one-step generation of gene engineered mice and rats have been reported by direct injection of the CRISPR/Cas9 system into one-cell embryos. Recently, it has been reported that vWF (von Willebrand factor) gene knock-out pigs have also been efficiently generated by zygote injection of CRISPR/Cas9 system in one step [347]. The high efficiency of one step generation of gene modified pigs by zygote injection of the CRISPR/Cas9 system will accelerate the development of gene engineered pigs applied in agriculture and biomedicine.

**Porcine cancer model** Generation of porcine models to mimic human cancers can bridge the gap between laboratory and clinical oncology and transit into practical benefits for human patients. Triple transgenic LSL-Kras<sup>G12D/+</sup>; LSL-Trp53<sup>R172H/+</sup>; PDX-1-Cre pigs will be generated as pancreatic cancer model. Pigs having a LSL-Kras<sup>G12D/+</sup>; LSL-Trp53<sup>R172H/+</sup> background can also be extended to the generation of other porcine cancer models, such as porcine model for human lung cancer, since human lung cancer is also linked to mutation of KRAS and Trp53. For this, pigs expressing Cre recombinase specific in the lung will be established. Afterwards, triple transgenic LSL-Kras<sup>G12D/+</sup>; LSL-Trp53<sup>R172H/+</sup>; lung specific Cre recombinase pig can be generated as a human lung cancer model.

**Pig used for other disease model**

Genomic modified porcine models also can be generated for other diseases, such as Alzheimer's disease, cardiovascular diseases, cystic fibrosis [151], retinitis pigmentosa [348,349], spinal muscular atrophy, Huntington's disease, xenotransplantation and so on. These porcine models provide the preclinical data for treatments of these diseases.

## 5 References:

1. Go VLW. *The Pancreas: biology, pathobiology, and disease*. Raven Press; 1993.
2. Hezel AF, Kimmelman AC, Stanger BZ, Bardeesy N, Depinho RA. Genetics and biology of pancreatic ductal adenocarcinoma. *Genes Dev* 2006; **20**:1218–1249.
3. Hariharan D, Saied A, Kocher HM. Analysis of mortality rates for pancreatic cancer across the world. *HPB* 2008; **10**:58–62.
4. Li D, Xie K, Wolff R, Abbruzzese JL. Pancreatic cancer. *The Lancet* 2004; **363**:1049–1057.
5. Bardeesy N, DePinho RA. Pancreatic cancer biology and genetics. *Nat Rev Cancer* 2002; **2**:897–909.
6. Hruban RH, Adsay NV, Albores-Saavedra J, *et al*. Pancreatic intraepithelial neoplasia: a new nomenclature and classification system for pancreatic duct lesions. *Am J Surg Pathol* 2001; **25**:579–586.
7. Matthaei H, Schulick RD, Hruban RH, Maitra A. Cystic precursors to invasive pancreatic cancer. *Nat Rev Gastroenterol Hepatol* 2011; **8**:141–150.
8. Hruban RH, Takaori K, Klimstra DS, *et al*. An illustrated consensus on the classification of pancreatic intraepithelial neoplasia and intraductal papillary mucinous neoplasms. *Am J Surg Pathol* 2004; **28**:977–987.
9. Macgregor-Das AM, Iacobuzio-Donahue CA. Molecular pathways in pancreatic carcinogenesis. *J Surg Oncol* 2013; **107**:8–14.
10. Thompson LD, Becker RC, Przygodzki RM, Adair CF, Heffess CS. Mucinous cystic neoplasm (mucinous cystadenocarcinoma of low-grade malignant potential) of the pancreas: a clinicopathologic study of 130 cases. *Am J Surg Pathol* 1999; **23**:1–16.
11. Maitra A, Fukushima N, Takaori K, Hruban RH. Precursors to invasive pancreatic cancer. *Adv Anat Pathol* 2005; **12**:81–91.
12. Delpu Y, Hanoun N, Lulka H, *et al*. Genetic and Epigenetic Alterations in Pancreatic Carcinogenesis. *Curr Genomics* 2011; **12**:15–24.
13. Qian J, Yang H, Li J, Wang J. Characterization of the Molecular Genetic Mechanisms that Contribute to Pancreatic Cancer Carcinogenesis. In: Srivastava S, ed. *Pancreatic Cancer - Molecular Mechanism and Targets*. InTech; 2012.
14. Yonezawa S, Higashi M, Yamada N, Goto M. Precursor Lesions of Pancreatic Cancer. *Gut Liver* 2008; **2**:137–154.



15. Kanda M, Matthaei H, Wu J, *et al.* Presence of somatic mutations in most early-stage pancreatic intraepithelial neoplasia. *Gastroenterology* 2012; **142**:730–733.e9.
16. Campbell SL, Khosravi-Far R, Rossman KL, Clark GJ, Der CJ. Increasing complexity of Ras signaling. *Oncogene* 1998; **17**:1395–1413.
17. Malumbres M, Barbacid M. RAS oncogenes: the first 30 years. *Nat Rev Cancer* 2003; **3**:459–465.
18. Hall BE, Bar-Sagi D, Nassar N. The structural basis for the transition from Ras-GTP to Ras-GDP. *Proc Natl Acad Sci U S A* 2002; **99**:12138–12142.
19. Scheffzek K, Ahmadian MR, Kabsch W, *et al.* The Ras-RasGAP complex: structural basis for GTPase activation and its loss in oncogenic Ras mutants. *Science* 1997; **277**:333–338.
20. Trahey M, McCormick F. A cytoplasmic protein stimulates normal N-ras p21 GTPase, but does not affect oncogenic mutants. *Science* 1987; **238**:542–545.
21. Schubbert S, Shannon K, Bollag G. Hyperactive Ras in developmental disorders and cancer. *Nat Rev Cancer* 2007; **7**:295–308.
22. Smit VT, Boot AJ, Smits AM, Fleuren GJ, Cornelisse CJ, Bos JL. KRAS codon 12 mutations occur very frequently in pancreatic adenocarcinomas. *Nucleic Acids Res* 1988; **16**:7773–7782.
23. Hruban RH, van Mansfeld AD, Offerhaus GJ, *et al.* K-ras oncogene activation in adenocarcinoma of the human pancreas. A study of 82 carcinomas using a combination of mutant-enriched polymerase chain reaction analysis and allele-specific oligonucleotide hybridization. *Am J Pathol* 1993; **143**:545–554.
24. Palmirotta R, Savonarola A, Formica V, *et al.* A Novel K-ras Mutation in Colorectal Cancer. A Case Report and Literature Review. *Anticancer Res* 2009; **29**:3369–3374.
25. Lin S-R, Hsu C-H, Tsai J-H, Wang J-Y, Hsieh T-J, Wu C-H. Decreased GTPase activity of K- ras mutants deriving from human functional adrenocortical tumours. *Br J Cancer* 2000; **82**:1035–1040.
26. Hofmann I, Weiss A, Elain G, *et al.* K-RAS Mutant Pancreatic Tumors Show Higher Sensitivity to MEK than to PI3K Inhibition In Vivo. *PLoS ONE* 2012; **7**:e44146.
27. Caldas C, Hahn SA, da Costa LT, *et al.* Frequent somatic mutations and homozygous deletions of the p16 (MTS1) gene in pancreatic adenocarcinoma. *Nat Genet* 1994; **8**:27–32.
28. Rozenblum E, Schutte M, Goggins M, *et al.* Tumor-suppressive pathways in pancreatic carcinoma. *Cancer Res* 1997; **57**:1731–1734.
29. Seemann S, Maurici D, Olivier M, Fromentel CC de, Hainaut P. The Tumor Suppressor Gene TP53: Implications for Cancer Management and Therapy. 2008.

- 
30. Amundson SA, Myers TG, Fornace AJ Jr. Roles for p53 in growth arrest and apoptosis: putting on the brakes after genotoxic stress. *Oncogene* 1998; **17**:3287–3299.
31. Maitra A, Adsay NV, Argani P, *et al.* Multicomponent analysis of the pancreatic adenocarcinoma progression model using a pancreatic intraepithelial neoplasia tissue microarray. *Mod Pathol Off J U S Can Acad Pathol Inc* 2003; **16**:902–912.
32. Vogelstein B, Kinzler KW. Cancer genes and the pathways they control. *Nat Med* 2004; **10**:789–799.
33. Melnikova VO, Ananthaswamy HN. p53 Protein and Nonmelanoma Skin Cancer. In: *Molecular Mechanisms of Basal Cell and Squamous Cell Carcinomas*. Medical Intelligence Unit. Springer US; 2006:66–79.
34. Pinho AV, Rومان I, Real FX. p53-dependent regulation of growth, epithelial-mesenchymal transition and stemness in normal pancreatic epithelial cells. *Cell Cycle Georget Tex* 2011; **10**:1312–1321.
35. Wilentz RE, Iacobuzio-Donahue CA, Argani P, *et al.* Loss of expression of Dpc4 in pancreatic intraepithelial neoplasia: evidence that DPC4 inactivation occurs late in neoplastic progression. *Cancer Res* 2000; **60**:2002–2006.
36. Hahn SA, Schutte M, Hoque AT, *et al.* DPC4, a candidate tumor suppressor gene at human chromosome 18q21.1. *Science* 1996; **271**:350–353.
37. Bierie B, Moses HL. Tumour microenvironment: TGFbeta: the molecular Jekyll and Hyde of cancer. *Nat Rev Cancer* 2006; **6**:506–520.
38. Massagué J. TGFβ in Cancer. *Cell* 2008; **134**:215–230.
39. Derynck R, Zhang YE. Smad-dependent and Smad-independent pathways in TGF-beta family signalling. *Nature* 2003; **425**:577–584.
40. Siegel PM, Massagué J. Cytostatic and apoptotic actions of TGF-beta in homeostasis and cancer. *Nat Rev Cancer* 2003; **3**:807–821.
41. Miyaki M, Kuroki T. Role of Smad4 (DPC4) inactivation in human cancer. *Biochem Biophys Res Commun* 2003; **306**:799–804.
42. Herreros-Villanueva M, Hijona E, Cosme A, Bujanda L. Mouse models of pancreatic cancer. *World J Gastroenterol WJG* 2012; **18**:1286–1294.
43. Cheon D-J, Orsulic S. Mouse Models of Cancer. *Annu Rev Pathol Mech Dis* 2011; **6**:95–119.
44. Olive KP, Tuveson DA. The Use of Targeted Mouse Models for Preclinical Testing of Novel Cancer Therapeutics. *Clin Cancer Res* 2006; **12**:5277–5287.

- 
45. Ornitz DM, Hammer RE, Messing A, Palmiter RD, Brinster RL. Pancreatic neoplasia induced by SV40 T-antigen expression in acinar cells of transgenic mice. *Science* 1987; **238**:188–193.
46. Quaife CJ, Pinkert CA, Ornitz DM, Palmiter RD, Brinster RL. Pancreatic neoplasia induced by ras expression in acinar cells of transgenic mice. *Cell* 1987; **48**:1023–1034.
47. Hingorani SR, Petricoin EF, Maitra A, *et al.* Preinvasive and invasive ductal pancreatic cancer and its early detection in the mouse. *Cancer Cell* 2003; **4**:437–450.
48. Hingorani SR, Wang L, Multani AS, *et al.* Trp53R172H and KrasG12D cooperate to promote chromosomal instability and widely metastatic pancreatic ductal adenocarcinoma in mice. *Cancer Cell* 2005; **7**:469–483.
49. Aguirre AJ, Bardeesy N, Sinha M, *et al.* Activated Kras and Ink4a/Arf deficiency cooperate to produce metastatic pancreatic ductal adenocarcinoma. *Genes Dev* 2003; **17**:3112–3126.
50. Kojima K, Vickers SM, Adsay NV, *et al.* Inactivation of Smad4 accelerates Kras(G12D)-mediated pancreatic neoplasia. *Cancer Res* 2007; **67**:8121–8130.
51. Tuveson DA, Zhu L, Gopinathan A, *et al.* Mist1-KrasG12D knock-in mice develop mixed differentiation metastatic exocrine pancreatic carcinoma and hepatocellular carcinoma. *Cancer Res* 2006; **66**:242–247.
52. Ijichi H, Chytil A, Gorska AE, *et al.* Aggressive pancreatic ductal adenocarcinoma in mice caused by pancreas-specific blockade of transforming growth factor-beta signaling in cooperation with active Kras expression. *Genes Dev* 2006; **20**:3147–3160.
53. Flisikowska T, Kind A, Schnieke A. Genetically modified pigs to model human diseases. *J Appl Genet* 2013.
54. Whyte JJ, Prather RS. Genetic modifications of pigs for medicine and agriculture. *Mol Reprod Dev* 2011; **78**:879–891.
55. Lai L, Kolber-Simonds D, Park K-W, *et al.* Production of  $\alpha$ -1,3-Galactosyltransferase Knockout Pigs by Nuclear Transfer Cloning. *Science* 2002; **295**:1089–1092.
56. Du Z-Q, Vincent-Naulleau S, Gilbert H, *et al.* Detection of novel quantitative trait loci for cutaneous melanoma by genome-wide scan in the MeLiM swine model. *Int J Cancer J Int Cancer* 2007; **120**:303–320.
57. Flisikowska T, Merkl C, Landmann M, *et al.* A Porcine Model of Familial Adenomatous Polyposis. *Gastroenterology* 2012; **143**:1173–1175.e7.
58. Dyson MC, Alloosh M, Vuchetich JP, Mokolke EA, Sturek M. Components of metabolic syndrome and coronary artery disease in female Ossabaw swine fed excess atherogenic diet. *Comp Med* 2006; **56**:35–45.

- 
59. Turk JR, Laughlin MH. Physical activity and atherosclerosis: which animal model? *Can J Appl Physiol Rev Can Physiol Appliquée* 2004; **29**:657–683.
60. Ishii A, Viñuela F, Murayama Y, *et al.* Swine model of carotid artery atherosclerosis: experimental induction by surgical partial ligation and dietary hypercholesterolemia. *AJNR Am J Neuroradiol* 2006; **27**:1893–1899.
61. Dick IP, Scott RC. Pig ear skin as an in-vitro model for human skin permeability. *J Pharm Pharmacol* 1992; **44**:640–645.
62. Graham JS, Reid FM, Smith JR, *et al.* A cutaneous full-thickness liquid sulfur mustard burn model in weanling swine: clinical pathology and urinary excretion of thiodiglycol. *J Appl Toxicol JAT* 2000; **20 Suppl 1**:S161–172.
63. Shatos M a., Klassen H, Schwartz P h., *et al.* Isolation of progenitor cells from retina and brain of the GFP-transgenic pig. *ARVO Meet Abstr* 2004; **45**:5406.
64. Gama Sosa MA, De Gasperi R, Elder GA. Animal transgenesis: an overview. *Brain Struct Funct* 2010; **214**:91–109.
65. Jaenisch R, Mintz B. Simian Virus 40 DNA Sequences in DNA of Healthy Adult Mice Derived from Preimplantation Blastocysts Injected with Viral DNA. *Proc Natl Acad Sci U S A* 1974; **71**:1250–1254.
66. Gordon JW, Scangos GA, Plotkin DJ, Barbosa JA, Ruddle FH. Genetic transformation of mouse embryos by microinjection of purified DNA. *Proc Natl Acad Sci U S A* 1980; **77**:7380–7384.
67. Hammer RE, Pursel VG, Rexroad CE Jr, *et al.* Production of transgenic rabbits, sheep and pigs by microinjection. *Nature* 1985; **315**:680–683.
68. Robl JM, Wang Z, Kasinathan P, Kuroiwa Y. Transgenic animal production and animal biotechnology. *Theriogenology* 2007; **67**:127–133.
69. Wolf E, Schernthaner W, Zakhartchenko V, Prella K, Stojkovic M, Brem G. Transgenic technology in farm animals--progress and perspectives. *Exp Physiol* 2000; **85**:615–625.
70. Tesson L, Cozzi J, Ménoret S, *et al.* Transgenic modifications of the rat genome. *Transgenic Res* 2005; **14**:531–546.
71. Lavitrano M, Camaioni A, Fazio VM, Dolci S, Farace MG, Spadafora C. Sperm cells as vectors for introducing foreign DNA into eggs: genetic transformation of mice. *Cell* 1989; **57**:717–723.
72. Hirabayashi M, Takahashi R, Ito K, *et al.* A comparative study on the integration of exogenous DNA into mouse, rat, rabbit, and pig genomes. *Exp Anim Jpn Assoc Lab Anim Sci* 2001; **50**:125–131.

73. Niemann H, Verhoeyen E, Wonigeit K, *et al.* Cytomegalovirus early promoter induced expression of hCD59 in porcine organs provides protection against hyperacute rejection. *Transplantation* 2001; **72**:1898–1906.
74. Lavitrano M, Busnelli M, Cerrito MG, Giovannoni R, Manzini S, Vargiolu A. Sperm-mediated gene transfer. *Reprod Fertil Dev* 2006; **18**:19–23.
75. Manzini S, Vargiolu A, Stehle IM, *et al.* Genetically modified pigs produced with a nonviral episomal vector. *Proc Natl Acad Sci U S A* 2006; **103**:17672–17677.
76. Reh binder E, Engelhard M, Hagen K, *et al.* *Pharming: Promises and risks of biopharmaceuticals derived from genetically modified plants and animals*. Springer; 2008.
77. Dupuy AJ, Clark K, Carlson CM, *et al.* Mammalian germ-line transgenesis by transposition. *Proc Natl Acad Sci U S A* 2002; **99**:4495–4499.
78. Tan WS, Carlson DF, Walton MW, Fahrenkrug SC, Hackett PB. Precision editing of large animal genomes. *Adv Genet* 2012; **80**:37–97.
79. Chan AWS, Homan EJ, Ballou LU, Burns JC, Bremel RD. Transgenic cattle produced by reverse-transcribed gene transfer in oocytes. *Proc Natl Acad Sci U S A* 1998; **95**:14028–14033.
80. Pinkert CA. Genetic Engineering and Competitiveness of Livestock Production. *Agric Conspec Sci ACS* 2003; **68**:45–54.
81. Goff SP. Genetics of retroviral integration. *Annu Rev Genet* 1992; **26**:527–544.
82. Brown PO, Bowerman B, Varmus HE, Bishop JM. Retroviral integration: structure of the initial covalent product and its precursor, and a role for the viral IN protein. *Proc Natl Acad Sci U S A* 1989; **86**:2525–2529.
83. Kulkosky J, Skalka AM. Molecular mechanism of retroviral DNA integration. *Pharmacol Ther* 1994; **61**:185–203.
84. Jähner D, Jaenisch R. Chromosomal position and specific demethylation in enhancer sequences of germ line-transmitted retroviral genomes during mouse development. *Mol Cell Biol* 1985; **5**:2212–2220.
85. Naldini L, Blömer U, Gallay P, *et al.* In vivo gene delivery and stable transduction of nondividing cells by a lentiviral vector. *Science* 1996; **272**:263–267.
86. Poeschla E, Corbeau P, Wong-Staal F. Development of HIV vectors for anti-HIV gene therapy. *Proc Natl Acad Sci U S A* 1996; **93**:11395–11399.
87. Pfeifer A, Ikawa M, Dayn Y, Verma IM. Transgenesis by lentiviral vectors: Lack of gene silencing in mammalian embryonic stem cells and preimplantation embryos. *Proc Natl Acad Sci* 2002; **99**:2140–2145.

- 
88. Miyoshi H, Blömer U, Takahashi M, Gage FH, Verma IM. Development of a Self-Inactivating Lentivirus Vector. *J Virol* 1998; **72**:8150–8157.
89. Zufferey R, Dull T, Mandel RJ, *et al.* Self-inactivating lentivirus vector for safe and efficient in vivo gene delivery. *J Virol* 1998; **72**:9873–9880.
90. Blesch A, Conner J, Pfeifer A, *et al.* Regulated lentiviral NGF gene transfer controls rescue of medial septal cholinergic neurons. *Mol Ther J Am Soc Gene Ther* 2005; **11**:916–925.
91. Lois C, Hong EJ, Pease S, Brown EJ, Baltimore D. Germline Transmission and Tissue-Specific Expression of Transgenes Delivered by Lentiviral Vectors. *Science* 2002; **295**:868–872.
92. Hofmann A, Kessler B, Ewerling S, *et al.* Efficient transgenesis in farm animals by lentiviral vectors. *EMBO Rep* 2003; **4**:1054–1060.
93. Whitelaw CBA, Radcliffe PA, Ritchie WA, *et al.* Efficient generation of transgenic pigs using equine infectious anaemia virus (EIAV) derived vector. *FEBS Lett* 2004; **571**:233–236.
94. Hofmann A, Zakhartchenko V, Weppert M, *et al.* Generation of transgenic cattle by lentiviral gene transfer into oocytes. *Biol Reprod* 2004; **71**:405–409.
95. McGrew MJ, Sherman A, Ellard FM, *et al.* Efficient production of germline transgenic chickens using lentiviral vectors. *EMBO Rep* 2004; **5**:728–733.
96. Rong YS, Golic KG. Gene Targeting by Homologous Recombination in Drosophila. *Science* 2000; **288**:2013–2018.
97. Capecchi MR. Altering the genome by homologous recombination. *Science* 1989; **244**:1288–1292.
98. Koller BH, Smithies O. Inactivating the beta 2-microglobulin locus in mouse embryonic stem cells by homologous recombination. *Proc Natl Acad Sci* 1989; **86**:8932–8935.
99. Wilson JH, Vasquez KM. Gene Targeting by Homologous Recombination. In: eLS. John Wiley & Sons, Ltd; 2001.
100. Terada R, Urawa H, Inagaki Y, Tsugane K, Iida S. Efficient gene targeting by homologous recombination in rice. *Nat Biotechnol* 2002; **20**:1030–1034.
101. Zwaka TP, Thomson JA. Homologous recombination in human embryonic stem cells. *Nat Biotechnol* 2003; **21**:319–321.
102. Porteus M. Using homologous recombination to manipulate the genome of human somatic cells. *Biotechnol Genet Eng Rev* 2007; **24**:195–212.
103. Vasquez KM, Marburger K, Intody Z, Wilson JH. Manipulating the mammalian genome

- by homologous recombination. *Proc Natl Acad Sci* 2001; **98**:8403–8410.
104. Lee K, Prather RS. Advancements in somatic cell nuclear transfer and future perspectives. *Anim Front* 2013; **3**:56–61.
105. Willadsen SM. Nuclear transplantation in sheep embryos. *Nature* 1986; **320**:63–65.
106. Wilmut I, Schnieke AE, McWhir J, Kind AJ, Campbell KHS. Viable offspring derived from fetal and adult mammalian cells. *Nature* 1997; **385**:810–813.
107. Schnieke AE, Kind AJ, Ritchie WA, *et al.* Human factor IX transgenic sheep produced by transfer of nuclei from transfected fetal fibroblasts. *Science* 1997; **278**:2130–2133.
108. Baguisi A, Behboodi E, Melican DT, *et al.* Production of goats by somatic cell nuclear transfer. *Nat Biotechnol* 1999; **17**:456–461.
109. Wells DN, Misica PM, Tervit HR, Vivanco WH. Adult somatic cell nuclear transfer is used to preserve the last surviving cow of the Enderby Island cattle breed. *Reprod Fertil Dev* 1998; **10**:369–378.
110. Polejaeva IA, Chen SH, Vaught TD, *et al.* Cloned pigs produced by nuclear transfer from adult somatic cells. *Nature* 2000; **407**:86–90.
111. Betthausen J, Forsberg E, Augenstein M, *et al.* Production of cloned pigs from in vitro systems. *Nat Biotechnol* 2000; **18**:1055–1059.
112. Onishi A, Iwamoto M, Akita T, *et al.* Pig cloning by microinjection of fetal fibroblast nuclei. *Science* 2000; **289**:1188–1190.
113. Flisikowska T, Thorey IS, Offner S, *et al.* Efficient immunoglobulin gene disruption and targeted replacement in rabbit using zinc finger nucleases. *PLoS One* 2011; **6**:e21045.
114. Gaj T, Gersbach CA, Barbas III CF. ZFN, TALEN, and CRISPR/Cas-based methods for genome engineering. *Trends Biotechnol* 2013; **31**:397–405.
115. Wei C, Liu J, Yu Z, Zhang B, Gao G, Jiao R. TALEN or Cas9 - rapid, efficient and specific choices for genome modifications. *J Genet Genomics Yi Chuan Xue Bao* 2013; **40**:281–289.
116. Joung JK, Sander JD. TALENs: a widely applicable technology for targeted genome editing. *Nat Rev Mol Cell Biol* 2013; **14**:49–55.
117. Hsu PD, Scott DA, Weinstein JA, *et al.* DNA targeting specificity of RNA-guided Cas9 nucleases. *Nat Biotechnol* 2013; **31**:827–832.
118. Mali P, Yang L, Esvelt KM, *et al.* RNA-Guided Human Genome Engineering via Cas9. *Science* 2013; **339**:823–826.
119. Zu Y, Tong X, Wang Z, *et al.* TALEN-mediated precise genome modification by

- homologous recombination in zebrafish. *Nat Methods* 2013; **10**:329–331.
120. White FF, Potnis N, Jones JB, Koebnik R. The type III effectors of *Xanthomonas*. *Mol Plant Pathol* 2009; **10**:749–766.
121. Li T, Huang S, Jiang WZ, *et al.* TAL nucleases (TALNs): hybrid proteins composed of TAL effectors and FokI DNA-cleavage domain. *Nucleic Acids Res* 2011; **39**:359–372.
122. Bonas U, Stall RE, Staskawicz B. Genetic and structural characterization of the avirulence gene *avrBs3* from *Xanthomonas campestris* pv. *vesicatoria*. *Mol Gen Genet MGG* 1989; **218**:127–136.
123. Cermak T, Doyle EL, Christian M, *et al.* Efficient design and assembly of custom TALEN and other TAL effector-based constructs for DNA targeting. *Nucleic Acids Res* 2011; **39**:e82.
124. Moscou MJ, Bogdanove AJ. A simple cipher governs DNA recognition by TAL effectors. *Science* 2009; **326**:1501.
125. Vanamee ES, Santagata S, Aggarwal AK. FokI requires two specific DNA sites for cleavage. *J Mol Biol* 2001; **309**:69–78.
126. Wah DA, Bitinaite J, Schildkraut I, Aggarwal AK. Structure of FokI has implications for DNA cleavage. *Proc Natl Acad Sci U S A* 1998; **95**:10564–10569.
127. Wah DA, Hirsch JA, Dorner LF, Schildkraut I, Aggarwal AK. Structure of the multimodular endonuclease FokI bound to DNA. *Nature* 1997; **388**:97–100.
128. Bedell VM, Wang Y, Campbell JM, *et al.* In vivo genome editing using a high-efficiency TALEN system. *Nature* 2012; **advance online publication**.
129. Miller JC, Tan S, Qiao G, *et al.* A TALE nuclease architecture for efficient genome editing. *Nat Biotechnol* 2011; **29**:143–148.
130. Wang B, Zhou J. Specific genetic modifications of domestic animals by gene targeting and animal cloning. *Reprod Biol Endocrinol RBE* 2003; **1**:103.
131. Smithies O, Gregg RG, Boggs SS, Koralewski MA, Kucherlapati RS. Insertion of DNA sequences into the human chromosomal  $\beta$ -globin locus by homologous recombination. *Nature* 1985; **317**:230–234.
132. Martin GR. Isolation of a pluripotent cell line from early mouse embryos cultured in medium conditioned by teratocarcinoma stem cells. *Proc Natl Acad Sci U S A* 1981; **78**:7634–7638.
133. Evans MJ, Kaufman MH. Establishment in culture of pluripotential cells from mouse embryos. *Nature* 1981; **292**:154–156.
134. Müller U. Ten years of gene targeting: targeted mouse mutants, from vector design to



- phenotype analysis. *Mech Dev* 1999; **82**:3–21.
135. Thomas KR, Capecchi MR. Site-directed mutagenesis by gene targeting in mouse embryo-derived stem cells. *Cell* 1987; **51**:503–512.
136. Doetschman T, Gregg RG, Maeda N, *et al.* Targetted correction of a mutant HPRT gene in mouse embryonic stem cells. *Nature* 1987; **330**:576–578.
137. Mansour SL, Thomas KR, Capecchi MR. Disruption of the proto-oncogene int-2 in mouse embryo-derived stem cells: a general strategy for targeting mutations to non-selectable genes. *Nature* 1988; **336**:348–352.
138. Schwartzberg PL, Goff SP, Robertson EJ. Germ-line transmission of a c-abl mutation produced by targeted gene disruption in ES cells. *Science* 1989; **246**:799–803.
139. Thomson JA, Kalishman J, Golos TG, *et al.* Isolation of a primate embryonic stem cell line. *Proc Natl Acad Sci U S A* 1995; **92**:7844–7848.
140. Thomson JA, Itskovitz-Eldor J, Shapiro SS, *et al.* Embryonic Stem Cell Lines Derived from Human Blastocysts. *Science* 1998; **282**:1145–1147.
141. Ueda S, Kawamata M, Teratani T, *et al.* Establishment of Rat Embryonic Stem Cells and Making of Chimera Rats. *PLoS ONE* 2008; **3**:e2800.
142. Clark AJ, Burl S, Denning C, Dickinson P. Gene targeting in livestock: a preview. *Transgenic Res* 2000; **9**:263–275.
143. McCreath KJ, Howcroft J, Campbell KH, Colman A, Schnieke AE, Kind AJ. Production of gene-targeted sheep by nuclear transfer from cultured somatic cells. *Nature* 2000; **405**:1066–1069.
144. Dai Y, Vaught TD, Boone J, *et al.* Targeted disruption of the alpha1,3-galactosyltransferase gene in cloned pigs. *Nat Biotechnol* 2002; **20**:251–255.
145. Richt JA, Kasinathan P, Hamir AN, *et al.* Production of cattle lacking prion protein. *Nat Biotechnol* 2007; **25**:132–138.
146. Phelps CJ, Koike C, Vaught TD, *et al.* Production of alpha 1,3-galactosyltransferase-deficient pigs. *Science* 2003; **299**:411–414.
147. Ratjen FA. Cystic Fibrosis: Pathogenesis and Future Treatment Strategies. *Respir Care* 2009; **54**:595–605.
148. Rogers CS, Hao Y, Rokhlina T, *et al.* Production of CFTR-null and CFTR-DeltaF508 heterozygous pigs by adeno-associated virus-mediated gene targeting and somatic cell nuclear transfer. *J Clin Invest* 2008; **118**:1571–1577.
149. Grubb BR, Boucher RC. Pathophysiology of gene-targeted mouse models for cystic

fibrosis. *Physiol Rev* 1999; **79**:S193–214.

150. Guilbault C, Saeed Z, Downey GP, Radzioch D. Cystic Fibrosis Mouse Models. *Am J Respir Cell Mol Biol* 2007; **36**:1–7.

151. Rogers CS, Stoltz DA, Meyerholz DK, *et al.* Disruption of the CFTR gene produces a model of cystic fibrosis in newborn pigs. *Science* 2008; **321**:1837–1841.

152. Luo Y, Li J, Liu Y, *et al.* High efficiency of BRCA1 knockout using rAAV-mediated gene targeting: developing a pig model for breast cancer. *Transgenic Res* 2011; **20**:975–988.

153. Leuchs S, Saalfrank A, Merkl C, *et al.* Inactivation and Inducible Oncogenic Mutation of p53 in Gene Targeted Pigs. *PLoS ONE* 2012; **7**.

154. Hoess R, Abremski K, Irwin S, Kendall M, Mack A. DNA specificity of the cre recombinase resides in the 25 kDa carboxyl domain of the protein. *J Mol Biol* 1990; **216**:873–882.

155. Abremski K, Hoess R, Sternberg N. Studies on the properties of P1 site-specific recombination: evidence for topologically unlinked products following recombination. *Cell* 1983; **32**:1301–1311.

156. Semprini S, Troup TJ, Kotelevtseva N, *et al.* Cryptic loxP sites in mammalian genomes: genome-wide distribution and relevance for the efficiency of BAC/PAC recombineering techniques. *Nucleic Acids Res* 2007; **35**:1402–1410.

157. Nagy A. Cre recombinase: the universal reagent for genome tailoring. *Genes N Y N* 2000 2000; **26**:99–109.

158. Zhang J, Zhao J, Jiang W, Shan X, Yang X, Gao J. Conditional gene manipulation: Cre-ating a new biological era. *J Zhejiang Univ Sci B* 2012; **13**:511–524.

159. Orban PC, Chui D, Marth JD. Tissue- and site-specific DNA recombination in transgenic mice. *Proc Natl Acad Sci U S A* 1992; **89**:6861–6865.

160. Sauer B, Henderson N. Site-specific DNA recombination in mammalian cells by the Cre recombinase of bacteriophage P1. *Proc Natl Acad Sci U S A* 1988; **85**:5166–5170.

161. Alam J, Cook JL. Reporter genes: Application to the study of mammalian gene transcription. *Anal Biochem* 1990; **188**:245–254.

162. Bronstein I, Fortin J, Stanley PE, Stewart GS, Kricka LJ. Chemiluminescent and bioluminescent reporter gene assays. *Anal Biochem* 1994; **219**:169–181.

163. Wood KV. Marker proteins for gene expression. *Curr Opin Biotechnol* 1995; **6**:50–58.

164. Schwartz O, Virelizier J-L, Montagnier L, Hazan U. A microtransfection method using the luciferase-encoding reporter gene for the assay of human immunodeficiency virus LTR

promoter activity. *Gene* 1990; **88**:197–205.

165. Williams TM, Burlein JE, Ogden S, Kricka LJ, Kant JA. Advantages of firefly luciferase as a reporter gene: application to the interleukin-2 gene promoter. *Anal Biochem* 1989; **176**:28–32.

166. Pazzagli M, Devine JH, Peterson DO, Baldwin TO. Use of bacterial and firefly luciferases as reporter genes in DEAE-dextran-mediated transfection of mammalian cells. *Anal Biochem* 1992; **204**:315–323.

167. Guarente L, Ptashne M. Fusion of *Escherichia coli* lacZ to the cytochrome c gene of *Saccharomyces cerevisiae*. *Proc Natl Acad Sci U S A* 1981; **78**:2199–2203.

168. Shimomura O, Johnson FH, Saiga Y. Extraction, Purification and Properties of Aequorin, a Bioluminescent Protein from the Luminous Hydromedusan, *Aequorea*. *J Cell Comp Physiol* 1962; **59**:223–239.

169. Prendergast FG, Mann KG. Chemical and physical properties of aequorin and the green fluorescent protein isolated from *Aequorea forskålea*. *Biochemistry (Mosc)* 1978; **17**:3448–3453.

170. Tsien RY. The green fluorescent protein. *Annu Rev Biochem* 1998; **67**:509–544.

171. Chudakov DM, Matz MV, Lukyanov S, Lukyanov KA. Fluorescent proteins and their applications in imaging living cells and tissues. *Physiol Rev* 2010; **90**:1103–1163.

172. Tsien RY. The Green Fluorescent Protein. *Annu Rev Biochem* 1998; **67**:509–544.

173. Phillips GJ. Green fluorescent protein--a bright idea for the study of bacterial protein localization. *FEMS Microbiol Lett* 2001; **204**:9–18.

174. Okabe M, Ikawa M, Kominami K, Nakanishi T, Nishimune Y. "Green mice" as a source of ubiquitous green cells. *FEBS Lett* 1997; **407**:313–319.

175. Hadjantonakis AK, Nagy A. FACS for the isolation of individual cells from transgenic mice harboring a fluorescent protein reporter. *Genes N Y N 2000* 2000; **27**:95–98.

176. Srinivas S, Watanabe T, Lin CS, *et al.* Cre reporter strains produced by targeted insertion of EYFP and ECFP into the ROSA26 locus. *BMC Dev Biol* 2001; **1**:4.

177. Li L, Pang D, Wang T, *et al.* Production of a reporter transgenic pig for monitoring Cre recombinase activity. *Biochem Biophys Res Commun* 2009; **382**:232–235.

178. Deng W, Yang D, Zhao B, *et al.* Use of the 2A Peptide for Generation of Multi-Transgenic Pigs through a Single Round of Nuclear Transfer. *PLoS ONE* 2011; **6**:e19986.

179. Anon. Imaging Neuronal Subsets in Transgenic Mice Expressing Multiple Spectral Variants of GFP. *Neuron* 2000; **28**:41–51.

180. Stepanenko OV, Stepanenko OV, Shcherbakova DM, Kuznetsova IM, Turoverov KK, Verkhusha VV. Modern fluorescent proteins: from chromophore formation to novel intracellular applications. *BioTechniques* 2011; **51**:313–314, 316, 318 passim.
181. Subach FV, Verkhusha VV. Chromophore Transformations in Red Fluorescent Proteins. *Chem Rev* 2012; **112**:4308–4327.
182. Baird GS, Zacharias DA, Tsien RY. Biochemistry, mutagenesis, and oligomerization of DsRed, a red fluorescent protein from coral. *Proc Natl Acad Sci* 2000; **97**:11984–11989.
183. Hadjantonakis A-K, Macmaster S, Nagy A. Embryonic stem cells and mice expressing different GFP variants for multiple non-invasive reporter usage within a single animal. *BMC Biotechnol* 2002; **2**:11.
184. Verkhusha VV, Otsuna H, Awasaki T, Oda H, Tsukita S, Ito K. An Enhanced Mutant of Red Fluorescent Protein DsRed for Double Labeling and Developmental Timer of Neural Fiber Bundle Formation. *J Biol Chem* 2001; **276**:29621–29624.
185. Bevis BJ, Glick BS. Rapidly maturing variants of the Discosoma red fluorescent protein (DsRed). *Nat Biotechnol* 2002; **20**:83–87.
186. Vintersten K, Monetti C, Gertsenstein M, *et al.* Mouse in red: red fluorescent protein expression in mouse ES cells, embryos, and adult animals. *Genes N Y N* 2000 2004; **40**:241–246.
187. Campbell RE, Tour O, Palmer AE, *et al.* A monomeric red fluorescent protein. *Proc Natl Acad Sci U S A* 2002; **99**:7877–7882.
188. Long JZ, Lackan CS, Hadjantonakis A-K. Genetic and spectrally distinct in vivo imaging: embryonic stem cells and mice with widespread expression of a monomeric red fluorescent protein. *BMC Biotechnol* 2005; **5**:20.
189. Armstrong JJ, Larina IV, Dickinson ME, Zimmer WE, Hirschi KK. Characterization of bacterial artificial chromosome transgenic mice expressing mCherry fluorescent protein substituted for the murine smooth muscle alpha-actin gene. *Genes N Y N* 2000 2010; **48**:457–463.
190. Fink D, Wohrer S, Pfeffer M, Tombe T, Ong CJ, Sorensen PHB. Ubiquitous expression of the monomeric red fluorescent protein mcherry in transgenic mice. *genesis* 2010; **48**:723–729.
191. Larina IV, Shen W, Kelly OG, Hadjantonakis A-K, Baron MH, Dickinson ME. A membrane associated mCherry fluorescent reporter line for studying vascular remodeling and cardiac function during murine embryonic development. *Anat Rec Hoboken NJ* 2007 2009; **292**:333–341.
192. Poché RA, Larina IV, Scott ML, Saik JE, West JL, Dickinson ME. The Flk1-myr::mCherry

mouse as a useful reporter to characterize multiple aspects of ocular blood vessel development and disease. *Dev Dyn Off Publ Am Assoc Anat* 2009; **238**:2318–2326.

193. Sunmonu NA, Chen L, Li JYH. Misexpression of Gbx2 throughout the mesencephalon by a conditional gain-of-function transgene leads to deletion of the midbrain and cerebellum in mice. *Genes N Y N 2000* 2009; **47**:667–673.

194. Muzumdar MD, Tasic B, Miyamichi K, Li L, Luo L. A global double-fluorescent Cre reporter mouse. *genesis* 2007; **45**:593–605.

195. Niwa H, Yamamura K, Miyazaki J. Efficient selection for high-expression transfectants with a novel eukaryotic vector. *Gene* 1991; **108**:193–199.

196. Rhee JM, Purity MK, Lackan CS, *et al.* In vivo imaging and differential localization of lipid-modified GFP-variant fusions in embryonic stem cells and mice. *genesis* 2006; **44**:202–218.

197. Griswold SL, Sajja KC, Jang C-W, Behringer RR. Generation and characterization of iUBC-KikGR photoconvertible transgenic mice for live time-lapse imaging during development. *Genes N Y N 2000* 2011; **49**:591–598.

198. Schorpp M, Jager R, Schellander K, *et al.* The human ubiquitin C promoter directs high ubiquitous expression of transgenes in mice. *Nucleic Acids Res* 1996; **24**:1787–1788.

199. Kisseberth WC, Brettingen NT, Lohse JK, Sandgren EP. Ubiquitous Expression of Marker Transgenes in Mice and Rats. *Dev Biol* 1999; **214**:128–138.

200. Chen C, Krohn J, Bhattacharya S, Davies B. A Comparison of Exogenous Promoter Activity at the ROSA26 Locus Using a PhiC31 Integrase Mediated Cassette Exchange Approach in Mouse ES Cells. *PLoS ONE* 2011; **6**.

201. Abe T, Sakaue-Sawano A, Kiyonari H, *et al.* Visualization of cell cycle in mouse embryos with Fucci2 reporter directed by Rosa26 promoter. *Development* 2013; **140**:237–246.

202. Sternberg N, Hamilton D. Bacteriophage P1 site-specific recombination: I. Recombination between loxP sites. *J Mol Biol* 1981; **150**:467–486.

203. Lakso M, Sauer B, Mosinger B, *et al.* Targeted oncogene activation by site-specific recombination in transgenic mice. *Proc Natl Acad Sci U S A* 1992; **89**:6232–6236.

204. Araki K, Araki M, Miyazaki J, Vassalli P. Site-specific recombination of a transgene in fertilized eggs by transient expression of Cre recombinase. *Proc Natl Acad Sci* 1995; **92**:160–164.

205. Novak A, Guo C, Yang W, Nagy A, Lobe CG. Z/EG, a double reporter mouse line that expresses enhanced green fluorescent protein upon Cre-mediated excision. *Genes N Y N 2000* 2000; **28**:147–155.

206. Lobe CG, Koop KE, Kreppner W, Lomeli H, Gertsenstein M, Nagy A. Z/AP, a Double Reporter for Cre-Mediated Recombination. *Dev Biol* 1999; **208**:281–292.
207. Trichas G, Begbie J, Srinivas S. Use of the viral 2A peptide for bicistronic expression in transgenic mice. *BMC Biol* 2008; **6**:40.
208. Abe T, Kiyonari H, Shioi G, *et al.* Establishment of conditional reporter mouse lines at ROSA26 locus for live cell imaging. *genesis* 2011; **49**:579–590.
209. Stewart MD, Jang C-W, Hong NW, Austin AP, Behringer RR. Dual fluorescent protein reporters for studying cell behaviors in vivo. *genesis* 2009; **47**:708–717.
210. Zambrowicz BP, Imamoto A, Fiering S, Herzenberg LA, Kerr WG, Soriano P. Disruption of overlapping transcripts in the ROSA beta geo 26 gene trap strain leads to widespread expression of beta-galactosidase in mouse embryos and hematopoietic cells. *Proc Natl Acad Sci U S A* 1997; **94**:3789–3794.
211. Friedrich G, Soriano P. Promoter traps in embryonic stem cells: a genetic screen to identify and mutate developmental genes in mice. *Genes Dev* 1991; **5**:1513–1523.
212. Soriano P. Generalized lacZ expression with the ROSA26 Cre reporter strain. *Nat Genet* 1999; **21**:70–71.
213. Nyabi O, Naessens M, Haigh K, *et al.* Efficient mouse transgenesis using Gateway-compatible ROSA26 locus targeting vectors and F1 hybrid ES cells. *Nucleic Acids Res* 2009; **37**:e55.
214. Irion S, Luche H, Gadue P, Fehling HJ, Kennedy M, Keller G. Identification and targeting of the ROSA26 locus in human embryonic stem cells. *Nat Biotechnol* 2007; **25**:1477–1482.
215. Kobayashi T, Kato-Itoh M, Yamaguchi T, *et al.* Identification of rat Rosa26 locus enables generation of knock-in rat lines ubiquitously expressing tdTomato. *Stem Cells Dev* 2012; **21**:2981–2986.
216. Madisen L, Zwingman TA, Sunkin SM, *et al.* A robust and high-throughput Cre reporting and characterization system for the whole mouse brain. *Nat Neurosci* 2010; **13**:133–140.
217. Snippert HJ, van der Flier LG, Sato T, *et al.* Intestinal Crypt Homeostasis Results from Neutral Competition between Symmetrically Dividing Lgr5 Stem Cells. *Cell* 2010; **143**:134–144.
218. Tchorz JS, Suply T, Ksiazek I, *et al.* A Modified RMCE-Compatible Rosa26 Locus for the Expression of Transgenes from Exogenous Promoters. *PLoS ONE* 2012; **7**:e30011.
219. Imayoshi I, Hirano K, Sakamoto M, *et al.* A multifunctional teal-fluorescent Rosa26 reporter mouse line for Cre- and Flp-mediated recombination. *Neurosci Res* 2012; **73**:85–91.
220. Abe T, Fujimori T. Reporter mouse lines for fluorescence imaging. *Dev Growth Differ*

2013; **55**:390–405.

221. Teruel MN, Blanpied TA, Shen K, Augustine GJ, Meyer T. A versatile microporation technique for the transfection of cultured CNS neurons. *J Neurosci Methods* 1999; **93**:37–48.

222. Randhawa VK, Ishikura S, Talior-Volodarsky I, *et al.* GLUT4 vesicle recruitment and fusion are differentially regulated by Rac, AS160, and Rab8A in muscle cells. *J Biol Chem* 2008; **283**:27208–27219.

223. Okada A, Lansford R, Weimann JM, Fraser SE, McConnell SK. Imaging cells in the developing nervous system with retrovirus expressing modified green fluorescent protein. *Exp Neurol* 1999; **156**:394–406.

224. McKeown L, Robinson P, Greenwood SM, Hu W, Jones OT. PIN-G – A novel reporter for imaging and defining the effects of trafficking signals in membrane proteins. *BMC Biotechnol* 2006; **6**:15.

225. Llopis J, McCaffery JM, Miyawaki A, Farquhar MG, Tsien RY. Measurement of cytosolic, mitochondrial, and Golgi pH in single living cells with green fluorescent proteins. *Proc Natl Acad Sci* 1998; **95**:6803–6808.

226. Kanda T, Sullivan KF, Wahl GM. Histone–GFP fusion protein enables sensitive analysis of chromosome dynamics in living mammalian cells. *Curr Biol* 1998; **8**:377–385.

227. Rizzuto R, Brini M, Pizzo P, Murgia M, Pozzan T. Chimeric green fluorescent protein as a tool for visualizing subcellular organelles in living cells. *Curr Biol CB* 1995; **5**:635–642.

228. Kimble M, Kuzmiak C, McGovern KN, de Hostos EL. Microtubule organization and the effects of GFP-tubulin expression in dictyostelium discoideum. *Cell Motil Cytoskeleton* 2000; **47**:48–62.

229. Iioka H, Ueno N, Kinoshita N. Essential role of MARCKS in cortical actin dynamics during gastrulation movements. *J Cell Biol* 2004; **164**:169–174.

230. Westphal M, Jungbluth A, Heidecker M, *et al.* Microfilament dynamics during cell movement and chemotaxis monitored using a GFP-actin fusion protein. *Curr Biol CB* 1997; **7**:176–183.

231. Petit V, Boyer B, Lentz D, Turner CE, Thiery JP, Valles AM. Phosphorylation of Tyrosine Residues 31 and 118 on Paxillin Regulates Cell Migration through an Association with Crk in Nbt-II Cells. *J Cell Biol* 2000; **148**:957–970.

232. Kretzschmar K, Watt FM. Lineage Tracing. *Cell* 2012; **148**:33–45.

233. Nowak JA, Polak L, Pasolli HA, Fuchs E. Hair follicle stem cells are specified and function in early skin morphogenesis. *Cell Stem Cell* 2008; **3**:33–43.

234. Livet J, Weissman TA, Kang H, *et al.* Transgenic strategies for combinatorial expression

- of fluorescent proteins in the nervous system. *Nature* 2007; **450**:56–62.
235. Jensen KB, Collins CA, Nascimento E, *et al.* Lrig1 expression defines a distinct multipotent stem cell population in mammalian epidermis. *Cell Stem Cell* 2009; **4**:427–439.
236. Van Keymeulen A, Rocha AS, Ousset M, *et al.* Distinct stem cells contribute to mammary gland development and maintenance. *Nature* 2011; **479**:189–193.
237. Karasawa S, Araki T, Nagai T, Mizuno H, Miyawaki A. Cyan-emitting and orange-emitting fluorescent proteins as a donor/acceptor pair for fluorescence resonance energy transfer. *Biochem J* 2004; **381**:307–312.
238. Karasawa S, Araki T, Yamamoto-Hino M, Miyawaki A. A green-emitting fluorescent protein from Galaxeidae coral and its monomeric version for use in fluorescent labeling. *J Biol Chem* 2003; **278**:34167–34171.
239. Dubey P. Reporter Gene Imaging of Immune Responses to Cancer: Progress and Challenges. *Theranostics* 2012; **2**:355–362.
240. Croxford AL, Buch T. Cytokine reporter mice in immunological research: perspectives and lessons learned. *Immunology* 2011; **132**:1–8.
241. Mohrs M, Shinkai K, Mohrs K, Locksley RM. Analysis of type 2 immunity in vivo with a bicistronic IL-4 reporter. *Immunity* 2001; **15**:303–311.
242. Gessner A, Mohrs K, Mohrs M. Mast cells, basophils, and eosinophils acquire constitutive IL-4 and IL-13 transcripts during lineage differentiation that are sufficient for rapid cytokine production. *J Immunol Baltim Md 1950* 2005; **174**:1063–1072.
243. Grogan JL, Mohrs M, Harmon B, Lacy DA, Sedat JW, Locksley RM. Early transcription and silencing of cytokine genes underlie polarization of T helper cell subsets. *Immunity* 2001; **14**:205–215.
244. Mohrs K, Wakil AE, Killeen N, Locksley RM, Mohrs M. A two-step process for cytokine production revealed by IL-4 dual-reporter mice. *Immunity* 2005; **23**:419–429.
245. Shinkai K, Mohrs M, Locksley RM. Helper T cells regulate type-2 innate immunity in vivo. *Nature* 2002; **420**:825–829.
246. Voehringer D, Shinkai K, Locksley RM. Type 2 immunity reflects orchestrated recruitment of cells committed to IL-4 production. *Immunity* 2004; **20**:267–277.
247. Stetson DB, Mohrs M, Reinhardt RL, *et al.* Constitutive Cytokine mRNAs Mark Natural Killer (NK) and NK T Cells Poised for Rapid Effector Function. *J Exp Med* 2003; **198**:1069–1076.
248. Brombacher F, Schäfer T, Weissenstein U, *et al.* IL-2 promoter-driven lacZ expression as a monitoring tool for IL-2 expression in primary T cells of transgenic mice. *Int Immunol*



1994; **6**:189–197.

249. Saporov A, Wagner FH, Zheng R, *et al.* Interleukin-2 expression by a subpopulation of primary T cells is linked to enhanced memory/effector function. *Immunity* 1999; **11**:271–280.

250. Repass JF, Laurent MN, Carter C, *et al.* IL7-hCD25 and IL7-Cre BAC transgenic mouse lines: new tools for analysis of IL-7 expressing cells. *Genes N Y N 2000* 2009; **47**:281–287.

251. Shalapour S, Deiser K, Sercan O, *et al.* Commensal microflora and interferon-gamma promote steady-state interleukin-7 production in vivo. *Eur J Immunol* 2010; **40**:2391–2400.

252. Kamanaka M, Kim ST, Wan YY, *et al.* Expression of interleukin-10 in intestinal lymphocytes detected by an interleukin-10 reporter knockin tiger mouse. *Immunity* 2006; **25**:941–952.

253. Maynard CL, Harrington LE, Janowski KM, *et al.* Regulatory T cells expressing interleukin 10 develop from Foxp3<sup>+</sup> and Foxp3<sup>[-]</sup> precursor cells in the absence of interleukin 10. *Nat Immunol* 2007; **8**:931–941.

254. Calado DP, Paixão T, Holmberg D, Haury M. Stochastic monoallelic expression of IL-10 in T cells. *J Immunol Baltim Md 1950* 2006; **177**:5358–5364.

255. Lee YK, Turner H, Maynard CL, *et al.* Late developmental plasticity in the T helper 17 lineage. *Immunity* 2009; **30**:92–107.

256. Croxford AL, Kurschus FC, Waisman A. Cutting Edge: An IL-17F-CreEYFP Reporter Mouse Allows Fate Mapping of Th17 Cells. *J Immunol* 2009; **182**:1237–1241.

257. Yang XO, Nurieva R, Martinez GJ, *et al.* Molecular antagonism and plasticity of regulatory and inflammatory T cell programs. *Immunity* 2008; **29**:44–56.

258. Azadniv M, Dugger K, Bowers WJ, Weaver C, Crispe IN. Imaging CD8<sup>+</sup> T cell dynamics in vivo using a transgenic luciferase reporter. *Int Immunol* 2007; **19**:1165–1173.

259. Chewning JH, Dugger KJ, Chaudhuri TR, Zinn KR, Weaver CT. Bioluminescence-based visualization of CD4 T cell dynamics using a T lineage-specific luciferase transgenic model. *BMC Immunol* 2009; **10**:44.

260. Lyons SK, Patrick PS, Brindle KM. Imaging mouse cancer models in vivo using reporter transgenes. *Cold Spring Harb Protoc* 2013; **2013**:685–699.

261. Peitz M, Pfannkuche K, Rajewsky K, Edenhofer F. Ability of the hydrophobic FGF and basic TAT peptides to promote cellular uptake of recombinant Cre recombinase: A tool for efficient genetic engineering of mammalian genomes. *Proc Natl Acad Sci* 2002; **99**:4489–4494.

262. Müntz B, Patsch C, Edenhofer F. Engineering cell-permeable protein. *J Vis Exp JoVE* 2009.

263. Kucherlapati RS, Eves EM, Song KY, Morse BS, Smithies O. Homologous recombination between plasmids in mammalian cells can be enhanced by treatment of input DNA. *Proc Natl Acad Sci U S A* 1984; **81**:3153–3157.
264. Li P, Burlak C, Estrada J, Cowan PJ, Tector AJ. Identification and cloning of the porcine ROSA26 promoter and its role in transgenesis. *Transplant Technol* 2014; **2**:1.
265. Abe T, Kiyonari H, Shioi G, *et al.* Establishment of conditional reporter mouse lines at ROSA26 locus for live cell imaging. *Genes N Y N* 2000 2011; **49**:579–590.
266. Li X, Yang Y, Bu L, *et al.* Rosa26-targeted swine models for stable gene over-expression and Cre-mediated lineage tracing. *Cell Res* 2014; **24**:501–504.
267. Gossler A, Joyner AL, Rossant J, Skarnes WC. Mouse embryonic stem cells and reporter constructs to detect developmentally regulated genes. *Science* 1989; **244**:463–465.
268. Peckham I, Sobel S, Comer J, Jaenisch R, Barklis E. Retrovirus activation in embryonal carcinoma cells by cellular promoters. *Genes Dev* 1989; **3**:2062–2071.
269. Brenner DG, Lin-Chao S, Cohen SN. Analysis of mammalian cell genetic regulation in situ by using retrovirus-derived “portable exons” carrying the Escherichia coli lacZ gene. *Proc Natl Acad Sci U S A* 1989; **86**:5517–5521.
270. De Angioletti M, Lacerra G, Sabato V, Carestia C. Beta+45 G --> C: a novel silent beta-thalassaemia mutation, the first in the Kozak sequence. *Br J Haematol* 2004; **124**:224–231.
271. Chen Y-T, Tsai M-S, Yang T-L, *et al.* R26R-GR: a Cre-activable dual fluorescent protein reporter mouse. *PLoS One* 2012; **7**:e46171.
272. Prather RS, Lorson M, Ross JW, Whyte JJ, Walters E. Genetically Engineered Pig Models for Human Diseases. *Annu Rev Anim Biosci* 2013; **1**:203–219.
273. Muzumdar MD, Tasic B, Miyamichi K, Li L, Luo L. A global double-fluorescent Cre reporter mouse. *genesis* 2007; **45**:593–605.
274. Imayoshi I, Hirano K, Sakamoto M, *et al.* A multifunctional teal-fluorescent Rosa26 reporter mouse line for Cre- and Flp-mediated recombination. *Neurosci Res* 2012; **73**:85–91.
275. Hoess RH, Wierzbicki A, Abremski K. The role of the loxP spacer region in P1 site-specific recombination. *Nucleic Acids Res* 1986; **14**:2287–2300.
276. Turan S, Galla M, Ernst E, *et al.* Recombinase-mediated cassette exchange (RMCE): traditional concepts and current challenges. *J Mol Biol* 2011; **407**:193–221.
277. Bethke B, Sauer B. Segmental genomic replacement by Cre-mediated recombination: genotoxic stress activation of the p53 promoter in single-copy transformants. *Nucleic Acids Res* 1997; **25**:2828–2834.

278. Kolb AF. Selection-marker-free modification of the murine beta-casein gene using a lox2272 [correction of lox2722] site. *Anal Biochem* 2001; **290**:260–271.
279. Osipovich AB, Singh A, Ruley HE. Post-entrapment genome engineering: First exon size does not affect the expression of fusion transcripts generated by gene entrapment. *Genome Res* 2005; **15**:428–435.
280. Araki K, Araki M, Yamamura K. Site-directed integration of the cre gene mediated by Cre recombinase using a combination of mutant lox sites. *Nucleic Acids Res* 2002; **30**:e103.
281. Cibelli JB, Stice SL, Golueke PJ, *et al.* Cloned transgenic calves produced from nonquiescent fetal fibroblasts. *Science* 1998; **280**:1256–1258.
282. Reggio BC, James AN, Green HL, *et al.* Cloned Transgenic Offspring Resulting from Somatic Cell Nuclear Transfer in the Goat: Oocytes Derived from Both Follicle-Stimulating Hormone-Stimulated and Nonstimulated Abattoir-Derived Ovaries. *Biol Reprod* 2001; **65**:1528–1533.
283. Park KW, Cheong HT, Lai L, *et al.* Production of nuclear transfer-derived swine that express the enhanced green fluorescent protein. *Anim Biotechnol* 2001; **12**:173–181.
284. Kurome M, Geistlinger L, Kessler B, *et al.* Factors influencing the efficiency of generating genetically engineered pigs by nuclear transfer: multi-factorial analysis of a large data set. *BMC Biotechnol* 2013; **13**:43.
285. Faast R, Harrison SJ, Beebe LFS, McIlpatrick SM, Ashman RJ, Nottle MB. Use of adult mesenchymal stem cells isolated from bone marrow and blood for somatic cell nuclear transfer in pigs. *Cloning Stem Cells* 2006; **8**:166–173.
286. Jin H-F, Kumar BM, Kim J-G, *et al.* Enhanced development of porcine embryos cloned from bone marrow mesenchymal stem cells. *Int J Dev Biol* 2007; **51**:85–90.
287. Kumar BM, Jin H-F, Kim J-G, *et al.* Differential gene expression patterns in porcine nuclear transfer embryos reconstructed with fetal fibroblasts and mesenchymal stem cells. *Dev Dyn* 2007; **236**:435–446.
288. Richter A, Kurome M, Kessler B, *et al.* Potential of primary kidney cells for somatic cell nuclear transfer mediated transgenesis in pig. *BMC Biotechnol* 2012; **12**:84.
289. Kubota C, Tian XC, Yang X. Serial bull cloning by somatic cell nuclear transfer. *Nat Biotechnol* 2004; **22**:693–694.
290. Cho S-K, Kim J-H, Park J-Y, *et al.* Serial cloning of pigs by somatic cell nuclear transfer: restoration of phenotypic normality during serial cloning. *Dev Dyn Off Publ Am Assoc Anat* 2007; **236**:3369–3382.
291. Peura TT, Lane MW, Lewis IM, Trounson AO. Development of bovine embryo-derived

- clones after increasing rounds of nuclear recycling. *Mol Reprod Dev* 2001; **58**:384–389.
292. Xing X, Magnani L, Lee K, Wang C, Cabot RA, Machaty Z. Gene expression and development of early pig embryos produced by serial nuclear transfer. *Mol Reprod Dev* 2009; **76**:555–563.
293. Wilmut I, Beaujean N, de Sousa PA, *et al.* Somatic cell nuclear transfer. *Nature* 2002; **419**:583–587.
294. Young LE, Fernandes K, McEvoy TG, *et al.* Epigenetic change in IGF2R is associated with fetal overgrowth after sheep embryo culture. *Nat Genet* 2001; **27**:153–154.
295. Inoue K, Kohda T, Lee J, *et al.* Faithful expression of imprinted genes in cloned mice. *Science* 2002; **295**:297.
296. Daniels R, Hall V, Trounson AO. Analysis of gene transcription in bovine nuclear transfer embryos reconstructed with granulosa cell nuclei. *Biol Reprod* 2000; **63**:1034–1040.
297. Prather RS, Sutovsky P, Green JA. Nuclear remodeling and reprogramming in transgenic pig production. *Exp Biol Med Maywood NJ* 2004; **229**:1120–1126.
298. Campbell KH, Loi P, Otaegui PJ, Wilmut I. Cell cycle co-ordination in embryo cloning by nuclear transfer. *Rev Reprod* 1996; **1**:40–46.
299. Campbell KH, McWhir J, Ritchie WA, Wilmut I. Sheep cloned by nuclear transfer from a cultured cell line. *Nature* 1996; **380**:64–66.
300. Miyoshi K, Rzucidlo SJ, Gibbons JR, Arat S, Stice SL. Development of porcine embryos reconstituted with somatic cells and enucleated metaphase I and II oocytes matured in a protein-free medium. *BMC Dev Biol* 2001; **1**:12.
301. Wakayama T, Perry AC, Zuccotti M, Johnson KR, Yanagimachi R. Full-term development of mice from enucleated oocytes injected with cumulus cell nuclei. *Nature* 1998; **394**:369–374.
302. Nagashima H, Ashman RJ, Nottle MB. Nuclear transfer of porcine embryos using cryopreserved delipated blastomeres as donor nuclei. *Mol Reprod Dev* 1997; **48**:339–343.
303. Wakayama T, Rodriguez I, Perry AC, Yanagimachi R, Mombaerts P. Mice cloned from embryonic stem cells. *Proc Natl Acad Sci U S A* 1999; **96**:14984–14989.
304. Tani YK. Direct exposure of chromosomes to nonactivated ovum cytoplasm is effective for bovine somatic cell nucleus reprogramming. *Biol Reprod* 2001; **64**:324–30.
305. Wood AJ, Lo T-W, Zeitler B, *et al.* Targeted Genome Editing Across Species Using ZFNs and TALENs. *Science* 2011; **333**:307–307.
306. Christian M, Cermak T, Doyle EL, *et al.* Targeting DNA double-strand breaks with TAL

- effector nucleases. *Genetics* 2010; **186**:757–761.
307. Zhang F, Cong L, Lodato S, Kosuri S, Church GM, Arlotta P. Efficient construction of sequence-specific TAL effectors for modulating mammalian transcription. *Nat Biotechnol* 2011; **29**:149–153.
308. Hockemeyer D, Wang H, Kiani S, *et al.* Genetic engineering of human pluripotent cells using TALE nucleases. *Nat Biotechnol* 2011; **29**:731–734.
309. Chang N, Sun C, Gao L, *et al.* Genome editing with RNA-guided Cas9 nuclease in zebrafish embryos. *Cell Res* 2013; **23**:465–472.
310. Cong L, Ran FA, Cox D, *et al.* Multiplex genome engineering using CRISPR/Cas systems. *Science* 2013; **339**:819–823.
311. Terns MP, Terns RM. CRISPR-Based Adaptive Immune Systems. *Curr Opin Microbiol* 2011; **14**:321–327.
312. Wiedenheft B, Sternberg SH, Doudna JA. RNA-guided genetic silencing systems in bacteria and archaea. *Nature* 2012; **482**:331–338.
313. Bhaya D, Davison M, Barrangou R. CRISPR-Cas systems in bacteria and archaea: versatile small RNAs for adaptive defense and regulation. *Annu Rev Genet* 2011; **45**:273–297.
314. Garneau JE, Dupuis M-È, Villion M, *et al.* The CRISPR/Cas bacterial immune system cleaves bacteriophage and plasmid DNA. *Nature* 2010; **468**:67–71.
315. Jinek M, Chylinski K, Fonfara I, Hauer M, Doudna JA, Charpentier E. A Programmable Dual-RNA-Guided DNA Endonuclease in Adaptive Bacterial Immunity. *Science* 2012; **337**:816–821.
316. Gasiunas G, Barrangou R, Horvath P, Siksnys V. Cas9-crRNA ribonucleoprotein complex mediates specific DNA cleavage for adaptive immunity in bacteria. *Proc Natl Acad Sci U S A* 2012; **109**:E2579–2586.
317. Sapranauskas R, Gasiunas G, Fremaux C, Barrangou R, Horvath P, Siksnys V. The *Streptococcus thermophilus* CRISPR/Cas system provides immunity in *Escherichia coli*. *Nucleic Acids Res* 2011; **39**:9275–9282.
318. Magadán AH, Dupuis M-È, Villion M, Moineau S. Cleavage of Phage DNA by the *Streptococcus thermophilus* CRISPR3-Cas System. *PLoS ONE* 2012; **7**:e40913.
319. Taylor GK, Heiter DF, Pietrokovski S, Stoddard BL. Activity, specificity and structure of I-Bth0305I: a representative of a new homing endonuclease family. *Nucleic Acids Res* 2011; **39**:9705–9719.
320. Shen B, Zhang J, Wu H, *et al.* Generation of gene-modified mice via

- Cas9/RNA-mediated gene targeting. *Cell Res* 2013; **23**:720–723.
321. Ran FA, Hsu PD, Wright J, Agarwala V, Scott DA, Zhang F. Genome engineering using the CRISPR-Cas9 system. *Nat Protoc* 2013; **8**:2281–2308.
322. Fu Y, Foden JA, Khayter C, *et al.* High-frequency off-target mutagenesis induced by CRISPR-Cas nucleases in human cells. *Nat Biotechnol* 2013; **31**:822–826.
323. Pattanayak V, Lin S, Guilinger JP, Ma E, Doudna JA, Liu DR. High-throughput profiling of off-target DNA cleavage reveals RNA-programmed Cas9 nuclease specificity. *Nat Biotechnol* 2013; **31**:839–843.
324. Cho SW, Kim S, Kim Y, *et al.* Analysis of off-target effects of CRISPR/Cas-derived RNA-guided endonucleases and nickases. *Genome Res* 2013.
325. Ran FA, Hsu PD, Lin C-Y, *et al.* Double nicking by RNA-guided CRISPR Cas9 for enhanced genome editing specificity. *Cell* 2013; **154**:1380–1389.
326. Mali P, Aach J, Stranges PB, *et al.* CAS9 transcriptional activators for target specificity screening and paired nickases for cooperative genome engineering. *Nat Biotechnol* 2013; **31**:833–838.
327. Fu Y, Sander JD, Reyon D, Cascio VM, Joung JK. Improving CRISPR-Cas nuclease specificity using truncated guide RNAs. *Nat Biotechnol* 2014; **32**:279–284.
328. Sharma S, Leonard J, Lee S, Chapman HD, Leiter EH, Montminy MR. Pancreatic islet expression of the homeobox factor STF-1 relies on an E-box motif that binds USF. *J Biol Chem* 1996; **271**:2294–2299.
329. Stoffel M, Stein R, Wright CV, Espinosa R 3rd, Le Beau MM, Bell GI. Localization of human homeodomain transcription factor insulin promoter factor 1 (IPF1) to chromosome band 13q12.1. *Genomics* 1995; **28**:125–126.
330. Inoue H, Riggs AC, Tanizawa Y, *et al.* Isolation, characterization, and chromosomal mapping of the human insulin promoter factor 1 (IPF-1) gene. *Diabetes* 1996; **45**:789–794.
331. Yokoi N, Serikawa T, Walther R. Pdx1, a homeodomain transcription factor required for pancreas development, maps to rat chromosome 12. *Exp Anim Jpn Assoc Lab Anim Sci* 1997; **46**.
332. Gerrish K, Van Velkinburgh JC, Stein R. Conserved transcriptional regulatory domains of the pdx-1 gene. *Mol Endocrinol Baltim Md* 2004; **18**:533–548.
333. Thomas MK, Devon ON, Lee JH, *et al.* Development of diabetes mellitus in aging transgenic mice following suppression of pancreatic homeoprotein IDX-1. *J Clin Invest* 2001; **108**:319–329.
334. Ahlgren U, Jonsson J, Jonsson L, Simu K, Edlund H. beta-cell-specific inactivation of the

mouse *Ipf1/Pdx1* gene results in loss of the beta-cell phenotype and maturity onset diabetes. *Genes Dev* 1998; **12**:1763–1768.

335. Stoffers DA, Zinkin NT, Stanojevic V, Clarke WL, Habener JF. Pancreatic agenesis attributable to a single nucleotide deletion in the human *IPF1* gene coding sequence. *Nat Genet* 1997; **15**:106–110.

336. Stoffers DA, Ferrer J, Clarke WL, Habener JF. Early-onset type-II diabetes mellitus (MODY4) linked to *IPF1*. *Nat Genet* 1997; **17**:138–139.

337. Mountford PS, Smith AG. Internal ribosome entry sites and dicistronic RNAs in mammalian transgenesis. *Trends Genet TIG* 1995; **11**:179–184.

338. Mizuguchi H, Xu Z, Ishii-Watabe A, Uchida E, Hayakawa T. IRES-dependent second gene expression is significantly lower than cap-dependent first gene expression in a bicistronic vector. *Mol Ther J Am Soc Gene Ther* 2000; **1**:376–382.

339. Doronina VA, Wu C, de Felipe P, Sachs MS, Ryan MD, Brown JD. Site-specific release of nascent chains from ribosomes at a sense codon. *Mol Cell Biol* 2008; **28**:4227–4239.

340. De Felipe P, Luke GA, Hughes LE, Gani D, Halpin C, Ryan MD. E unum pluribus: multiple proteins from a self-processing polyprotein. *Trends Biotechnol* 2006; **24**:68–75.

341. Heffner CS, Herbert Pratt C, Babiuk RP, *et al.* Supporting conditional mouse mutagenesis with a comprehensive cre characterization resource. *Nat Commun* 2012; **3**:1218.

342. Jaisser F. Inducible Gene Expression and Gene Modification in Transgenic Mice. *J Am Soc Nephrol* 2000; **11**:S95–S100.

343. Indra AK, Warot X, Brocard J, *et al.* Temporally-controlled site-specific mutagenesis in the basal layer of the epidermis: comparison of the recombinase activity of the tamoxifen-inducible Cre-ER(T) and Cre-ER(T2) recombinases. *Nucleic Acids Res* 1999; **27**:4324–4327.

344. Flisikowska T, Kind A, Schnieke A. The new pig on the block: modelling cancer in pigs. *Transgenic Res* 2013; **22**:673–680.

345. Flotte TR, Barraza-Ortiz X, Solow R, Afione SA, Carter BJ, Guggino WB. An improved system for packaging recombinant adeno-associated virus vectors capable of in vivo transduction. *Gene Ther* 1995; **2**:29–37.

346. Wadia JS, Dowdy SF. Protein transduction technology. *Curr Opin Biotechnol* 2002; **13**:52–56.

347. Hai T, Teng F, Guo R, Li W, Zhou Q. One-step generation of knockout pigs by zygote injection of CRISPR/Cas system. *Cell Res* 2014; **24**:372–375.

348. Ross JW, Fernandez de Castro JP, Zhao J, *et al.* Generation of an inbred miniature pig model of retinitis pigmentosa. *Invest Ophthalmol Vis Sci* 2012; **53**:501–507.
349. Petters RM, Alexander CA, Wells KD, *et al.* Genetically engineered large animal model for studying cone photoreceptor survival and degeneration in retinitis pigmentosa. *Nat Biotechnol* 1997; **15**:965–970.



## 6 Abbreviations

%	percent
°C	Degree Celsius
µg	Microgram
µM	Micromolar
µm	Micrometer
ADMSC	Adipose mesenchymal stem cell
APC	adenomatous polyposis coli
bFGF	Basic fibroblast growth factor
bmMSC	Bone marrow mesenchymal stem cell
bp	Base pair
<i>bsr</i>	Blasticidin S-resistance gene
BRCA1	breast cancer associated gene 1
β-geo	fusion gene of β-galactosidase and neomycine resistance
CAG	chicken beta-actin promoter combined with the cytomegalovirus enhancer element
CAT	Chloramphenicol acetyltransferase
cDNA	Complementary DNA
cm <sup>2</sup>	Square centimeter
CO <sub>2</sub>	Carbon dioxide
Cre	causes recombination
CRISPR	clustered regularly interspaced short palindromic repeats
CDKN2A	Cyclin-dependent kinase inhibitor 2A
ddH <sub>2</sub> O	Double distilled water
dNTP	Deoxynucleotide triphosphate
dUTP	Desoxyuridin-5'-triphosphate
DSB	Double strand break
DMSO	Dimethylsulfoxide
DMEM	Dulbecco's Modified Eagle's Medium
DNA	Desoxyribonucleic acid
DL	Deutsche Landrasse
EDTA	Ethylenediaminetetraacetic acid
ESC	Embryonic stem cell
ET	Embryo transfer
<i>E. coli</i>	Escherichia coli
EtOH	Ethanol
FCS	Fetal calf serum

---

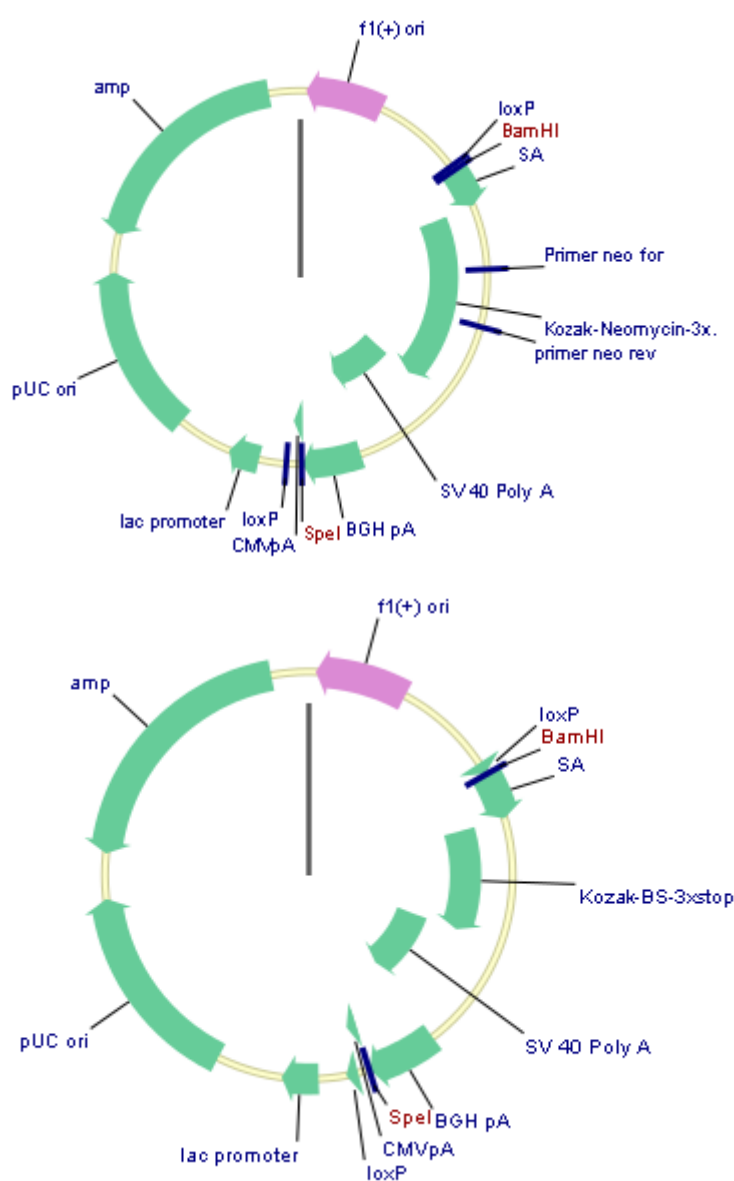
FAP	familial adenomatous polyposis
g	Gram
g	Gravitational acceleration
GAPDH	Glyceraldehyde 3-phosphate dehydrogenase
GFP	Green fluorescent protein
GGTA1	$\alpha$ -1,3-galactosyltransferase
GCROSA	ROSA26 $\beta$ -geo/mCherry gene targeting vector
G418	geneticin
HR	homologous recombination
HPRT	hypoxanthine phosphoribosyl transferase
HAR	hyperacute rejection
IRES	Internal ribosome entry site
IPMN	Intraductal Papillary Mucinous Neoplasm
KRAS	Kirsten rat sarcoma viral oncogene homolog
KDNF	Kidney fibroblast
kDa	kilodalton
L	Liter
LTRs	long-terminal-repeats
Min	Minute
ml	milliliter
mRNA	Messenger RNA
MCN	Mucinous Cystic Neoplasm
mCherry	monomeric cherry
NHEJ	non-homologous end joining
NaCl	sodium chloride
NaOH	sodium hydroxide
NaAC	Sodium Acetate
neo	neomycin
PBS	Phosphate buffered saline
PCR	Polymerase Chain Reaction
PDX-1	Pancreatic and duodenal homeobox 1
PDAC	Pancreatic ductal adenocarcinoma
PanIN	Pancreatic Intraepithelial Neoplasia
Ptf1a/P48	pancreas-specific transcription factor 1a
poFFs	porcine fetal fibroblasts
RT-PCR	Reverse transcriptase polymerase chain reaction
RACE	rapid amplification of cDNA end
RFP	Red fluorescent protein
s	Second

SCNT	Somatic cell nuclear transfer
SDS	Sodium dodecyl sulfate
SMAD4	SMAD family member 4
SMGT	Sperm mediated gene transfer
SV40	simian virus 40
TALENs	transcription activator-like (TAL) effector nucleases
tdTomato	tandem dimer Tomato
TGROSA	ROSA26 mTomato/mEGFP gene targeting vector
TP53	Tumour protein 53
U	Unit
UBC	human ubiquitin C
UV	Ultraviolet
V	Volt
X-Gal	5-Brom-4-chlor-3-indolyl- $\beta$ -D-galactopyranosid
ZFN	zinc finger nuclease

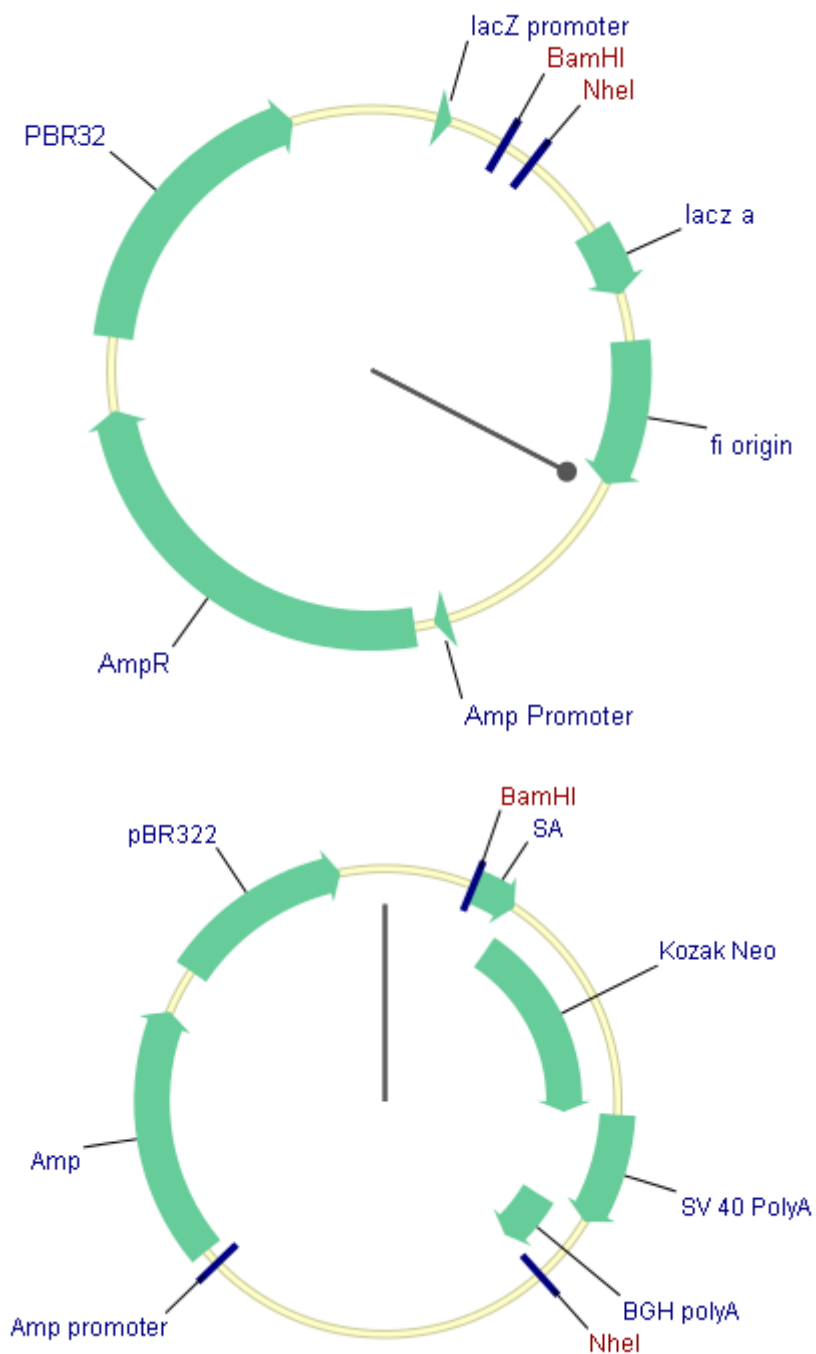
## 7 Appendix

### A.1 Molecular cloning of TGROSA targeting vector

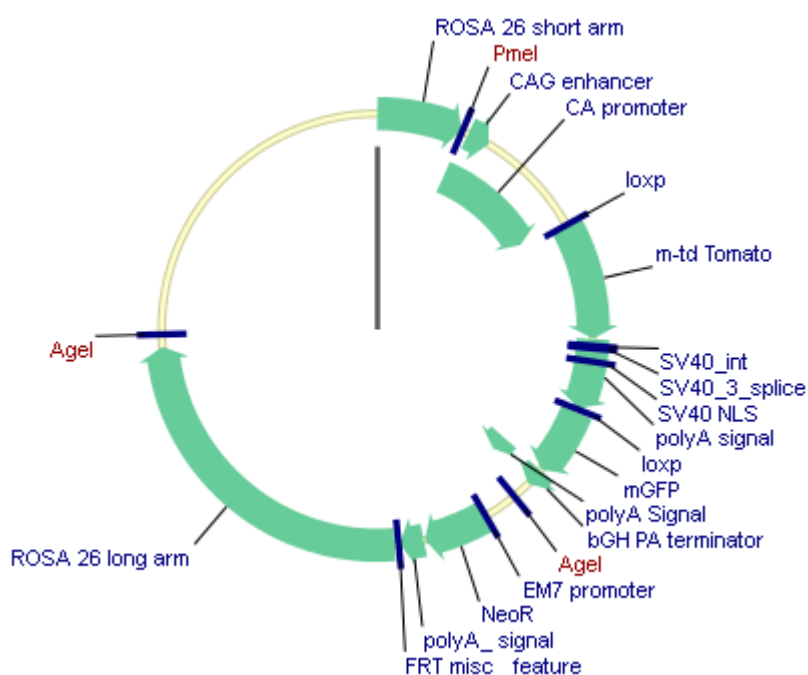
1, The pBluescript LSL SA-neo-PA and pBluescript LSL SA-BS-PA were double digested by *Bam*HI-HF and *Spe*I to get the 1562 bp SA-neo-PA and 1203 bp SA-BS-PA cassette, respectively.



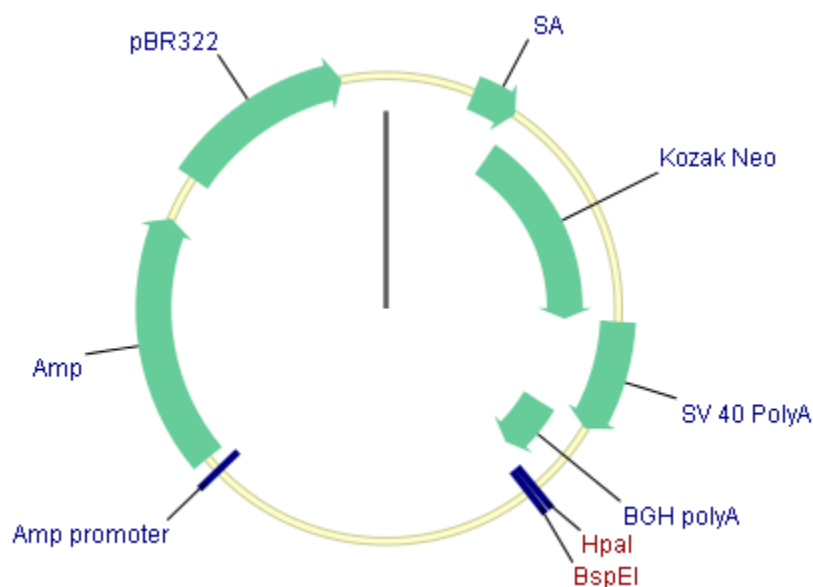
2, The pSL1180 (3422 bp) was double digested by *Bam*HI and *Nhe*I, and 1562 bp SA-neo-PA and 1203 bp SA-BS-PA were subcloned into double digested pSL1180 plasmid to get pSL1180-SA-neo-PA and pSL1180-SA-BS-PA. (pSL1180-SA-neo-PA is shown below)

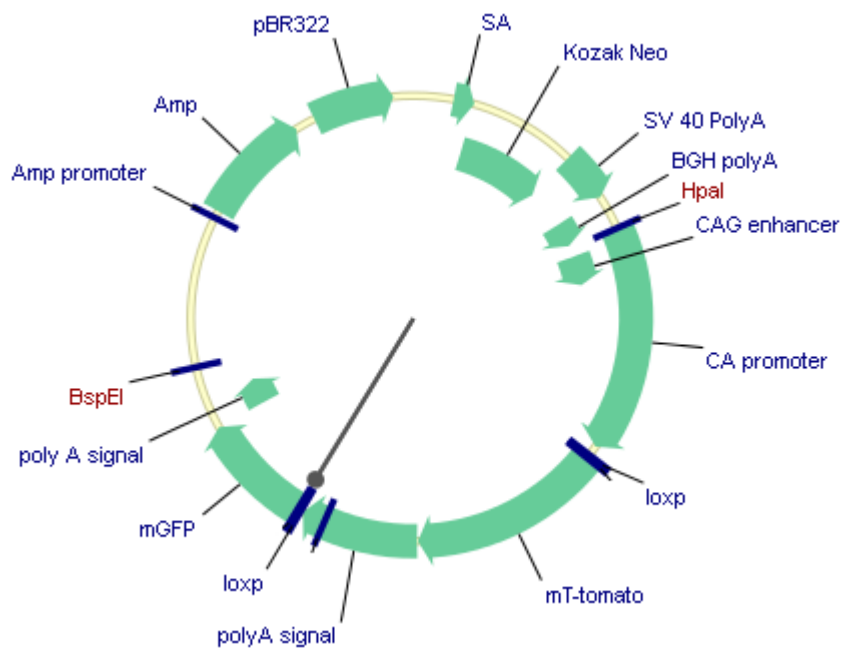


3, The mouse ROSA26 CAG mT/mG was double digested by *PmeI* and *AgeI* to get the CAG mT/mG cassette.

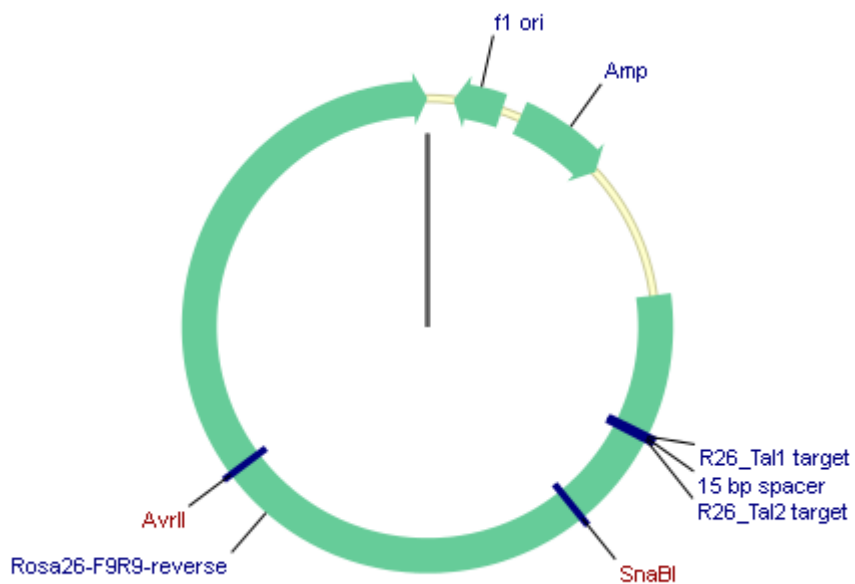


4, pSL1180-SA-neo-PA and pSL1180-SA-BS-PA were double digested by *HpaI* and *BspEI*, and CAG mT/mG cassette was subcloned into double digested pSL1180-SA-neo-PA or pSL1180-SA-BS-PA to get pSL1180-SA-neo-PA-CAG mT/mG or pSL1180-SA-BS-PA-CAG mT/mG, respectively. (pSL1180-SA-neo-PA-CAG mT/mG is shown in below).

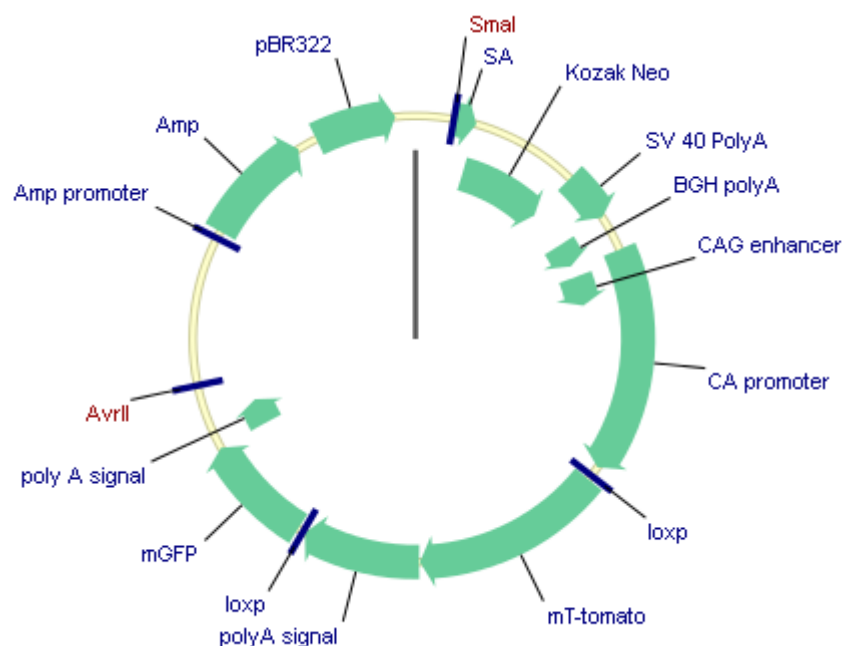




5, ROSA26 F9R9 was double digested by *SnaBI* and *AvrII*.



pSL1180-SA-neo-PA-CAG mT/mG was double digested by *SmaI* and *AvrII*.



6, Subclone double digested pSL1180-SA-neo-PA-CAG mT/mG into double digested ROSA26F9R9 to generate GCROSA and TGROSA targeting vector.

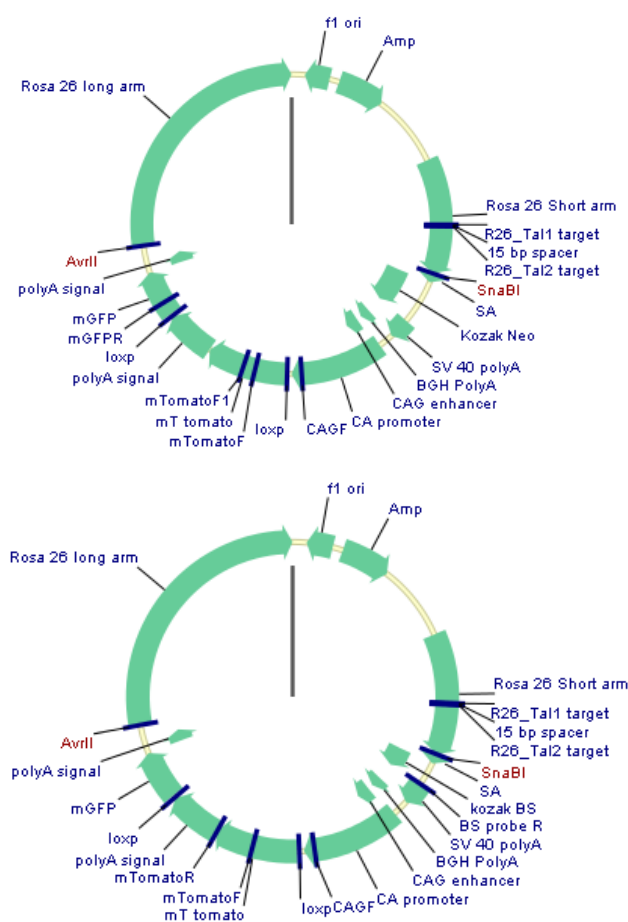






**Figure A.1** DNA sequence alignment of the promoter region and exon1 of *ROSA26* in mouse, rat, pig and human. The porcine sequence shown is located on chromosome 13 (NCBI *Sus Scrofa* 10.2 porcine genome NW\_003611693: 29648-30716). The mouse, rat and human *ROSA26* sequences shown are located on chromosome 6 (AC\_000028), chromosome 4 (NC\_005103) and chromosome 3 (NC\_000003) respectively.

**GGAAGCCGCCGGGGCCGCTAGAGAAGAGGCTGTGCTCTGGGGCTCCGGCTCCTCA**  
**GAGAGCCTCGGCTAGTTTTAATTTCTAGTATGGTAAATACTGGTAAACAAAGCATT**  
**GGGACCCTCAGCTTTTAATAATGTGAAGATATCCTGAGACCAAGAAGTTGGAGGAAG**  
**CTGCTAAGCATACCAATGGATTATTATCGCCAGCAATATGGTAAACAGTTAGACCATT**  
**TGTAGCCCCCTAAAAGACAAGAGAATATATTTAAAGAGAAGTAACAAACTGCAAAAC**  
**AGAAAAGATTAAAGGGCCACACTTGCATCATATGAAGAACTCTAGAGGTTGAATTGG**  
**AGCTGTAGCGGCCAGCCTATGTTACAGCCACAGCAACCTGGGATCCAAGCTCAATCT**  
**GTGACCTATAACACAGATCATGGCAATGCTGGATCCTTAACCCACTGAGCGAGGCCA**  
**GGGATCAAACCTACATCCTCATAGATCCTAGTCGGGCTCGTTAACTGCTGAGCCACAA**  
**AGGGAACCTCCCTTATTTATTTGCATTTTATTTTTGTCTTTTATAGGGCTGCATCCACAGCC**  
**TGTGTAAGTTCCCAGGCTAGGGGCTGAAGCGGAGCTATAGCTGTCAGCCTACACCAC**  
**AGCCACAGCAGTGCCAGATCCTAGTGGTGTCTGTGACCTACACCACAACTCACAGCA**  
**ATGCCGGATCCTTAACCACTGAGCCAGGACAGGGATTAACACACATCCTCATGGAT**  
**ACTAGTTGGGGTTCCTTATAGCTGAAGTCATCATG**

**Figure A.2** Porcine *ROSA26* cDNA with the four exons indicated by different colours.

## 8 Acknowledgement

First of all, I would like to thank my supervisor Prof. Angelika Schnieke for giving me the opportunity to participate in this promising and interesting project. Also, I thank her for the inspiration and her patient supervision and support.

I would like to thank the China Scholarship Council for the financial support for my PhD studies in Germany.

I would like to thank Dr. Alexander Kind for his useful advice on the project. I also would like to thank him for the patient correction of the publications. I also thank Dr. Tatiana Flisikowska and Dr. Krzysztof Flisikowski for all of their kind help, guidance and suggestions. When I was new at the chair, they provided me with a lot of help and supervision, making it easy for me to adapt to the new lab quickly.

I would like to thank Steffen and Viola Löbnitz in Thalhausen for dedicated animal husbandry. Also, I would like to thank Prof. Eckhard Wolf, Dr. Mayuko Kurome, Valeri Zakhartchenko, Dr. Barbara Kessler for performing nuclear and embryo transfers in Oberschleissheim.

I would like to express my gratitude to the colleagues in the Chair of Livestock Biotechnology for all of their kind help. Dr. Simone Kraner-Scheiber who arranged students for me; Barbara Bauer who helped me deal with many documents. I also would like to thank Sulith Christan, Marlene Edlinger, Peggy Mueller-Fliedner, Kristina Mosandl and Margret Bahnweg for their wonderful technical assistance.

Also, I would like to thank my fellow PhD students Konrad Fischer, Benedikt Baumer, Anja Saalfrank, Erica Schulze, Carolin Wander, Daniela Fellner, Beate Rieblinger, Tobias Richter, Simon Leuchs and Marina Durkovic for the help and discussions. I would like to thank my students Claudia Sturm, Judith Schäfers, Veronika Harant.

Special thanks to Denise Nguyen and Rahul Dutta for their help both in lab and in life, for their trust and encouragement and the wonderful English correction and professional photographing. I really cherish our friendship. Also, I would like to thank Xinxin Cui for her help and kind advice.

Furthermore, I also would like to thank all of my Chinese friends back at home and in Germany for all the help and the nice time we have spent together. Thanks to Kai Li for helping me a lot.

At last, I thank my relatives for endless support and my parents for their love and support. When I call my parents and relatives, I always get a lot of positive energy which let me overcome every difficulty during these years.

May, 2014, Freising

---

## Declaration

I hereby declare that I have produced this work without the prohibited assistance of third parties and without making use of aids other than those specifically indicated. This work has not been presented to any other examination board and has not been part of any other thesis.

Freising, June 17, 2014

Shun Li

---

# Curriculum Vitae

## Persönliche Daten

Name: Shun Li  
Geburtstag: 20.07.1986  
Geburtsort: Hubei, China  
Email: lishun86@126.com

## Ausbildung

09/2011-08/2014 Promotion am Lehrstuhl für Biotechnologie der Nutztiere, WZW, Technische Universität München  
Thema der Doktorarbeit: *ROSA26 dual fluorescent reporter pigs and generation of a porcine model for pancreatic cancer*

09/2008-06/2011 Master of Science, Tier Molekularbiologie  
Southwest University  
Thema der Masterarbeit: Cloning, mapping, imprinting status and tissue expression analysis of four porcine candidate imprinted genes

09/2004-06/2008 Bachelor of Science, Biologische Wissenschaften  
Zunyi Normal College  
Thema der Bachelorarbeit: Isolation and Molecular Identification of Bacteria from *Tinca tinca Linnaeus* of Net Cage Culture in the Wujiang River

09/2001-06/2004 Abitur, Erste Gymnasium der Qichun, Hubei, China

## Veröffentlichungen

1. **Shun Li**, Tatiana Flisikowska, Mayuko Kurome, Valeri Zakhartchenko, Barbara Kessler, Dieter Saur, Alexander Kind, Eckhard Wolf, Krzysztof Flisikowski, Angelika Schnieke. *Dual fluorescent reporter pig for Cre recombination; transgene placement at the ROSA26 locus*. PLoS one 9(7): e102455.doi:10.1371/journal.pone.0102455.
2. Heli Venhoranta<sup>#</sup>, **Shun Li**<sup>#</sup>(**co-first author**), Sylwia Salamonc, Tatiana Flisikowska, Magnus Andersson, Marek Switonski, Alexander Kind, Angelika Schnieke, Krzysztof Flisikowski. *Non-CpG hypermethylation in placenta of mutation-induced intrauterine growth restricted bovine fetuses*. Biochemical and Biophysical Research Communications, 2014, 444 (3): 391-394.
3. **Shun Li**, Juan Li, Jiawei Tian, Ranran Dong, Jin Wei, Xiaoyan Qiu, and Caode Jiang. *Characterization, Tissue Expression, and Imprinting Analysis of the Porcine CDKN1C and NAP1L4 Genes*. Journal of Biomedicine and Biotechnology, 2012, Volume 2012, Article ID 946527, doi: 10.1155/2012/946527.
4. Caode Jiang<sup>#</sup>, **Shun Li**<sup>#</sup>(**co-first author**), Ping Shi<sup>#</sup>, Ranran Dong, Jiawei Tian, Changyan Deng. *Characterization and imprinting analysis of COPG2 and MEST genes in pigs*. *Animal Science Papers and Reports*, 2011, 29(3):247-256.
5. Jiang CD, **Li S**, Deng CY. *Assessment of genomic imprinting of PPP1R9A, NAP1L5 and PEG3 in pigs*. *Russian Journal of Genetics*, 2011, 47(4): 467-472.
6. Caode Jiang, Ping Shi, **Shun Li**, Ranran Dong, Jiawei Tian, Jin Wei, and Shuang Luo. *Gene Expression Profiling of Skeletal Muscle of Nursing Piglets*. *International Journal of Biological Sciences*, 2010, 6(7):627-638.